Emulsion and miniemulsion polymerization stabilized with oligomeric surfactants (ASRs)

Sara Caballero Berasategui

Chemical Engineering Group
University of the Basque Country (UPV/EHU)
Donostia-San Sebastian
(2015)

Algunas personas hacen que el mundo sea
más especial sólo por estar en él...

A Jose, el amor de mi vida, por darme la felicidad
A mi padre, el recuerdo que siempre me dibuja una sonrisa
Y a mi madre por darmelo todo sin pedir nada a cambio, os quiero

Emulsion and miniemulsion polymerization stabilized with oligomeric surfactants (ASRs)

Contents

Agradecimientos

En primer lugar querría agradecer a Polymat y en exclusiva al grupo de Ingeniería Química la oportunidad de realizar la tesis doctoral bajo su tutela con especial mención a mis directores de tesis; a Txema Asua por su dedicación y la adquisición de tantos y variados conocimientos y a José Carlos de la Cal por su incondicional apoyo (ya que me distes paz en muchos momentos de tempestad), su gran paciencia y la inmensidad de consejos dados. También al resto de profesores que componen el grupo; a José Ramón Leiza por darme la oportunidad de comenzar mi andadura en la investigación, a Mariaje Barandiaran por estar siempre dispuesta a ayudar, a María Paulis por su generosidad y a las nuevas incorporaciones Radmila Tomovska y David Mecerreyes. También a otros profesores de Polymat por vuestros consejos; Jaquelin Forcada, Iñigo Legorburu, Mario Montes, Lourdes Cantón, Josepi Berridi, etc. Y como no, al secretariado del grupo, a Txoni, a Onintza y en especial a Inés Plaza, porque es imposible enumerar todo el bien que proporcionas (y siempre con una sonrisa); gracias por estar ahí.

También debo agradecer a BASF, Arkema, Cytec, ICI Paint, Romh & Haas, Euroresins, Nuplex Resins, Azko Nobel y Waker por la financiación aportada a traves del programa ILP (Industrial Liason Program) durante el desarrollo de esta tesis doctoral en el área de las dispersiones coloidales.

En particular, agradezco a Nuplex Resin Labs (en Wageningen, Holanda) la gran oportunidad que me dio Richard Brinkhuis de formar parte de su grupo y conocer la investigación desde un punto de vista más industrial. A Javier Bohorquez por ayudarme y apoyarme en esos duros momentos y al equipo humano que allí me encontré, Richard Van der Host, Tonny Busser, Peter-Jan Elfrink, etc.

A todos los doctorandos y doctores con los que he compartido muchos y variados momentos tanto en las instalaciones de la facultad como en Korta. Con los que comencé en la facultad, Amaia, Mónica, Aitziber, Josetxo, Alvaro, Gema, Ainara, Raquel, Iñigo, Adam, Txepe, Milton, Gaby, Savio que fue el instructor number one del excell, Maider que es todo corazón, Mihaela que amenizaba las horas con su canto, Sorin (digan lo que digan, no cambies nunca), Odinei que estuviste en mis primeros pasos apoyandome y Javier que fue el rockero del grupo además de un gran compañero. Al grupo de Catálisis, Orlando, Dora, Chendy, Ohiane que me distes fuerzas cuando no las tenía,

Eleta que es la alegría de la huerta, Javi Echave que además de un gran amigo, es un excelente profesor (¿te acuerdas de los controladores? Uff, que horror) y Luciano que daba el toque "brasileiro" a los acontecimientos. Y a los que llegaron trás el translado a las nuevas instalaciones, a Korta; Audrey, Ibón, Andoni (mi compi de pedidos), Arvind (el teacher hindú de inglés), Ibai, Ander, Amaia (patx), Edurne, Miren, Leire, Shagha, Ali, Jessica, Nick, Garbiñe, Aintzane, Yamal con el que tantos buenos ratos compartí en el laboratorio, Eshan, Alejandro, Freddy y Wendy con los que siempre puedes contar, Jone y Ziortza con las que he pasado buenisimos momentos, Itxaso con la que he vivido grandes momentos desde las clases en la carrera hasta interminables horas en el laboratorio, André, Roque y Pablo de los que tanto aprendí, Matek, Yuri nuestro mexicano más salado, Joseba que es una de las mejores personas que he conocido, Maitane, Paula y Raquel las postdoc más guays del grupo, Ana Margarida la ternura en si misma, Ana Belen la burgalesa con más entusiasmo, Urko (técnico del TEM), Antonio que por ser el técnico del MALDI le he vuelto loco con muestras imposibles y Patricia a la que siempre que necesito está ahí, gracias. En especial a mis compañeras y amigas por que habéis enriquecido mi vida y mi alma en tantos y tan buenos momentos, a Vesna por darnos fuerza, a Juliana por ser la cordura y la sensatez, a Karim por ser la alegría y la bondad y a Julieta por ser nuestra chica cosmopolitan y cinéfila (cuanto aprendimos contigo).

Otra parte de mi vida que no quiero dejar de nombrar en estas lineas es la de las personas que me han acompañado antes, durante y tras este reto personal y profesional. Mi familia que desde los más mayores hasta los más

pequeños (abuelos, aitonas, osabas, izebas y prim@s de todas las edades) siempre están ahí, a mi ama por dármelo todo y a la vez enseñarme que todo no es necesario (te quiero muchísimo) y a mi aita que ojala hubiera podido acompañarme en esta parte de mi vida (aunque sé, que desde donde estés lo habrás hecho). A mi otra familia, los Dominguez, por hacerme sentir parte de vosotros. A mi cuadrilla, Ane, Aitor, Yoli, Asier, Enrique, Juliana, Iosune, Javi C, Javi G, Cris, David, Eider, Marijo e Iban; por todo y en especial por mi despedida a Holanda (uno de los mejores fines de semana de mi vida) y por las visitas recibidas en aquellos duros momentos.

Con mención especial debo agradecer muchísimo a la persona que hace que haya luz en mi vida y deseos de seguir viviéndola. Gracias Jose por estar ahí noche y día y hacer que me sienta la persona más afortunada del mundo incluso en momentos duros y muy complicados.

Chapter 1: Alkali soluble resins as emulsifiers

Outline

1.1 Water-borne polymer dispersions

Water-borne polymer dispersions are polymer particles dispersed in an aqueous medium. These dispersions are commonly synthesized by emulsion or miniemulsion polymerization yielding versatile products called latexes. These solvent-free polymer latexes are environmentally friendly fulfilling the increasingly restrictive governmental regulations.

There is a wide variety of water-borne polymeric dispersions that are mainly used as paints, coatings and adhesives [1]. They are also used in a broad range of fields such as inks, carpet backing, non-woven fabrics, leather treatment, foam mattresses, drug delivery systems, medical assay kits and other biomedical and pharmaceutical applications [2]. In addition, latexes are also used as impact modifiers in plastic matrices [3], as additives [4] and as rheological modifiers [5].

The properties of the final product are mainly determined by the chemical composition of the polymer, the molecular weight distribution, the polymer microstructure, the particle morphology, the surface properties of the polymer particles and the particle size distribution. In addition, for the applications that require film formation, the morphology of the polymer film [6] plays a key role in the product performance.

Copolymer composition has a direct effect on the Tg (glass transition temperature) which determines the minimum film forming temperature

(MFFT). Copolymer composition also affects other properties such as resistance to hydrolysis [7] and weatherability.

The polymer particles are mostly spherical, but sometimes they have other morphologies that affect the final properties. The presence of acid at the surface of the polymer particles is beneficial for both the stability of the latex [8] and adhesion to substrates. The particle size distribution (PSD) and the particle surface functionality determine the rheology of the latex [9] that in turn controls mixing and heat transfer and the maximum solids content achievable in the reactor.

The great variety of properties achievable by varying these characteristics and the use of water as environment friendly dispersion medium are the main reasons to the continuous increase in the market share of these products.

By 2012, plastics had a worldwide annual production of 288 million tones [10], and in a wide variety of applications are substituting other materials such as metal and wood. Waterborne dispersed polymers represent about 6% of worldwide polymer production. These materials are used in a wide range of applications [7, 11-15], and a significant part of them are high value-added products.

1.2 Synthesis of polymeric dispersions

Most latexes are commercially produced by emulsion polymerization. Miniemulsion polymerization has the potential of synthesizing complex polymer-polymer and polymer-inorganic water borne dispersions but its presence in commercial products is still scarce [16].

In this Thesis, the synthesis of polymeric dispersions was carried out by free radical polymerization using emulsion and miniemulsion processes. A brief explanation of both techniques is presented to facilitate reading of the thesis. This information is extended in the Appendices I and II.

1.2.1 Emulsion polymerization

In batch reactors, emulsion polymerization basically follows the mechanism proposed by W.D. Harkins [17] in 1947 and depicted in Figure 1. First, the monomers are dispersed in water in the presence of surfactants, which adsorb on the surface of the monomer droplets. In almost all formulations, the amount of surfactant exceeds that needed to cover the monomer droplets and hence, micelles that are swollen with monomer are formed. As most initiators are water-soluble, the radicals are formed in the aqueous phase. These radicals are often too hydrophilic to directly enter into the organic phases. Therefore, they react with the monomer dissolved in the aqueous phase, forming oligoradicals hydrophobic enough to be able to enter

into or adsorb on the organic phases. As the total area of the micelles is about three orders of magnitude greater than that of the droplets, the entry of radicals into the micelles is more likely. In the monomer swollen micelles, the radicals grow fast forming polymer particles. This process is called *heterogeneous nucleation* or *micellar nucleation* [17]. Polymer particles can also be formed by *homogeneous nucleation* [18], which occurs when the oligoradicals grow in the aqueous phase beyond the length at which they precipitate. The precipitated polymer chains are stabilized by the emulsifier present in the aqueous phase, and monomer diffuses to the new organic phase, allowing a fast growth of the polymer particles. The rate of particle formation depends on the nucleation mechanism (see Appendix I).

The new particles are very small and suffer a tremendous increase in surface area when they grow. It is arguable that the emulsifier molecules may diffuse fast enough to the surface of these fast growing particles to stabilize them. Therefore, the species formed by entry of radicals in micelles and by precipitation of growing radicals in the aqueous phase may be regarded as precursor particles that only become stable particles upon growth by coagulation and polymerization [19-21]. This combined process is called *coagulative nucleation*.

The formation of particles ceases when there is no enough emulsifier to stabilize more particles. In the classical mechanism proposed by Harkins [17], this occurred when the micelles disappear but it is now recognized that the

formation of particles can extend beyond this point. The period in which particles are formed is known as Interval I.

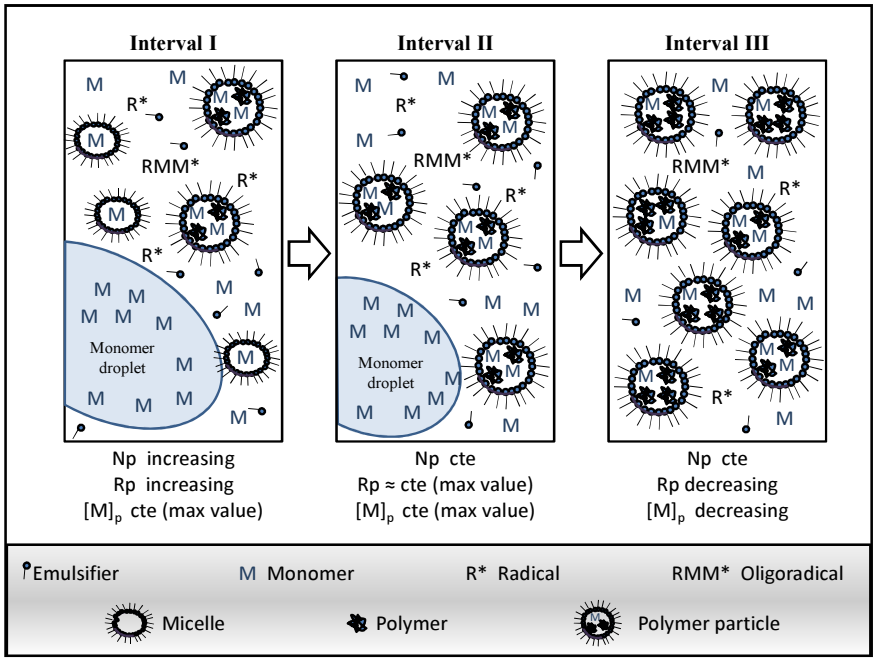

Figure 1: The classic Harkins theory

During Interval I the number of particles (N_p) increases and therefore the polymerization rate (R_p) also increases. During nucleation, monomer droplets, monomer swollen micelles and monomer swollen polymer particles coexist in the batch reactor. The monomer that is consumed in the polymer particles is replaced by the monomer that diffuses from the monomer droplets. Consequently, the size of the polymer particles increases and the size of monomer droplets decreases. After some time, all micelles disappear. The formation of new particles may occur after this point because particles

stabilization does not require a complete coverage of their surface and hence some surfactant may desorb from the existing particles to stabilize the new particles formed by homogeneous nucleation. The kinetics of the surfactant desorption is critical for the stabilization of the newly formed particles [22]. The disappearance of micelles, considered to be the end of the nucleation marks the end of Interval I.

In the Interval II, the system is composed of monomer droplets and polymer particles. The monomer consumed by polymerization in the polymer particles is replaced by monomer that diffuses from the monomer droplets through the aqueous phase. In the presence of monomer droplets, the concentration of the monomer in the polymer particles reaches a maximum value and remains constant. The transport of reactants with low water solubility from monomer droplets to polymer particles may be diffusionally limited. As the number of polymer particles and the monomer concentration in the particles are constant, the polymerization rate is roughly constant (some variation of the average number of radicals per particle may occur). The polymer particles grow in size and after some time, the monomer droplets disappear, marking the end of Interval II (see the Figure 1). The transition from Intervals II to III occurs at about 15-40% conversion depending on the nature of the monomer. In general, the higher the water solubility of the monomer the higher the maximum swelling of the polymer particles and the lower the conversion at which Interval II ends. Most of the monomer polymerizes during Interval III. In this interval, the monomer concentration in the polymer particles decreases continuously, and consequently the

polymerization rate also decreases, although increases due to gel effect have been reported [23].

In semi-continuous reactors, monomers and sometimes surfactant, initiator and water are continuously fed into the reactor. In these systems, emulsion polymerization does not follow the sequence of events described earlier. Nevertheless, the underlying processes are the same. Usually, monomers are continuously fed under starved conditions, namely, at high instantaneous conversions (polymer/monomer ratios close to 90/10 on weight basis). Under these circumstances, only the newly fed monomer droplets are present in the reactor, and their life-time is short because the monomers diffuse to the polymer particles where they are consumed. The concentration of monomer in the polymer particles depends on the relative values of mass transfer and polymerization rates.

The dispersed systems are thermodynamically unstable and kinetic stability is provided by emulsifiers or by incorporation of hydrophilic groups into the polymer. In emulsion polymerization, most of the polymerization occurs in the polymer particles. In these systems, radicals are distributed among the polymer particles. The amount of radicals present in the polymer particles is the most distinctive kinetic feature of emulsion polymerization and has profound implications in both the polymerization rate and polymer microstructure. Radicals in different particles cannot terminate by bimolecular termination and as a result, the overall radical concentration in emulsion polymerization is higher than in bulk polymerization. This means, that the

polymerization rate is significantly higher. The overall concentration of radicals increases as the number of particles increases, providing longer life-time to the radicals. As the life-time is inversely proportional to the entry frequency, this leads to higher molecular weights. Consequently, in emulsion polymerization it is possible to increase simultaneously the polymerization rate and the molecular weight by simply increasing the number of particles.

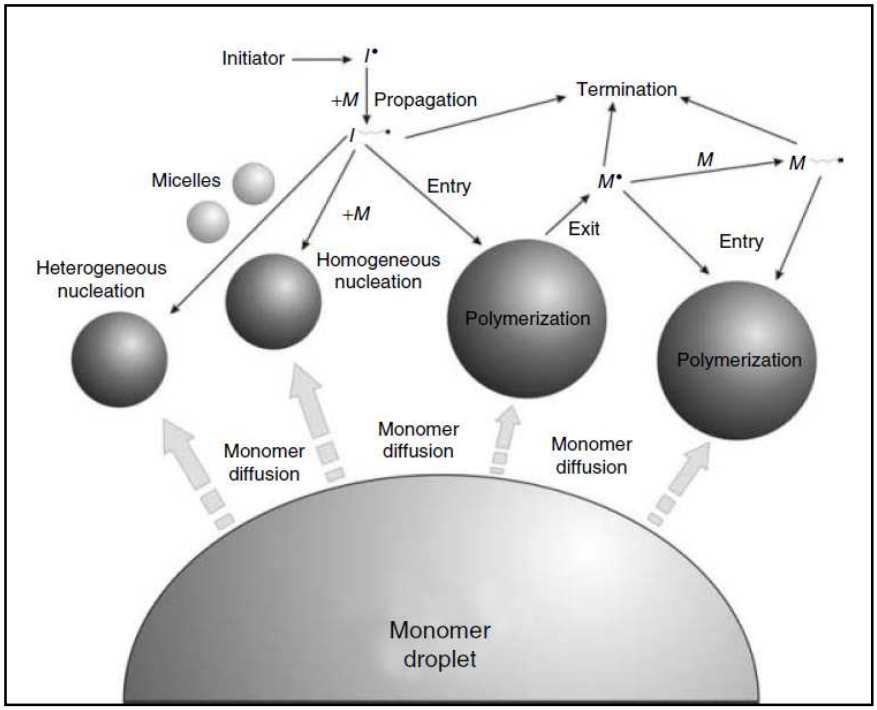

Figure 2: Mechanisms involved in emulsion polymerization [14]

Figure 2 summarizes the mechanisms involved in emulsion polymerization. Radicals formed in the aqueous phase from water-soluble initiators, react with the monomer dissolved in the aqueous phase forming

oligoradicals. These oligoradicals may: (1) enter into the polymer particles, (2) enter into the micelles (*heterogeneous nucleation*), (3) propagate in the aqueous phase until they become insoluble and precipitate forming new polymer particles (*homogeneous nucleation*) and (4) terminate with other radicals in the aqueous phase. The reactions that can occur within the polymer particles are the same as for bulk free radical polymerization. Small radicals formed by chain transfer to monomer or to chain transfer to agent (CTA) can desorb from the polymer particles provided they present some water solubility [24].

In emulsion polymerization, the rate of polymerization of monomer per unit volume of the reactor, R_p, measured in mol $L^{-1}s^{-1}$, is:

$$R_p = k_p[M]_p \frac{\bar{n}}{N_A} \frac{N_p}{V} \qquad (1)$$

where k_p is the propagation rate constant in $Lmol^{-1}s^{-1}$, $[M]_p$ the concentration of monomer in the polymer particles ($molL^{-1}$), $\bar{n}$ the average number of radicals per particle, N_A the Avogadro's number, N_p the number of polymer particles (measured as particles in the reactor) and V the volume of the reactor in L.

Depending on the frequency of radical entry and exit in the polymer particles, the value of $\bar{n}$ varies. Smith and Ewart [25] considered three limiting cases depending on the reactants involved and the experimental conditions:

a) Case 1: where $\bar{n}$«0.5 and it corresponds to a system in which the radical desorption rate is much faster than the rate of radical entry. The main features for this system are: (1) small particles (typically d_p<100 nm), (2) relatively water-soluble monomers or relatively water-soluble CTAs, (3) low rate of generation of radicals from the initiator and (4) large number of particles. Under these conditions, $\bar{n}$ is given by [25]:

$$\bar{n} = \frac{k_a[R]_w}{2k_a[R]_w + k_d} \quad (2)$$

where k_a is the entry rate coefficient in $Lmol^{-1}s^{-1}$, k_d (s^{-1}) the desorption rate coefficient and $[R]_w$ the radical concentration in aqueous phase ($molL^{-1}$).

b) Case 2: where $\bar{n}$=0.5 that corresponds to a system in which there is no radical desorption and instantaneous termination occurs when a radical enters into polymer particle already containing one radical. The characteristics for this system are: (1) no chain transfer to small molecules occurs (i.e., monomers and CTAs) or these small molecules are highly water insoluble, (2) fast bimolecular termination rate and (3) the polymer particles are relatively small (typically, d_p<200 nm).

c) Case 3: where the concentration of radicals in the polymer particle approaches that of bulk polymerization ($\bar{n}$»0.5). The system is formed by (1) large particles (d_p>200 nm), (2) high initiator concentrations or redox initiators and (3) slow termination rates (may be due to gel effect). In Case 3, $\bar{n}$ is given by:

$$\bar{n} = \left(\frac{k_a[R]_w}{2c}\right)^{0.5} \quad (3)$$

where c is defined as:

$$c = \frac{k_t}{2v_p N_A} \quad (4)$$

where k_t is the termination rate constant in $Lmol^{-1}s^{-1}$, v_p the volume of monomer(s) swollen polymer particle, and N_A the Avogadro's number.

In general, for Case 2, the polymerization rate is proportional to the number of particles and the molecular weight also increases with N_p. For Cases 1 and 3, the polymerization rate is independent of the number of polymer particles if radical termination in the aqueous phase is negligible, but R_p increases with N_p when termination in aqueous phase is considerable. In Case 1, the molecular weights are determined by chain transfer, and in Case 3, the molecular weights are similar to those in bulk. Further information is given in Appendix I.

1.2.2 Miniemulsion polymerization

Miniemulsion polymerization facilitates the synthesis of complex materials that cannot be produced otherwise [16]. These materials have a broad range of applications including adhesives [26-29]; antireflection [30],

anticorrosive [31, 32] and UV resistant [33] coatings; anti-counterfeiting [34]; textile pigments [35]; bio-based polymer dispersions [36]; gene and drug delivery [37-42]; anti-viral therapy [43]; low viscosity high solids dispersions [44-46], among others.

The word miniemulsion was coined [47] to describe submicron oil in water dispersions that are stable for a period ranging from hours to months. Ugelstad et al. [48] were the first to demonstrate that under conditions in which the droplet size is small enough, nucleation of monomer droplets could account for an important part of the particles formed. Miniemulsion polymerization has been reviewed broadly [16, 49-51].

The controlled synthesis of dispersed polymers by miniemulsion polymerization requires to form the initial miniemulsion making them colloidaly stable and stable with respect Ostwald ripening. This effect has been shown to cause miniemulsion degradation due to the fact the chemical potential of the monomer in the small droplets is highest than in large droplets. Consequently, monomer diffuses from small to large droplets leading to large droplets and emulsion destabilization. Higuchi and Misra [52] predicted that the addition of a small amount of a water-insoluble compound would retard the emulsion degradation by molecular diffusion because the slow rate of diffusion of the water-insoluble compound would permit the monomer remain essentially equilibrated among the droplets.

In an ideal miniemulsion system, coalescence and Ostwald ripening are suppressed by using an efficient surfactant and a water insoluble low molecular weight compound as costabilizer. The key aspects in the preparation of the monomer miniemulsions are the formulation and the method of preparation.

A typical formulation includes water, the monomer mixture, a costabilizer and the surfactant and initiator systems. Hexadecane [53, 54] and cetyl alcohol [55] are the costabilizers most often used in publications. However, these costabilizers remain in the polymer particles and may have deleterious effects on the properties of the polymer. Alduncin et al. [56] proposed to minimize these negative effects of the costabilizer by incorporating it into the polymer backbone by means of covalent bonds using high water insoluble initiators. Water insoluble monomers and polymers have also been used to reduce Ostwald ripening although they are not costabilizers but hydrophobes. Miller at al. [57] found that styrene miniemulsion could be prepared using 1wt% of polystyrene as hydrophobe. This miniemulsion creamed rather rapidly but it was stable enough to be polymerized. Reimers and Schork [58] used poly(methyl methacrylate) to stabilize methyl methacrylate miniemulsions finding that miniemulsion stability depends on polymer content and polymer molecular weight. Chern at al. [59] reported that a water-insoluble dye could offer resistance to diffusional degradation of styrene miniemulsion. However, the dye was less efficient than cetyl alcohol and stearyl or dodecyl methacrylate in stabilizing the miniemulsion.

Usually, for miniemulsion preparation, the surfactant system is dissolved in water, the costabilizer is dissolved in the monomers and mixed under stirring. Then, the mixture is subjected to high efficient homogenization. A huge range of equipment is commercially available for emulsification. The most important are sonifiers and high-pressure homogenizers. The sonifier produces ultrasound waves that cause the molecules to oscillate about their main position as the waves propagate. During the compression cycle, the average distance between the molecules decreases, whilst during rarefaction the distance increases. The rarefaction results in a negative pressure that may cause the formation of voids and cavities (cavitation bubbles) that may grow in size. In the succeeding compression cycle of the wave, the bubbles are forced to contract and may even disappear totally [60]. The shock waves produced on the total collapse of the bubbles cause the break up of the surrounding monomer droplets. A problem associated with the sonifier is that only a small region of the fluid around the sonifier tip is directly affected by the ultrasound waves. Therefore, an additional stirring must be used to allow all the fluid to pass through the sonication region. This process makes the miniemulsion characteristic dependent on the sonication time. Thus, there is evidence [61, 62] that droplet size decreases with sonication time. The decrease is initially pronounced and later the droplet size evolves asymptotically towards a value that depends on both the formulation and the energy input.

The Manton-Gaulin and the Microfluidizer are the most commonly used high-pressure homogenizers. Both of them have in common that coarse dispersions are pressurized using a positive displacement pump, and flow

through a narrow gap at high velocity. A strong pressure drop also occurs. In the Manton-Gaulin, the coarse emulsion is pumped through the narrow gap of a valve. The final droplet size was the result of two consecutive processes [63]: droplet break up (presumably occurring in the homogenizer's valve) and coagulation of newly formed droplets insufficiently covered by the emulsifier (likely occurring after the pass by the homogenizer's valve). Therefore, at high pressure in the valve, the droplets size depends on the emulsifier concentration and at high emulsifier concentration, it depends on the pressure of the valve. In the Microfluidizer, the emulsion is forced through the interaction chamber where the stream splits into precisely defined microchannels. In the microchannels, the streams accelerate to approximately 300-400 ms^{-1}, are turned at right angles upon each other in a region created by an orifice plate at the same time the liquid undergoes a pressure drop. Shear, impact and the cavitation forces are focused on a small area, which act to break up the dispersed phase.

Likely, the main difference between emulsion and miniemulsion polymerizations is the nucleation step. In miniemulsion process, droplet nucleation is the main nucleation mechanism (it may be accompanied by homogeneous nucleations). In the emulsion polymerization, the homogeneous and heterogeneous nucleations are the most important particle formation processes.

1.3 Surfactant systems

Surfactant (also referred as emulsifier or stabilizer) is a key component of the formulation of polymerization in dispersed media. The surfactants useful for miniemulsion or emulsion polymerizations [44, 55, 64-69] should meet the following requirements: (1) have a specific structure with polar and non-polar groups; (2) be more soluble in the aqueous phase so as to be readily available for adsorption on the droplet/particle surface; (3) adsorb strongly and not be easily displaced when two droplets/particles collide; (4) reduce the interfacial tension; (5) impart a sufficient electrokinetic potential to the droplets/particles; (6) work in small concentration; and (7) be relatively inexpensive, non-toxic and safe to handle.

A wide variety of commercial surfactants fulfill these requirements. It must be stressed that the role of emulsifier is crucial since it facilitates the formation of monomer droplets of the initial emulsion, contributes decisively to the nucleation process and imparts colloidal stability to polymer particles in the final latex [70]. There are three basic types of surfactants [71]:

(a) Ionic surfactants (anionic or cationic) which prevent coagulation by electrostatic repulsion arising from the charges located on the particle surface and the associated electrical double layer [72].

(b) Non-ionic surfactants (for example partially hydrolyzed polyvinyl alcohol) which stabilize mainly through the entropic repulsion caused when trying to pack two chains in the same space [73].

(c) Electrosteric stabilizer (such as polyelectrolytes) which display the characteristics of ionic and non-ionic surfactants.

Anionic emulsifiers are extensively used in many emulsion polymerization systems. They serve as strong particle generators and stabilize the latex particles via electrostatic repulsion mechanism. However, latexes stabilized with this type of emulsifiers are often unstable upon addition of electrolytes and in freeze-thaw cycles. Furthermore, these emulsifiers have limited stabilizing effectiveness at high solids content and their films present high water sensitivity. To overcome these problems, non-ionic emulsifiers can be used to stabilize the particles in the course of emulsion polymerization. The use of non-ionic surfactants reduces the water sensitivity of the films and improves the stability of latex against electrolytes, freeze-thaw cycles, and high shear rates. However, they are less efficient than ionic surfactants in particle nucleation because of their slow desorption [22]. Alkali soluble resins (ASRs) are electrosteric stabilizers that can impart enhanced colloidal stability due to the combined electrostatic and steric stabilization. In addition, ASRs can absorb strongly onto the surface of latex particles, reducing or avoiding emulsifier migration in the final applications.

1.4 Alkali soluble resins (ASRs)

The alkali soluble resins (ASRs) are random or block copolymers formed by copolymerization of hydrophobic monomers (such as styrene (S), methyl methacrylate (MMA) and butyl methacrylate (BMA)) and monomers containing carboxylic acid groups (e.g. methacrylic acid (MAA) and acrylic acid (AA)). At low pHs (typically below the pK_a of the carboxylic acids) the carboxylic acid is protonated and the ASR is not soluble in water. At high pH, a large fraction of the carboxylic groups are deprotonated and the polymer chain becomes charged and soluble in water, under these conditions, it is able to act as an electrosteric stabilizer.

The water solubility of the ASRs depends on the molecular weight (MW), the acid number (N_{Ac}) and the nature of the hydrophobic monomers. Usually, for copolymer chains of a given composition, the solubility in water decreases with the increase of the molecular weight, and precipitation of the chains occurs above a critical length. The acid number is defined as the milligrams of potassium hydroxide (KOH) that are needed to neutralize one gram of the resin (ASR), namely, it is a measure of the fraction of carboxylic groups in the copolymer chains. Water solubility increases as N_{Ac} increases. S, MMA and BMA are often used as hydrophobic monomers. The relative hydrophobicities between them are S>BMA>MMA. Therefore, for the rest of characteristics constant, the ASRs synthesized with S are less water soluble than those prepared with BMA.

Low molar mass alkali-soluble resins have been used as colloidal stabilizers in commercial emulsion polymerizations since the 1970s [74, 75] and it is claimed that ASRs can offer advantages, including substantial Newtonian flow, excellent mechanical and freeze thaw stability, good pigment dispersion and wetting properties [76, 77].

1.4.1 Synthesis of ASRs

To synthesize random ASRs, one or several non-acidic monomers are copolymerized with acidic monomers at low pH. If a block copolymer is desired, controlled radical polymerization may be used [78-80]. After polymerization, the pH is increased adding a base (such as ammonium hydroxide, NH_4OH) to dissolve the copolymer in alkali medium. This characteristic is the reason for the name: alkali soluble resins.

Pierre Castan [81] synthesized in 1943 one of the first synthetic resins with acidic groups. The invention refers to the production of thermosetting artificial resins [82], which were synthesized by condensing ethylene oxide or derivatives thereof with polyvalent carboxylic acids in alkaline solutions. In 1959, Greenlee et al. [83] patented the ASRs synthesis for use in removable protective coating compositions. The resins of this invention were useful in the manufacture of paints, varnishes, adhesives, and fabric-treating compositions. They were composed by polyhydric alcohol and dicarboxylic acid having 2-12 carbons and an N_{Ac} in the range of 40-100 $mg_{KOH}g_{Resin}^{-1}$.

In 1968, Stevens et al. [74] patented the low molecular weight ASRs and the method for their preparation and purification. These solvent-borne ASRs contained at least two monomers, one was a carboxylic monomer and other carboxyl-free monomer (MMA or/and ethyl acrylate (EA)) and had an N_{Ac} from 140 to 300 $mg_{KOH}g_{ASR}^{-1}$ and a number average molecular weight ($\overline{M}_n$) from 700 to 5000 $gmol^{-1}$ and were used as emulsifier, as well as leveling and film-former agents.

Kiehlbauch and Tsaur [76, 77] examined the feasibility of using ASR as surfactant. The ASRs were synthesized copolymerizing AA/S or AA/S/AMS (AMS: alpha methyl styrene) and had a number average molecular weight between 2000-3000 $gmol^{-1}$. The authors found that the resin fortified emulsion polymer offered many advantages, such as substantial Newtonian flow, excellent mechanical stability, freeze-thaw stability, good pigment dispersion and wetting properties. Lee and Kim [84] using surface tension and pyrene adsorbance measurements showed that above certain concentration, the ASRs formed aggregates (micelles) in aqueous medium. Other authors [85, 86] also demonstrated the presence of the aggregates in aqueous phase.

Hwu and Lee [86] showed that the surface tension measurement of ASR (copolymer S/AA) had a shape similar to that of a conventional emulsifier. They observed that the critical aggregates concentration of ASR ranges from 1.48 to 14.8 gL^{-1}, owing to the fact that the ASRs are composed of species with various molecular weights (dispersity of the molecular weight

distribution was 1.9 from GPC results). The authors also observed that the surface tension of the ASR aqueous solution before stirring was lower than after stirring. They argued that the phenomenon was due to the high molecular weight of the ASR that caused its slow diffusion to the liquid-air interface. The slow migration in the film allowed the polymeric surfactant to overcome the drawbacks of surfactant migration.

1.4.2 ASRs as emulsifiers in emulsion polymerization

Alkali soluble resins are a special type of polymeric surfactants that may provide advantages over conventional surfactants because they strongly adsorb onto the polymer particles minimizing the emulsifier migration during film formation. However, the knowledge of their behaviour in emulsion polymerization is limited. Several factors have been investigated using ASR as emulsifier which are detailed below:

a) Molecular weight of ASRs

Kato et al. [87] studied the kinetics and particle nucleation in the styrene emulsion polymerization using a random MMA/MAA ASR [84] with weight average molecular weights ($\overline{M}_w$) varying from 2500 to 67000 $gmol^{-1}$. They observed that for $\overline{M}_w$=67000 $gmol^{-1}$, both, the polymerization rate (R_p) and the number of particles (N_p) began to decrease after 30% conversion and the system was not always stable. The authors argued that bridging

agglomeration [88] may take place when the copolymer molecular weight is large. However, for $\overline{M}_w$ between 4500 and 9100 gmol^{-1}, the system was stable, the nucleation period takes place until 20-30% of conversion reaching for all the molecular weights a similar value of N_p and R_p. The authors also showed that for $\overline{M}_w$<4500, N_p become constant for conversions above 20-30%, but R_p and N_p decreased monotonously with decreasing $\overline{M}_w$ of ASRs. Therefore, three different behaviors were observed varying $\overline{M}_w$. On the contrary, Piirma et al. [89-91] reported that in the emulsion polymerization of styrene, the molecular weight of non-ionic graft and block amphiphilic copolymer did not affect either R_p or N_p.

Wang et al. [92] synthesized ASRs by cleavage of *tert*-butyl (*t*-butyl) groups in the chains of poly (*n*BMA-co-*t*BMA) and by radical polymerization between MAA and *n*BMA. All the polymers were produced by controlled radical polymerizations carried out using RAFT agent that provided a similar molecular weight for all the ASR chains (dispersity (Đ) around 1.3). It was found that an increase in the number average molecular weight ($\overline{M}_n$) between 14000 and 31000 gmol^{-1}, led to a slight increase in polymerization rate of styrene, which was attributed to the gel effect. The authors claimed that in the last stages of emulsion polymerization, the number of radicals in large particles was much higher than in the smaller particles, and this increase compensated the decrease in N_p.

b) Composition of ASRs

Kato et al. [87] studied the effect of the ASR composition on the kinetics and particle nucleation in the styrene emulsion polymerization. The random polymer composition was varied from 10/90 to 40/60 (wt/wt) of MMA/MAA [85]. All emulsion polymerizations proceeded without coagulum. The authors found that both N_p and R_p decreased monotonously with increasing the MAA content. The reason can be that the higher hydrophilicity leads to lower adsorption and hence less particles can be stabilized. On the other hand, Wang et al. [92] in the emulsion polymerization of styrene stabilized with a relative monodispersed ASR synthesized by RAFT polymerization, observed that N_p and R_p increased with increasing the carboxyl group content of the ASR. The authors explained that the carboxyl content may decrease the number of aggregation (Agg_N, number of molecules present in a micelle or in an aggregate) and consequently, this reduction provokes an increase in the number of aggregates (N_{agg}). This resulted in higher N_p and R_p.

c) Neutralization degree of ASRs

Lee and Kim [84] studied the effect of the neutralization degree of the ASR on the final particle size (d_p) and polydispersity of the particle size distribution (PSD) for S and MMA emulsion polymerizations. A commercial ASR with high acid number, N_{Ac}=190 $mg_{KOH}g_{Resin}^{-1}$, was used varying the neutralization degree; 80, 90 and 100%. The authors showed that for MMA, the polydispersity of PSD increased with the increase of the ASR's

neutralization. For 100% neutralization, the shape of the PSD was even bimodal. Therefore, they concluded that the degree of neutralization affected particle nucleation in MMA emulsion polymerization; due to the change of the dominant nucleation mechanism from micellar nucleation (low polydispersity) to micellar and homogeneous nucleations (bimodal) as the neutralization increases. In S emulsion polymerization, the micellar nucleation is the predominant mechanism, following the Harkins [17] theory. The average particle diameter decreased slightly as the neutralization degree increased. The authors concluded that with increasing the neutralization degree of the ASR, the number of aggregates (N_{agg}) increases.

On the other hand, Lee and Kim [93] used an alkali-soluble random copolymer (styrene/α-methylstyrene/acrylic acid) as polymeric emulsifier in S emulsion polymerization. The calorimetric technique was applied to study the kinetics varying the neutralization degree. The authors observed that the rate of polymerization (R_p) decreased with increasing the neutralization degree of ASR. They argued that highly neutralized ASRs are less efficient in solubilising the monomer and capturing initiator radicals than those with a lower neutralization.

d) ASR concentration

Kato et al. [85] used a MMA/MAA ASR as emulsifier in the styrene (S) emulsion polymerization varying the ASR concentration. The authors observed that the N_p and R_p increased with the ASR concentration, and some

coagulum was obtained at low emulsifier content. Moreover, the authors observed that the nucleation period was prolonged by increasing ASR concentration; but this period never extended beyond 30% conversion. They argued that the mechanism of particle nucleation using ASR must be somewhat different than using SLS [94] as emulsifier, because for SLS, N_p reached a constant value at very low conversion. Interestingly, the power dependence of the polymer particles and the polymerization rate with respect to the initial ASR concentration was 0.6 as predicted by Smith-Ewart theory [25].

Coen et al. [95] reported that an ASR prepared by copolymerization of AA/S reduced the entry and exit rate coefficients of radicals in emulsion polymerization, compared with a conventional ionic stabilizer. Lee and Kim [93] found that using a commercial ASR when the amount of ASR increased, d_p decreased (as for a conventional emulsifier). However, in spite of the increase of N_p they observed that R_p decreased because the thicker and denser layer of ASR reduced radical entry. Hwu and Lee [96] studied the emulsion polymerization of BMA using a commercial ASR (copolymer of S/AA) and their data of the aggregates number, swelling aggregates (before polymerization) and final d_p (after polymerization) suggested that the coagulative nucleation was the major mechanism. The authors reported that the effect of ASR concentration on N_p was in accordance with that of a conventional emulsifier, but, the ASR slowed down the radical entry into the polymer particles. This idea was further supported by the increase of the polymer molecular weight due to the low frequency of radical entry (giving

the polymer chain more time to growth). Hwu and Lee [96] reported also that particle nucleation occurred while there were monomer droplets in the system (around 50% of conversion). The long nucleation period was also confirmed by the broad PSD obtained that become even broader when ASR concentration increased.

Wang et al. [92] studied the effect of the concentration of ASR content (BMA/MAA using RAFT agent) on N_p in the emulsion polymerization of S. They showed that N_p increased with the ASR amount. However, above a certain concentration of ASR the viscosity of the final latex severely increased leading to coagulation during the last stages of the emulsion polymerization. The authors attributed the coagulation to the bridging flocculation caused by the ASRs chains dissolved in the aqueous phase (non adsorbed onto the particles). The adsorption was enhanced by the agitation.

e) Hydrophilicity of the monomers using ASRs as surfactant

Hwu and Lee [86] studied the effect of the hydrophobicity of the monomer in ASR (copolymer S/AA) stabilized emulsion polymerization of MMA, S and BA. It was reported that the average particle size of the BA latex was 3 times higher than those for S and MMA and the particle size distribution was the broader. In addition, the latex was unstable. This was attributed to the poor adsorption of ASR onto the poly(butyl acrylate) particles. In spite of the high propagation rate constant, R_p was the lowest for BA. MMA showed a somewhat higher d_p than S, which was attributed to the high amount of ASR

in the system that favours the micellar nucleation. This nucleation was faster than homogeneous nucleation because the adsorption of ASR onto the surface of new polymer particles was the slowest mechanism. Nevertheless, $R_p(MMA) > R_p(S)$, possibly due to the higher propagation rate constant of MMA. Hwu and Lee [86] evaluated the effect of ASR and SLS on MMA and S emulsion polymerizations, reporting that for styrene, R_p was similar for ASR and SLS. On the other hand, for MMA, $R_p(ASR) < R_p(SLS)$ although the number of particle was higher for ASR. The reason was that the average number of radicals per particle ($\bar{n}$) was lower for ASR. The authors suggested that the ASR acted as a chain transfer agent.

f) Initiator effect on emulsion polymerization stabilized with ASRs

Kuo and Chen [97] carried out the emulsion polymerization of S using the sodium salt of poly (dodecyl acrylate/ acrylic acid) as emulsifier. Both, water soluble (KPS, potassium persulfate) and oil soluble (AIBN, azobisisobutyronitrile) initiators were used. It was found that for both initiators a bimodal particle size distribution was obtained that was attributed to polymerization in monomer droplets and in ASR aggregates.

Kato et al. [85] studied the effect of the initiator concentration (KPS) using a MMA/MAA ASR as stabilizer. They found that for high concentrations of KPS, both R_p and N_p decreased above 40% of conversion and that the final system was unstable. The authors proposed that the high initiator concentration produced many polymer particles, and consequently,

the ASR absorbed per unit area of particle surface was low. In addition, the high electrolyte concentration reduced the electrostatic potential at the surface of the polymer particles, and hence the polymer particles become unstable. For smaller KPS concentrations, both the polymer particles and the polymerization rate were proportional to the 0.4 power of the initial initiator concentration, as predicted by Smith-Ewart theory [25].

1.4.3 ASR as emulsifier in miniemulsion polymerization

The great versatility of the miniemulsion polymerization technique to synthesize novel materials with high added value has attracted the interest of both, academic and industrial communities. Recently, processes based on the use of ASR as sole emulsifier in miniemulsion polymerization for high solids content latexes have been disclosed [46]. The new technology opens a vast field for the production of high performance latexes for industrial applications, as well as an interesting topic for academic research.

Using miniemulsion polymerization, do Amaral et al. [98] synthesized high solids content with low viscosity (BA, MMA and BA/MMA) latexes stabilized with commercial ASRs (Morez 101 and Morez 300). It was reported that stable aqueous polymer dispersions could be obtained using lower concentrations of ASR compared with other processes [71].

do Amaral et al. [99] found that persulfate initiators (APS and KPS) led to coagulation, likely due to the combined effect of an increase in the ionic strength of the medium and to a reduction of the pH during polymerization. The first effect reduces the thickness of the double layer and the second the surface charge density because of the protonation of the carboxyl groups of the ASR. Using non-charged initiators (either water-soluble, Luperox 256, or oil-soluble, VA-086) high solids stable latexes were obtained for BA and MMA. However, coagulum was observed for S. The authors proposed that the solubilisation of ASR into the monomer droplets may play a relevant role. The ASR may be buried into S monomer droplets due to the higher affinity between S and Morez 300. A similar behaviour has also been documented in the emulsion polymerization using no ionic surfactants, where the solubility of the surfactant in the monomer droplets reduced the effective concentration of surfactant in the aqueous phase [100-102]. In addition, do Amaral et al. [99] observed that BA and MAA miniemulsion polymerizations led to polymer particles bigger than the monomer droplets. They suggested that coagulative nucleation was operative.

The kinetics of the miniemulsion copolymerization of MMA and BA stabilized with ASR was studied by Peck et al. [103] using redox initiators able to generate radicals with different characteristics. The pair *t*-butyl hydroperoxide/ascorbic acid (TBHP/AsAc) yields uncharged hydrophobic radicals and the pair potassium persulfate/sodium bisulfite (KPS/NaBs) produces anionic hydrophilic radicals, both in the aqueous phase. They observed that using TBHP/AsAc, the presence of hairy layer of ASR around

the polymer particle reduced the entry rate, leading to substantially lower polymerization rate per particle (R_{pp}) than that obtained with classical anionic surfactants. The authors attributed this reduction to the diffusional limitations and/or to the formation of no reactive tertiary radicals in the ASR backbone by hydrogen abstraction. They observed that for the miniemulsion copolymerization initiated with KPS/NaBs, the use of ASR also led to a lower R_{pp}. In this case, they found two additional effects which were operative. First, the proper use of ASRs requires that the pH of the medium should be higher than the pK_a of the carboxylic groups. This high pH can reduce the radical generation rate from the initiator system. Second, the electrostatic repulsion between the anionic entering radical and the anionic groups of the ASR.

1.5 Main objectives

The goal of this thesis is to gain understanding on the kinetics and nucleation mechanism in emulsion and miniemulsion polymerization stabilized with ASRs of low molecular weight (number average molecular weight around 5000 $gmol^{-1}$) and acid number lower than that of the commercial ASRs (which have values around 200 $mg_{KOH}\, g_{ASR}^{-1}$).

1.6 Scope of the thesis

In this Thesis, different ASRs have been produced using methacrylates and/or acrylates as non-acidic monomers and methacrylic or acrylic acids as acidic monomers. Random ASR copolymers were synthesized in emulsion polymerization carried out at low pH to make the ASR insoluble in water.

In Chapter 2, a preliminary screening of MMA/BMA/MAA ASRs (varying the content of acid of the ASR backbone) for their use as sole stabilizer in emulsion polymerization was carried out. The colloidal behavior of these surfactants was also studied.

In Chapter 3, the mechanisms responsible to reduce the radical entry in ASR stabilized systems were investigated. It was found that the mechanism responsible for the reduction of the rate of radical entry depends on the type of ASR used (prone or not prone to suffer hydrogen abstraction), the type of radical produced from the initiator (charged or uncharged, oxygen centered or carbon centered), the phase where the radical are produced (aqueous or oil phase) and the hydrophobicity of the monomer.

In Chapter 4 a new family of low acid number ASRs (~100 $mg_{KOH}g_{ASR}^{-1}$) containing methyl methacrylate (MMA), butyl methacrylate (BMA), methacrylic acid (MAA) and acrylamide (AM) were synthesized and characterized. The effect of the MMA/BMA ratio and MAA content of the ASRs as well as the ASR concentration on the emulsion and

miniemulsion polymerizations was investigated. Different monomer systems such as MMA/BMA, S and MMA were used throughout this chapter to investigate their effect on particle nucleation and kinetics of the polymerizations.

In Chapter 5, which was carried out at Nuplex-Resins labs in The Netherlands, a relatively hydrophobic ASR able to form aggregates was synthesized. This very low acid number (50 $mg_{KOH}g_{ASR}^{-1}$) ASR containing MMA, BA, MAA and dimethyl acrylamide (DMAM) was shown capable of forming aggregates in presence of different monomers (S, BA and MMA). These aggregates were used as seeds to synthesize high solids content latexes in a two steps polymerization process. In addition, small particle size high solids content latexes were also obtained by using more hydrophobic ASRs synthesized by substituting part of MMA for lauryl methacrylate (LMA).

Appendices I and II provide a detailed description of the emulsion and miniemulsion polymerizations respectively.

1.7 References

1. Asua, J. M., Ed., *Polymeric dispersions: principles and applications*. Kluwer Academic Publishers: Netherlands, 1997; Vol. 335, p vii.

2. Urban, D.; Takamura, K., Eds., *Polymer dispersions and their industrial applications*. Wiley-VCH Weinheim, 2002; p i-xviii.

3. Gharieh, A.; Mahdavian, A. R.; Salehi-Mobarakeh, H. *Iranian Polymer Journal* **2014,** 23, (1), 27-35.

4. Vincent, B. *Advances in Colloid and Interface Science* **1974,** 4, (2), 193-277.

5. Kästner, U. *Colloids and Surfaces A: Physicochemical and Engineering Aspects* **2001,** 183, 805-821.

6. Schmidt-Thümmes, J.; Schwarzenbach, E.; Lee, D. I., Applications in the paper industry. In *Polymer dispersions and their industrial applications*, Urban, D.; Takamura, K., Eds. Wiley-VCH Weinheim: 2002; pp 75-101.

7. Anquetil, J. Y.; Vu, C., Latex à base d'acétate de vinyle. In *Les latex synthétiques: élaboration, propriétés, applications*, Daniel, J.-C.; Pichot, C., Eds. Lavoisier: Paris, 2006; pp 365-386.

8. Plessis, C.; Arzamendi, G.; Leiza, J. R.; Schoonbrood, H. A. S.; Charmot, D.; Asua, J. M. *Macromolecules* **2001,** 34, (15), 5147-5157.

9. Arevalillo, A.; do Amaral, M.; Asua, J. M. *Industrial & Engineering Chemistry Research* **2006,** 45, (9), 3280-3286.

10. Plastic Europe *Plastics - the Facts 2011. An analysis of European plastics production, demand and recovery for 2010.* PlasticsEurope, EuPC (the European Plastics Converters), EuPR (the European Plastics

Recyclers) and EPRO (the European Association of Plastics Recycling and Recovery Organisations). 2014/2015; pp 5-13.

11. Urban, D.; Takamura, K., In *Polymer dispersions and their industrial applications*, Urban, D.; Takamura, K., Eds. Wiley-VCH Weinheim, 2002; pp 1–14.

12. Lee, D. I., Latex aplications in paper coating. In *Polymeric dispersions: principles and applications*, Asua, J. M., Ed. Kluwer Academic Publishers: Netherland, 1997; Vol. 335, pp 497-513.

13. Pichot, C.; Delair, T.; Elaïssari, A., Polymer colloids for biomedical and pharmaceutical applications. In *Polymeric dispersions: principles and applications*, Asua, J. M., Ed. Kluwer Academic publishers: Netherlands 1997; Vol. 335.

14. Barandiaran, M. J.; de la Cal, J. C.; Asua, J. M., Emulsion polymerization. In *Polymer reaction engineering*, Asua, J. M., Ed. John Wiley & Sons: 2008; pp 233-272.

15. Asua, J. M. *Journal of Polymer Science Part A: Polymer Chemistry* **2004,** 42, (5), 1025-1041.

16. Asua, J. M. *Progress in Polymer Science* **2014,** 39, (10), 1797-1826.

17. Harkins, W. D. *Journal of the American Chemical Society* **1947,** 69, (6), 1428-1444.

18. Priest, W. *The Journal of Physical Chemistry* **1952,** 56, (9), 1077-1082.

19. Fitch, R. M.; Tsai, C. H., Particle formation in polymer colloids, III: Prediction of the number of particles by a homogeneous nucleation theory. In *Polymer Colloids*, Fitch, R. M., Ed. Plenun Press: New York, 1971; pp 73-102.

20. Ugelstad, J.; Hansen, F. K. *Rubber Chemistry and Technology* **1976,** 49, (3), 536-609.

21. Feeney, P. J.; Napper, D. H.; Gilbert, R. G. *Macromolecules* **1987,** 20, (11), 2922-2930.

22. Ballard, N.; Urrutia, J.; Eizagirre, S.; Schäfer, T.; Diaconu, G.; de la Cal, J. C.; Asua, J. M. *Langmuir* **2014,** 30, (30), 9053-9062.

23. Friis, N.; Hamielec, A. E. In *Gel effect in emulsion polymerization of vinyl monomers*, ACS Symp. Ser, 1976; pp 82-91.

24. Asua, J. M. *Macromolecules* **2003,** 36, (16), 6245-6251.

25. Smith, W. V.; Ewart, R. H. *The Journal of Chemical Physics* **1948,** 16, (6), 592-599.

26. Agirre, A.; de las Heras-Alarcón, C.; Wang, T.; Keddie, J. L.; Asua, J. M. *ACS Applied Materials & Interfaces* **2010,** 2, (2), 443-451.

27. Fonseca, G. E.; McKenna, T. F.; Dubé, M. A. *Chemical Engineering Science* **2010,** 65, (9), 2797-2810.

28. Lopez, A.; Degrandi-Contraires, E.; Canetta, E.; Creton, C.; Keddie, J. L.; Asua, J. M. *Langmuir* **2011,** 27, (7), 3878-3888.

29. Udagama, R.; Degrandi-Contraires, E.; Creton, C.; Graillat, C.; McKenna, T. F.; Bourgeat-Lami, E. *Macromolecules* **2011,** 44, (8), 2632-2642.

30. Sun, Z.; Luo, Y. *Soft Matter* **2011,** 7, (3), 871-875.

31. Bhadra, S.; Singha, N. K.; Khastgir, D. *Journal of Chemical Engineering and Materials Science* **2011,** 2, (1), 1-11.

32. Nabih, N.; Herrmann, U.; Glasser, G.; Lieberwirth, I.; Landfester, K.; Taden, A. *Progress in Organic Coatings* **2013,** 76, (4), 555-562.

33. Aguirre, M.; Paulis, M.; Leiza, J. R. *Journal of Materials Chemistry A* **2013,** 1, (9), 3155-3162.

34. Harun, N. A.; Horrocks, B. R.; Fulton, D. A. *Nanoscale* **2011,** 3, (11), 4733-4741.

35. Abdou, L. A. W.; El-Molla, M. M.; Hakeim, O. A.; El-Gammal, M. S.; Shamey, R. *Industrial & Engineering Chemistry Research* **2013,** 52, (6), 2195-2200.

36. Moreno, M.; Goikoetxea, M.; Barandiaran, M. J. *Journal of Polymer Science Part A: Polymer Chemistry* **2012,** 50, (22), 4628-4637.

37. Lorenz, S.; Hauser, C. P.; Autenrieth, B.; Weiss, C. K.; Landfester, K.; Mailänder, V. *Macromolecular Bioscience* **2010,** 10, (9), 1034-1042.

38. Tautzenberger, A.; Lorenz, S.; Kreja, L.; Zeller, A.; Musyanovych, A.; Schrezenmeier, H.; Landfester, K.; Mailänder, V.; Ignatius, A. *Biomaterials* **2010,** 31, (8), 2064-2071.

39. Ramos, J.; Forcada, J. *Langmuir* **2011,** 27, (11), 7222-7230.

40. Baier, G.; Musyanovych, A.; Mailänder, V.; Landfester, K. *The International Journal of Artificial Organs* **2012,** 35, (1), 77-83.

41. Zhang, J.; Sun, W.; Bergman, L.; Rosenholm, J. M.; Lindén, M.; Wu, G.; Xu, H.; Gu, H.-C. *Materials Letters* **2012,** 67, (1), 379-382.

42. Fonseca, L. B.; Nele, M.; Volpato, N. M.; Seiceira, R. C.; Pinto, J. C. *Macromolecular Reaction Engineering* **2013,** 7, (1), 54-63.

43. Sankarakumar, N.; Tong, Y. W. *Journal of Materials Chemistry B* **2013,** 1, (15), 2031-2037.

44. Unzué, M. J.; Asua, J. M. *Journal of Applied Polymer Science* **1993,** 49, (1), 81-90.

45. Guyot, A.; Chu, F.; Schneider, M.; Graillat, C.; McKenna, T. F. *Progress in Polymer Science* **2002,** 27, (8), 1573-1615.

46. do Amaral, M.; Asua, J. M. *Journal of Polymer Science Part A: Polymer Chemistry* **2004,** 42, (17), 4222-4227.

47. Chou, Y. J.; El-Aasser, M. S.; Vanderhoff, J. W. *Journal of Dispersion Science and Technology* **1980,** 1, (2), 129-150.

48. Ugelstad, J.; El-Aasser, M.; Vanderhoff, J. *Journal of Polymer Science: Polymer Letters Edition* **1973,** 11, (8), 503-513.

49. Asua, J. M. *Progress in Polymer Science* **2002,** 27, (7), 1283-1346.

50. Antonietti, M.; Landfester, K. *Progress in Polymer Science* **2002,** 27, (4), 689-757.

51. Schork, F. J.; Luo, Y.; Smulders, W.; Russum, J. P.; Butté, A.; Fontenot, K., Miniemulsion polymerization. In *Polymer Particles*, Okubo, M., Ed. Springer Heidelberg, 2005; Vol. 175, pp 129-255.

52. Higuchi, W.; Misra, J. *Journal of Pharmaceutical Sciences* **1962,** 51, (5), 459-466.

53. Tang, P. L.; Sudol, E. D.; Adams, M.; El-Aasser, M. S.; Asua, J. M. *Journal of Applied Polymer Science* **1991,** 42, (7), 2019-2028.

54. Lim, M.-S.; Chen, H. *Journal of Polymer Science Part A: Polymer Chemistry* **2000,** 38, (10), 1818-1827.

55. Choi, Y. T.; El-Aasser, M. S.; Sudol, E. D.; Vanderhoff, J. W. *Journal of Polymer Science: Polymer Chemistry Edition* **1985,** 23, (12), 2973-2987.

56. Alduncin, J. A.; Forcada, J.; Asua, J. M. *Macromolecules* **1994,** 27, (8), 2256-2261.

57. Miller, C. M.; Blythe, P. J.; Sudol, E. D.; Silebi, C. A.; El-Aasser, M. S. *Journal of Polymer Science Part A: Polymer Chemistry* **1994,** 32, (12), 2365-2376.

58. Reimers, J.; Schork, F. J. *Journal of Applied Polymer Science* **1996,** 59, (12), 1833-1841.

59. Chern, C. S.; Chen, T. J.; Liou, Y. C. *Polymer* **1998,** 39, (16), 3767-3777.

60. Lorimer, J. P.; Mason, T. J., Ultrasonics. In *Sonochemistry: Theory, Applications and Uses of Ultrasound in Chemistry*, Lorimer, J. P.; Mason, T. J., Eds. Ellis Horwood: Chichester, 1988; p 27.

61. Rodriguez, V. S.; El-Aasser, M. S.; Asua, J. M.; Silebi, C. A. *Journal of Polymer Science Part A: Polymer Chemistry* **1989,** 27, (11), 3659-3671.

62. Fontenot, K.; Schork, F. J. *Industrial & Engineering Chemistry Research* **1993,** 32, (2), 373-385.

63. Manea, M.; Chemtob, A.; Paulis, M.; de la Cal, J. C.; Barandiaran, M. J.; Asua, J. M. *AIChE Journal* **2008,** 54, (1), 289-297.

64. Landfester, K.; Bechthold, N.; Tiarks, F.; Antonietti, M. *Macromolecules* **1999,** 32, (16), 5222-5228.

65. Chern, C.-S.; Liou, Y.-C. *Polymer* **1999,** 40, (13), 3763-3772.

66. Masa, J. A.; López de Arbina, L.; Asua, J. M. *Journal of Applied Polymer Science* **1993,** 48, (2), 205-213.

67. Kitzmiller, E. L.; Miller, C. M.; David Sudol, E.; El-Aasser, M. S. In *Miniemulsion polymerization: an approach to control copolymer composition*, Macromolecular Symposia, 1995; Wiley Online Library: pp 157-168.

68. El-Aasser, M. S.; Miller, C. M., Preparation of latexes using miniemulsions. In *Polymeric dispersions: principles and applications*, Asua, J. M., Ed. Kluwer Academic Publishers: Netherlands, 1997; Vol. 335, pp 109-126.

69. Becher, P., *Emulsions: Theory and Practice*. Reinhold Publishing Crop.: New York, 1965.

70. Hansen, F. K., Is There Life Beyond Micelles? Mechanisms of Latex Particle Nucleation. In *Polymer latexes: Preparation, Characterization, and Applications*, Daniels, E. S.; Sudol, E. D.; El-Aasser, M. S., Eds. American Chemical Society: Washington, DC 1992; Vol. 492, pp 12-27.

71. Gilbert, R. G., *Emulsion Polymerization: A Mechanistic Approach*. Academic Press: San Diego, 1995.

72. Hunter, R. J., Charge and potential distribution at interface. In *Zeta Potential in Colloid Science: Principles and Applications*, Hunter, R. J., Ed. Academic Press: San Diego, 2013; pp 11-58.

73. Napper, D. H., *Polymeric stabilization of colloidal dispersions*. Academic Press London, 1983; Vol. 7.

74. Stevens; Langers; Parry; Rollison. Alkali soluble resin polymer and method of preparing the same. GB 1107249 (A) Johnson & Son S. C., 1968.

75. Kaminski, L. A.; Brafford, R. A.; Dragner, L. R. Ethylenically unsaturated carboxyl-free/carboxyl-containing copolymers. CA 814528 A, Johnson & Son Inc S. C., 1969.

76. Tsaur, S. L. Resin-fortified emulsion polymers and methods of preparing the same. EP 0257567 A2, Johnson & Son, Inc., S.C., 1988.

77. Kiehlbauch, R. A.; Tsaur, S. L. Resin-fortified emulsion polymers and methods of preparing the same. US 4839413 A, S.C. Johnson & Son, Inc., 1989.

78. Matyjaszewski, K.; Miller, P. J.; Shukla, N.; Immaraporn, B.; Gelman, A.; Luokala, B. B.; Siclovan, T. M.; Kickelbick, G.; Vallant, T.; Hoffmann, H. *Macromolecules* **1999,** 32, (26), 8716-8724.

79. Zhang, X.; Matyjaszewski, K. *Macromolecules* **1999,** 32, (6), 1763-1766.

80. Hawker, C. J. *Journal of the American Chemical Society* **1994,** 116, (24), 11185-11186.

81. Castan, P.; Switzerland, Z. Process of preparing synthetic resins. US 2324483 A, Castan, P., 1943.

82. Castan, P. Production of thermosetting artificial resins US 250225, Castan, P., 1939.

83. Greenlee, S. O. Alkali soluble resins and compositions containing the same. US 2890189 A, Johnson & Son, Inc., Racine, Wis., 1959.

84. Lee, D. Y.; Kim, J. H. *Journal of Applied Polymer Science* **1998,** 69, (3), 543-550.

85. Kato, S.; Suzuki, K.; Nomura, M. *e-Polymers* **2005,** 5, (1), 338-352.

86. Hwu, H.-D.; Lee, Y.-D. *Polymer* **2000,** 41, (15), 5695-5705.

87. Kato, S.; Sato, K.; Maeda, D.; Nomura, M. *Colloids and Surfaces A: Physicochemical and Engineering Aspects* **1999,** 153, (1), 127-131.

88. Sato, T. *Journal of Coatings Technology* **1993,** 65, (825), 113-121.

89. Piirma, I.; Lenzotti, J. R. *British Polymer Journal* **1989,** 21, (1), 45-51.

90. Jialanella, G. L.; Firer, E. M.; Piirma, I. *Journal of Polymer Science Part A: Polymer Chemistry* **1992,** 30, (9), 1925-1933.

91. Jialanella, G. L.; Piirma, I. *Journal of Applied Polymer Science* **1991,** 42, (5), 1423-1431.

92. Wang, S.; Qiang, Y.; Zhang, Z.; Wang, X. *Colloids and Surfaces A: Physicochemical and Engineering Aspects* **2006,** 281, (1), 156-162.

93. Lee, D. Y.; Kim, J. H. *Journal of Polymer Science Part A: Polymer Chemistry* **1998,** 36, (16), 2865-2872.

94. Ringsdorf, H.; Venzmer, J.; Winnik, F. M. *Macromolecules* **1991,** 24, (7), 1678-1686.

95. Coen, E. M.; Lyons, R. A.; Gilbert, R. G. *Macromolecules* **1996,** 29, (15), 5128-5135.

96. Hwu, H.-D.; Lee, Y.-D. *Journal of Polymer Research* **2000,** 7, (2), 115-123.

97. Kuo, P.-L.; Chen, C.-J. *Journal of Polymer Science Part A: Polymer Chemistry* **1993,** 31, (1), 99-111.

98. do Amaral, M.; Asua, J. M. *Macromolecular Rapid Communications* **2004,** 25, (22), 1883-1888.

99. do Amaral, M.; de Brouwer, H.; Van Es, S.; Asua, J. M. In *Novel Industrial Application of Miniemulsion Polymerization–Use of Alkali Soluble Resin as Surfactant in Miniemulsion Polymerization*, Macromolecular Symposia, 2005; Wiley Online Library: pp 167-176.

100. Emelie, B.; Pichot, C.; Guillot, J. *Macromolecular Chemistry and Physics. Supplement* **1985**, (10-11), 43-57.

101. Unzueta, E.; Forcada, J. *Polymer* **1995,** 36, (5), 1045-1052.

102. Özdeğer, E.; Sudol, E. D.; El-Aasser, M. S.; Klein, A. *Journal of Polymer Science Part A: Polymer Chemistry* **1997,** 35, (17), 3813-3825.

103. Peck, A. N.; Asua, J. M. *Macromolecules* **2008,** 41, (21), 7928-7932.

Chapter 2: Screening ASRs as emulsifiers

Outline

2.1 Introduction

ASRs are often synthesized in solution polymerization [1-4]. This process is convenient form the point of view of the homogeneity of the ASR produced, but it presents serious environmental and practical drawbacks (transferring of the ASR from the solvent phase to the water phase). Therefore, in this Chapter the synthesis of MMA/BMA/MAA ASRs in emulsion polymerization was explored. Both batch and semicontinuous processes were employed. The suitability of these ASRs to stabilize batch emulsion polymerization of two monomers with widely different water solubilities (S and MMA) was assessed.

2.2 Synthesis of ASRs

Technical monomers methyl methacrylate (MMA, Quimidroga), butyl methacrylate (BMA, Aldrich) and methacrylic acid (MAA, Aldrich) were all used as received. Ammonium persulfate (APS, Panreac) and sodium lauryl sulfate (SLS, Aldrich) were used as initiator and emulsifier, respectively. 2-mercaptoethanol (M-Et, Aldrich) and 1-octanethiol (OcT, Aldrich) were employed as water soluble and oil soluble chain transfer agents. Sodium bicarbonate ($NaHCO_3$, Aldrich) was used as buffer.

The amount of acidic monomer needed to produce ASRs with an acid number (N_{Ac} expressed as $mg_{KOH}g_{ASR}^{-1}$) is given by:

$$N_{Ac} = 1000 \frac{Ac_{(g)}}{ASR_{(g)}} \frac{M_{KOH}}{M_{Ac}} \quad (1)$$

where $Ac_{(g)}$ is the amount in grams of acidic monomer (MAA) in the ASR; $ASR_{(g)}$ is the total amount in grams of ASR and M_{KOH} and M_{Ac} are the molecular weights of KOH and acidic monomer, respectively. In order to maintain the N_{Ac} below $100 mg_{KOH}/g_{ASR}$, the weight fraction of MAA in the ASR should be lower than 15wt%. Therefore, 14wt% of MAA was used ($N_{Ac} = 91 mg_{KOH}/g_{ASR}$). The MMA/BMA monomer ratio was 3/4 wt/wt. Then, the composition of the ASR synthesized was: 14wt% MAA, 37wt% MMA and 49wt% BMA.

2.2.1 Synthesis of ASRs by means of batch emulsion polymerization

The synthesis of ASR by means of batch emulsion polymerization was carried out in a 1L jacketed glass reactor equipped with reflux condenser, stainless-steel stirrer and nitrogen inlet using the formulation given in Table 1. The pre-emulsion of monomers (30wt% solids content), emulsifier (SLS), water and the oil-soluble chain transfer agent (OcT which will be referred as CTA_{Oil}) was added to the reactor, and then heated to 70ºC under stirring (180 rpm) and nitrogen atmosphere. Polymerization was started adding the initiator (APS) as a shot. The polymerization was maintained during 3 hours to obtain total conversion.

In the formulation shown in Table 1, the CTA_{Oil} concentration was varied (1.5; 3 and 6wt% with respect to the monomers). At the same time, the SLS was varied in order to check any possible effect on the molecular weight of the ASRs ([SLS] affects particle size, which influences the frequency of radical entry and exit, and hence the molecular weight of the polymer formed in the particles), which in turn may affect the final solubility of the chains in alkali medium. The amounts of SLS used were 2, 4, 6 and 8wt% with respect to the monomers.

Table 1: Formulation used in batch emulsion polymerization

Ingredient	**Total charge (g)**		**Concentration (wt%)**	
MMA	180	66.6	30	37
BMA		88.2		49
MAA		25.2		14
SLS	3.6 / 7.2 / 10.8 / 14.4		2 / 4 / 6 / 8 [(a)]	
CTA_{Oil}	2.7 / 5.4 / 10.8		1.5 / 3 / 6 [(a)]	
APS	1.80		1 [(a)]	
$NaHCO_3$	1.33		0.74 [(a)]	
Water	420		70	
(a) wt% with respect to the monomers				

Table 2 shows that for all the reactions, the conversion was complete and the final pH higher than 4. The molecular weights decreased with the CTA_{Oil} concentration and only for the smallest CTA_{Oil} concentration they showed the expected decrease with particle size. This suggests that for higher

CTA_{Oil} concentration, chain transfer to CTA was the main termination event of the growing polymer chains.

Table 2: ASRs obtained varying the concentration of CTA_{Oil} and SLS

ASR		X (-)	dp (nm)	pH (-)	$\bar{M}_n$ (g/mol)	$\bar{M}_w$ (g/mol)	$Đ$ (-)	Transparency of neutralized latex
1.5% CTA_{Oil}	2%SLS	1.0	104	4.7	27000	36700	1.4	50-60%
	4%SLS	1.0	91	4.7	34000	50000	1.5	50-60%
	6%SLS	1.0	94	4.8	32700	49000	1.5	60-70%
	8%SLS	1.0	99	4.7	29500	47300	1.6	60-70%
3.0% CTA_{Oil}	2%SLS	1.0	118	5.0	5500	12200	2.2	90-100%
	4%SLS	1.0	131	4.6	5400	11600	2.1	90-100%
	6%SLS	1.0	156	4.6	4600	9800	2.1	90-100%
	8%SLS	1.0	174	4.7	4800	10300	2.1	90-100%
6.0% CTA_{Oil}	2%SLS	1.0	138	4.7	2100	4600	2.2	90-100%
	4%SLS	1.0	192	4.2	2200	4500	2.0	90-100%
	6%SLS	1.0	204	4.4	2100	4300	2.0	90-100%
	8%SLS	1.0	209	4.8	2100	4500	2.1	90-100%

The particle size measured by DLS (dynamic light scattering) increased with both CTA_{Oil} and (very surprisingly) with SLS for 3 and 6wt% of CTA_{Oil}. The particle sizes obtained with high concentrations of CTA_{Oil} and SLS were much larger (175-200nm) than what is commonly obtained with this SLS concentration for more hydrophobic monomer mixtures and 30wt% solids content. Therefore, something special occurred in these polymerizations.

Taking into account that what is measured in DLS is the hydrodynamic diameter, one may speculate that the observed differences are at least in part due to different swelling of the polymer particles. Swelling of the carboxyl rich copolymer with water is expected to increase as the content of carboxyl groups increases and the molecular weight of the polymer decreases. This second effect, in agreement with the experimental findings, would lead to larger particle sizes for increasing CTA_{Oil} concentrations. The expected effect of the increase of the SLS concentration is an increase in the number of particles, which will enhance the incorporation of the acidic monomer into the copolymer, which in turn, will increase swelling and the observed particle size.

However, although these effects may be operative, material balances show that this cannot be the only reason. Thus, if the unswollen volume of a particle formed with 8wt% SLS is 100 nm (taken from the size measured with 1.5wt% of CTA_{Oil} and 8wt% of SLS), but the observed size is 209nm, this is a 8 times increase in volume, namely, there is no water in the system for such a huge increase. Taking this into account, the following (admittedly highly speculative) mechanism is proposed. Particles are nucleated by micellar and heterogeneous nucleation and stabilized by the SLS present in the system. The number of particles nucleated increases with the SLS concentration. These particles swell according to the MAA content of the copolymer (that increases with the number of particles, i.e., with SLS concentration) and the molecular weight of the polymer (that decreases with CTA_{Oil} concentration). The

particle-particle distance in the high swollen cases (high concentration of SLS and CTA_{Oil}) decreases and coagulation occurs leading to large particles.

Table 2 also includes the transparency of the neutralized latex, which is related to the solubility of the neutralized ASRs. It can be seen that the ASRs synthesized with 1.5wt% of CTA_{Oil} did not show good solubility, whereas those prepared with higher concentrations of CTA_{Oil} were basically soluble in water. In addition, the ASR obtained with 3wt% of CTA_{Oil} had the intended molecular weight ($\overline{M}_n$). Figure 1 shows that no effect of the SLS concentration on molecular weight was observed.

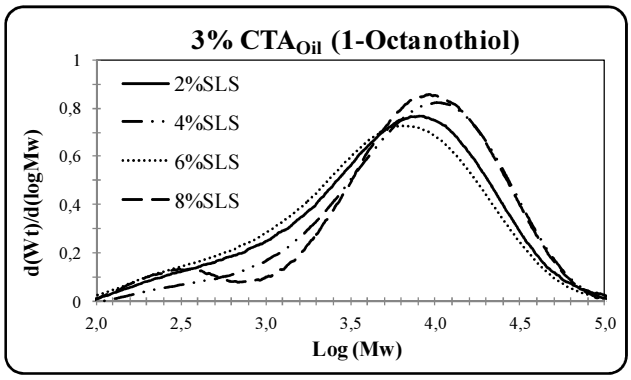

Figure 1: Molecular weight distributions with different wt% of SLS

2.2.2 Synthesis of ASRs by means of semicontinuous emulsion polymerization

2.2.2.1 Oil-soluble chain transfer agent

The synthesis of ASRs by means of semicontinuous emulsion polymerization was carried out in a 1L jacketed glass reactor equipped with reflux condenser, stainless-steel stirrer (180rpm) and nitrogen inlet. The formulation given in Table 3 was used. The APS was added as a shot when the initial charge reached 70ºC and 20min later, the rest of the recipe was fed during 3 hours ($R_{feed} \approx 3.14$ g min^{-1}).

Table 3: Formulation used to synthesize ASRs by means of semicontinuous emulsion polymerization

Ingredient	**Initial charge (g)**		**Feed (g)**	
MMA	25.50	9.435	229.50	84.915
BMA		12.495		112.455
MAA		3.570		32.130
CTA_{Oil}	0.77		6.88	
SLS	0 / 0.51 / 2.04		0 / 2.04 / 8.16	
APS	2.55		0	
$NaHCO_3$	1.88		0	
Water	214.20		380.80	

Table 4 shows the particle sizes obtained with different concentrations of SLS (wt% with respect to the monomers). It can be seen that in this case, particle size substantially decreased with SLS concentration. The difference with respect to the batch process is that in the initial charge, particle nucleation occurred at very low solids content (about 12wt%) and under these conditions, coagulation is unlikely. These results support the mechanism proposed above.

Table 4: Effect of SLS concentration on the solubility of ASRs

wt% SLS	**dp (nm)**	**Neutralization (pH~8.5)**
0	800	Insoluble after 1 week
1	180	Soluble in aprox. 30 hours
4	85	Soluble instantaneously

Table 4 also shows that the ASRs presented a very different behavior upon neutralization. In particular, the ASR obtained with 4wt% of SLS become soluble immediately after neutralization, the ASR obtained with 1wt% needed approximately 30 hours, and the one prepared without SLS could not be solubilized after 1 week. These behavior may be due to the differences in MAA incorporation or/and the different particle size.

Changes in MAA content in the polymer backbone might be due to the expected higher incorporation of MAA to smaller particles. If this is the case, the MAA content in the serum should increase with the particle size. In order to check this point, non neutralized latexes (pH=3) were centrifugated at 20,000rpm for 1 hour at 20ºC and the serum and the polymer rich phases

separated. This serum is expected to contain the non adsorbed water-soluble polymer. It can be argued that the water soluble polymer may be surface active and hence be adsorbed on the polymer particles. As the kinetics of desorption is very slow [5] the adsorbed chains will not be in the serum and hence the fraction of MAA in the water soluble polymer underestimated. The latex were brought to pH=8 for 24hours and then subjected to the same centrifugation process. The serum collected this way likely contained a fraction of polymer chains that are not soluble at pH=3, but they serve to establish an upper limit. The MAA content of the serum was determined by conductomeric titration [6] with 0.1N NaOH (a feed rate of 0.2ml min^{-1} was used). Previously, all the carboxyl groups were protonated by adding HCl until pH=2.

Figure 2 and Table 5 present the results of the conductometric titration versus NaOH volume per gram of ASR. The first decrease of the conductivity corresponded of the H^+ from de HCl; the relatively flat part is the consequence of the neutralization of the carboxyl groups and the final increase is the accumulation of NaOH. Therefore, the difference between the points at which the slope of the line changes abruptly is a measure of the MAA units of the serum. For the serum collected from the latex at pH=3, it can be seen that the amount of MAA in the serum was maximum (24.9%) for the ASR prepared without SLS and decreased with the SLS concentration until reaching a value of 1.3wt% for 4wt% SLS. This means that the decrease in particle size reduced the amount of water soluble polymer at pH=3.

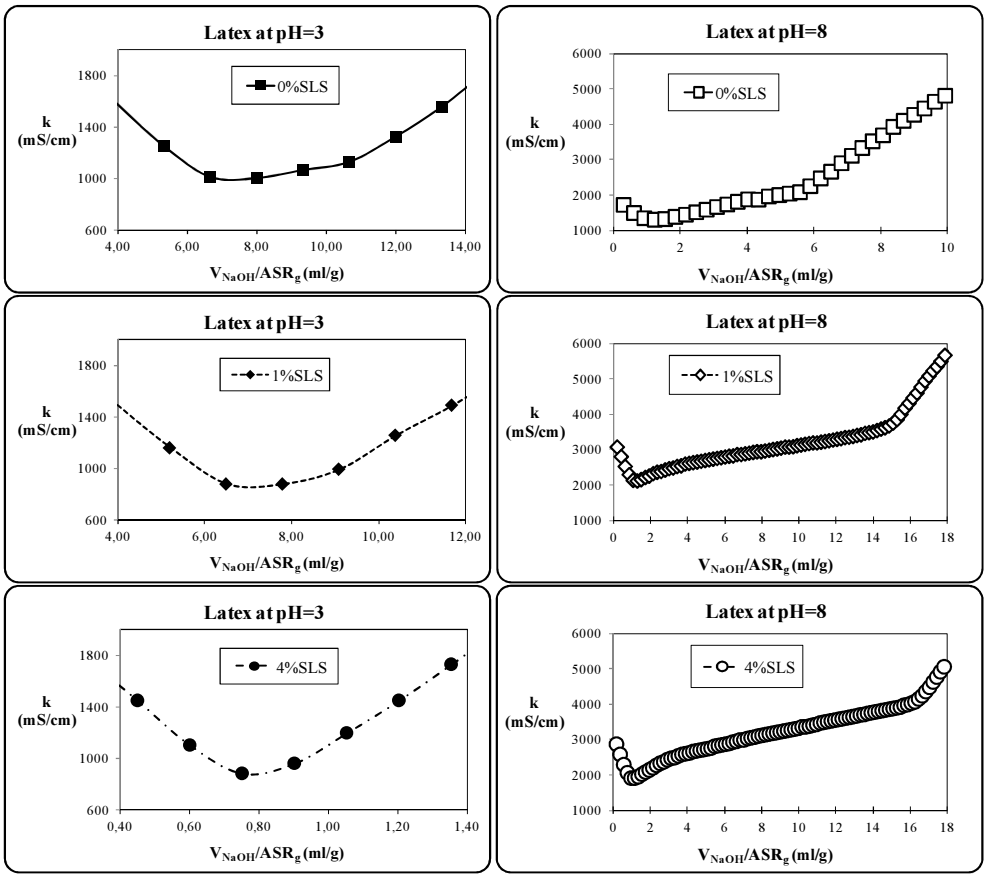

Figure 2: Conductometric titration of the serum. Left: serum from latex at pH=3, and right: serum from latex at pH=8

The pH of the latex had a relatively small effect on the fraction of the MAA in the serum for the latex prepared without SLS. This means that only a small fraction of soluble polymer was adsorbed on the surface. Therefore, for this latex, most of MAA was buried in the polymer particles and the size of the particles makes difficult the access to this MAA. It may be argued that the size

effect is reinforced by the decrease in the MAA concentration caused by the about 25% that forms part of the serum.

Table 5: Effect of the concentration of SLS on the fraction of MAA in the serum

wt % SLS	Latex at pH=3			Latex at pH=8		
	$V_{NaOH}/ASR_{(g)}$ (ml/g)	$Ac_g/ASR_{(g)}$ (g/g)	Acid (wt%)	$V_{NaOH}/ASR_{(g)}$ (ml/g)	$Ac_g/ASR_{(g)}$ (g/g)	Acid (wt%)
0	4.06	0.0349	24.9	4.62	0.0398	28.4
1	2.46	0.0212	15.1	13.97	0.1203	85.9
4	0.21	0.0018	1.3	15.81	0.1361	97.2

For the latexes synthesized with SLS, it was not possible to estimate the fraction of soluble polymer adsorbed on the particles because at pH=8 they basically dissolved. Nevertheless, the latex synthesized with 4wt% of SLS was the only one that underwent a fast dissolution.

2.2.2.2 Oil-soluble and water-soluble CTAs

Because MAA is highly water soluble, it may occur that by only using an oil-soluble CTA, the length of the chains formed in the aqueous phase can not be controlled. Therefore, oil-soluble and water-soluble CTAs were used in this section.

The semicontinuous emulsion copolymerizations were carried out using the formulation in Table 6 and the procedure used in the previous section.

Table 6: Final recipe of ASRs with and without water soluble CTA

Components	**ASR_A**		**ASR_B**	
MMA	30wt%	37wt%	30wt%	37wt%
BMA		49wt%		49wt%
MAA		14wt%		14wt%
CTA_{Oil}	3wt%*			
CTA_{Water}	0wt%*		1wt%*	
$NaHCO_3$	0.74wt%*			
SLS	4wt%*			
APS	1wt%*			
H_2O	70wt%			
* wt% with respect to the monomers				

Figures 3 and 4 present the evolution of the monomer conversion and the number of particles, respectively. In both, the feeding time is marked by two lines. It can be seen that the processes were carried out under starved conditions and the number of particles was similar for both ASRs.

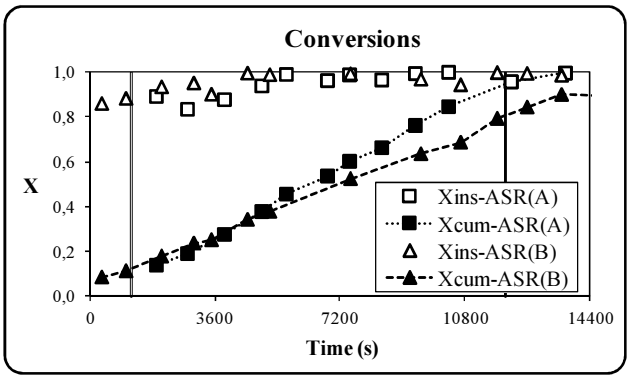

Figure 3: Instantaneous and cumulative conversions of the ASRs synthesized with and without water-soluble CTA

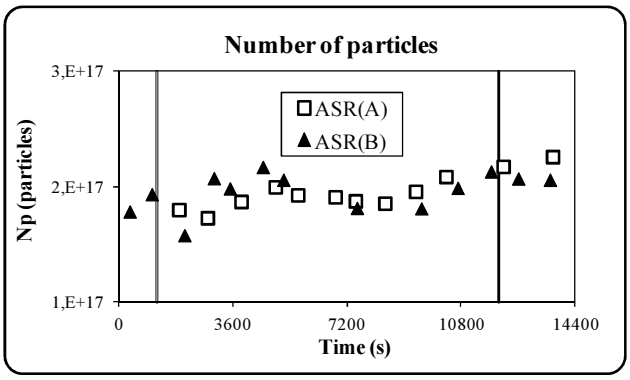

Figure 4: Number of particles of the ASRs synthesized with and without water-soluble CTA

The effect of the CTA_{Water} on the molecular weight distribution of the ASRs is presented in Figure 5. It can be seen that the molecular weight slightly decreased when CTA_{Water} was used. In addition, the shapes of the curves were very similar.

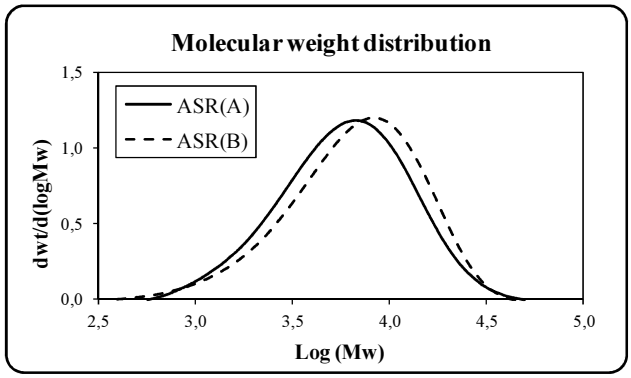

ASR_A

$\overline{M}_n$= 4600gmol^{-1}
$\overline{M}_w$=8500gmol^{-1}
$Đ$=1.85

ASR_B

$\overline{M}_n$= 4300gmol^{-1}
$\overline{M}_w$=7600gmol^{-1}
$Đ$=1.77

Figure 5: Molecular weight distributions and average molecular weights for ASR_A and ASR_B.

The CMCs of ASR_A and ASR_B were measured using a tensiometer (SIGMA KSV 70). Figure 6 shows the effect of the concentration of ASRs on the surface tension for ASR_A and ASR_B. It can be seen that the surface tension (γ) decreased with ASR concentration and that beyond a certain concentration the surface tension was roughly constant. The decrease is caused by the adsorption of surface tension species on the water-air interface (Gibbs adsorption equation) and the point at which γ was constant marks the saturation of the water-air interface. Beyond this point, which is called critical micellar concentration (CMC), the additional surfactant forms aggregates (micelles).

It can be seen that the ASRs presented a completely different behavior. ASR_A showed a rather standard curve with a CMC about 0.54gL^{-1}. It is worth pointing out that because ASRs had a distribution of chain lengths and compositions they did not show a sharp break point at the CMC.

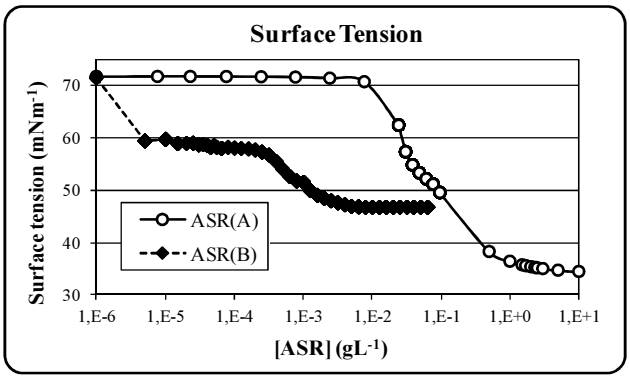

Figure 6: Surface tension vs. ASR concentration for both ASRs, with CTA_{Water} (ASR_B) and without CTA_{Water} (ASR_A)

ASR_B showed a peculiar behavior, with a significant decrease in γ at very low concentrations followed by a plateau and the final decrease to the CMC. The CMC was substantially lower than that of ASR_A and the final γ was relatively high ($47mNm^{-1}$). A possible explanation for the initial decrease to $60mNm^{-1}$ is that the MAA rich small chains, which have been formed in aqueous phase by the addition of the CTA_{Water}, move very fast to the air-water interface. The high value of the final γ suggests a limited adsorption of the ASR at the air-water interface, which may be due to the repulsion between the polymer chains rich in deprotonated MAA. For ASR_B, the value of the CMC is $0.002gL^{-1}$. All these data suggests that the use of water-soluble CTA led to a lower incorporation of MAA in the main polymer chains and to the formation of short polymer chains rich in MAA.

In order to check if the ASR_B is able to form aggregates in aqueous phase, aqueous solutions at different concentrations were prepared to measure

the size of the aggregates using light scattering (Coulter N_4^+). In Figure 7, the volume average diameter (D_{agg}) and the surface tension were plotted versus ASR_B concentration.

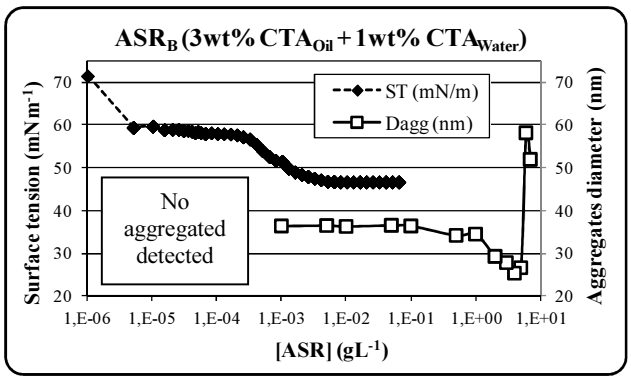

Figure 7: Surface tension (ST) and aggregate diameter (D_{agg}) versus ASR_B concentration

Focusing on the surface tension curve, for the first fall and the continuous plateau, no aggregates were detected by DLS. It is not clear if there were not aggregates or if they could not be detected by the equipment. However, for the second plateau (equilibrium region), aggregated were detected and between 10^{-3} and $10^{-1}gL^{-1}$ of ASR_B aggregates with a diameter of around 36nm were observed. For ASR concentrations higher than $1gL^{-1}$, a clear decrease followed by a sharp increase of the size was observed. The initial decrease in the diameter can be attributed to the SLS included in the ASR solution. Even if the SLS concentration is very low to form micelles, they can interact with the ASR decreasing the particle diameter. Finally, at

higher concentrations of ASR the aggregates tend to collapse increasing the particle diameter.

The parking area (a_s, $Å^2 molecule^{-1}$) is the area that covers one molecule of surfactant onto a specific surface at saturation conditions. A simple way to calculate a_s is by comparing the effective CMC in the presence and absence of the surface. To obtain these data, the particles of PMMA and PS were cleaned to remove the rest of surfactants or salts that may affect drastically the results. To clean the particles, the serum replacement [7] was used. In this technique, the latex is placed in a well mixed continuous cell equipped with a membrane that prevents the exit of the particles, but allows the exit of surfactant. A continuous flow of deionized water is fed into the cell and the latex is considered to be clean when the conductivity of the exit current is virtually the same as that of the entry water.

Figure 8 shows the variation of surface tension with ASR concentration in the presence and absence of polymer particles. The value of a_s was estimated using equation 2:

$$a_s = \frac{\pi d_p^2 N_p}{\frac{[CMC_{Particles} - CMC_{Water}]V}{M_E/N_A}} = \frac{6V_{Polym} * M_E}{d_p[CMC_{Particles} - CMC_{Water}]N_A V} \qquad (2)$$

where d_p is the average particle diameter, N_p the number of particles, $CMC_{Particles}$ and CMC_{Water} the CMC in the presence and absence of particles, V the total volume of aqueous phase, V_{Polym} the volume of the polymer particles,

M_E the molecular weight of the emulsifier (8500 $gmol^{-1}$ for ASR_A and 7600 $gmol^{-1}$ for ASR_B) and N_A the Avogadro's number.

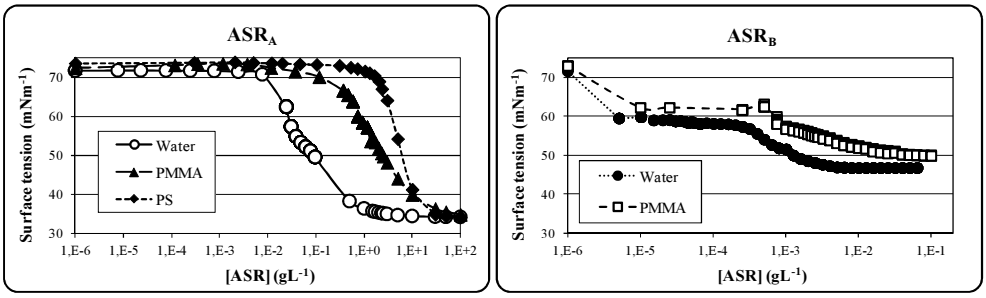

Figure 8: Surface tension measurements using polymer particles (PMMA and PS) and water for ASR_A and ASR_B

Table 7 shows the values of parking area (a_s) obtained by surface tension evolution (Figure 8) and the literature values for SLS. It can be seen that the parking area increased with polymer hydrophilicity; $a_s^{(PS)}<a_s^{(PBA)}<a_s^{(PMMA)}$ using SLS as emulsifier. The same trend is observed for ASR_A owing to the $a_s^{(PMMA)}$ is 3 times higher than $a_s^{(PS)}$. ASR_B had a large value for $a_s^{(PMMA)}$, which suggest a weak adsorption.

Table 7: Parking area obtained using equation 2

Polymers particles	**a_s^b(SLS)**	**a_s^a(ASR_A)**	**a_s^a(ASR_B)**
PolyStyrene	47	74	---
PolyButylAcrylate	66	---	---
PolyMethylMethacrylate	119	215	781
(^{a}) a_s measured in $Å^2 molecule^{-1}$ (^{b}) a_s from P. Roose, P. De Doncker [8]			

2.3 ASRs as emulsifiers in emulsion polymerization

The use of ASR_A and ASR_B as sole stabilizer in batch emulsion polymerization of styrene and methyl methacrylate was explored. Table 8 summarizes the formulation used. The redox system *tert*-butyl hydroperoxide with ascorbic acid (TBHP/AsAc) was used as initiator, feeding the components in two separate streams for 1hour.

Table 8: Batch emulsion polymerization using ASRs as sole stabilizers for MMA and S systems.

Recipe		**wt%**			**Grams**		
MMA	S	30			135		
ASR_A	ASR_B	10*	20*	30*	13.5	27.0	40.5
TBHP		1*			0,68		
AsAc					0,67		
Water		70			315		
(*) wt % respect to the monomer							

2.3.1 Styrene batch emulsion polymerization

Figures 9 and 10 present the evolution of the monomer conversion and number of particles respectively for styrene batch emulsion polymerization. It can be seen (Figure 10) that for the two ASRs the number of particles increased with the ASR concentration.

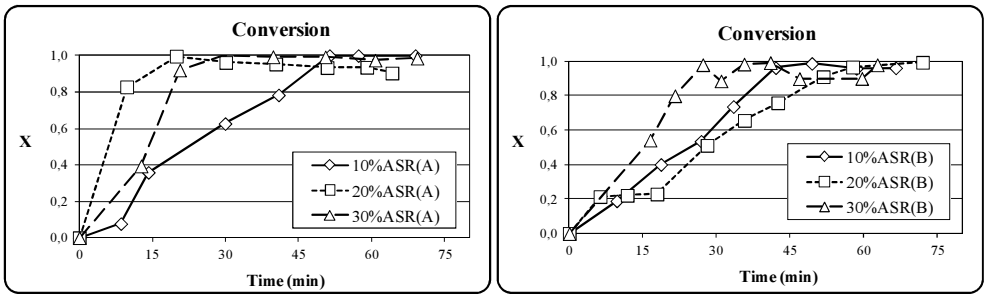

Figure 9: Effect of the ASR type and concentration on evolution of monomer conversion in the styrene batch emulsion polymerization

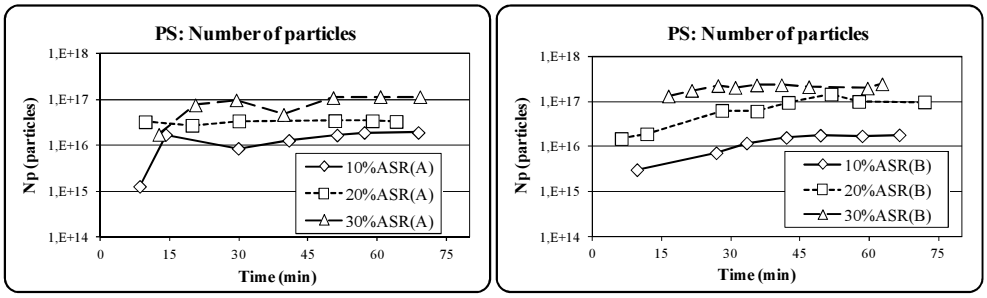

Figure 10: Effect of the ASR type and concentration on evolution of the number of particles in the styrene batch emulsion polymerization

Figure 11 shows that for ASR_A, $N_p \div [ASR]^{1.7}$, whereas for ASR_B, $N_p \div [ASR]^{2.4}$. This deviation of particle formation kinetics from the Smith-Ewart theory [9] (0.6^{th} power) was attributed [10] to the solubilization of the ASRs in the monomer droplets. The results suggested that burying of the ASR_B into the monomer droplets was higher than for ASR_A. This agrees with the more hydrophobic nature of ASR_B.

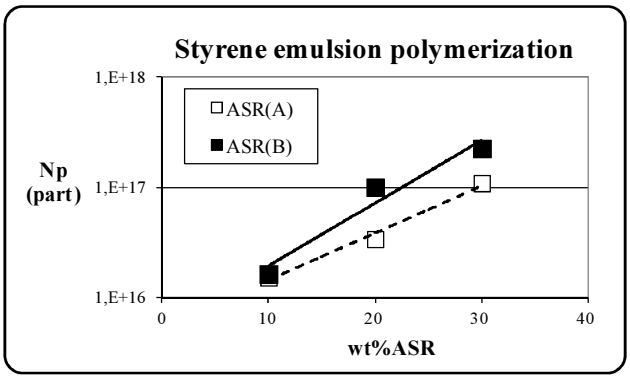

Figure 11: Effect of ASR concentration on the number of particles

On the other hand, Figures 9 and 10 suggest that the particle nucleation continues until a relatively high conversion was reached. The high concentration of ASR used and the burying of the ASR in the monomer droplets were likely responsible for the long nucleation period. The nucleation period was longer for ASR_B, which further supports the burying hypothesis.

Figure 11 shows that the number of particles obtained with ASR_B was higher than with ASR_A, which may be attributed to both the higher a_s and the small molecular weight fraction of the ASR_B that can stabilize precursor particles more efficiently than the longer ASR chains [5].

A striking result in Figures 9 and 10 is that polymerization rate did not correlate with N_p. Thus, for ASR_A, the polymerization rates ordered as $R_{p10}<R_{p30}<R_{p20}$ whereas for ASR_B the order was $R_{p20}<R_{p10}<R_{p30}$. Interestingly, the polymerization rate per particle (R_{pp}) decreased with the concentration of ASR and with the surface concentration of ASR in the particles (Figure 12).

These results agree with the observation of Coen et al. [11] and Lee and Kim [12] that reported that the hairy layer of ASR caused a reduction in radical entry and exit rates in the emulsion polymerization of styrene. Because the redox system yielded non-charged hydrophobic radicals and the ASR were made out of methacrylates (which are not prone to suffer polymer chain transfer) the most likely reason for the observed effect is that the hairy layer of ASR acted as a physical barrier for diffusion.

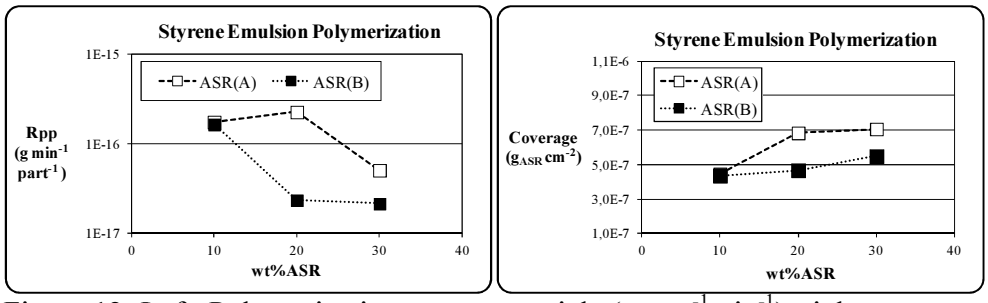

Figure 12: Left: Polymerization rate per particle (g $part^{-1}min^{-1}$); right: coverage of the polymer particles by ASR ($g_{ASR}cm^{-2}$) in styrene emulsion polymerization

Figure 12 shows that the effect was stronger for ASR_B, as a smaller coverage caused a stronger decrease in R_{pp}. This suggests denser hairy layer, but the reason for this result is not clear.

2.3.2 Methyl methacrylate batch emulsion polymerization

Figures 13 and 14 present the results obtained in the batch emulsion polymerization of MMA.

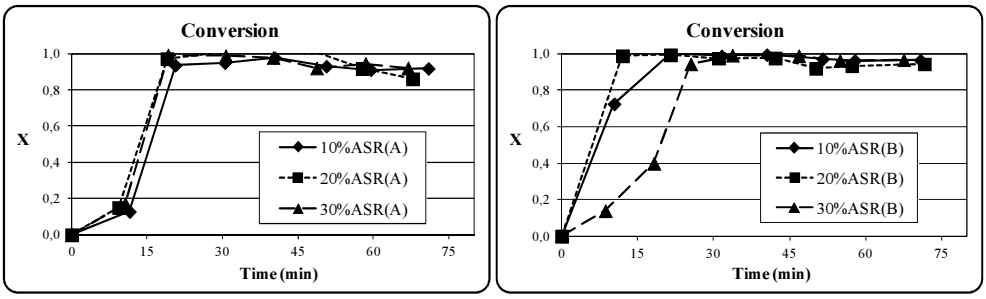

Figure 13: Effect of the ASR type and concentration on the evolution of monomer conversion in the methyl methacrylate batch emulsion polymerization

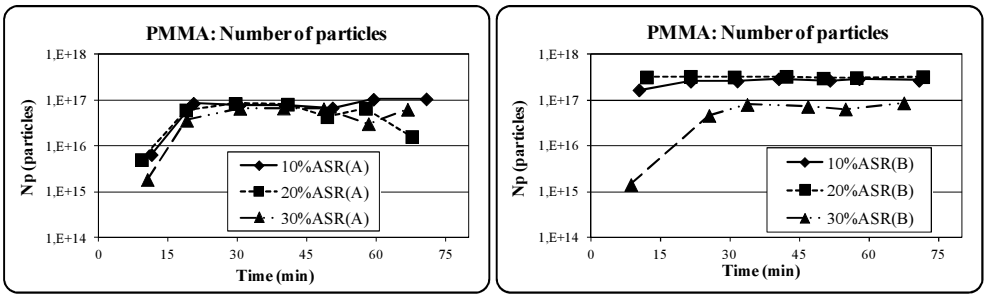

Figure 14: Effect of the ASR type and concentration on the evolution of the number of particles in the methyl methacrylate batch emulsion polymerization

Using ASR_A, the polymerization was so fast that no effect of the ASR concentration on polymerization rate could be observed. On the other hand, it was surprising that the number of particles was independent of the ASR concentration. Comparison with Figures 9 and 10 shows that the number of particles was higher for MMA than for S, which might be due to the combined effect of the contribution of homogeneous nucleation in the case of MMA and the large parking area of the surfactant for poly(methyl methacrylate).

Figures 13 and 14 also present the results using ASR_B. It can be seen that for 10 and 20wt% of ASR_B the differences in conversion and number of particles were small although both R_p and N_p increased with ASR_B concentration. On the other hand, a further increase of $[ASR_B]$ to 30wt% resulted in a much lower number of particles and consequently, lower polymerization rate. No explanation can be offered for this observation.

2.3.3 Effect of the SLS on the study

In the previous study, SLS was included in the formulation because the ASRs were synthesized by emulsion polymerization using SLS as surfactant. Obviously, the SLS may affect the results obtained. The amount of SLS used in each reaction may be estimated as follows:

$$[SLS]\left(\frac{SLS_{(g)}}{L}\right) = [M]\left(\frac{M_{(g)}}{L}\right) * ASR_{wt\%}\left(\frac{ASR_{(g)}}{M_{(g)}}\right) * SLS_{wt\%}\left(\frac{SLS_{(g)}}{ASR_{(g)}}\right) \qquad (3)$$

where [SLS] are the grams of SLS per liter, [M] is the mass of the monomer per liter (S or MMA), $ASR_{wt\%}$ is the weight fractions of ASR in emulsion polymerization (0.1, 0.2 or 0.3) and $SLS_{wt\%}$ is the weight fractions of SLS in the synthesis of ASR (0.04).

The concentrations of SLS for the previous cases were: 1.2g/L (10wt% of ASR); $2.4gL^{-1}$ (20wt%) and $3.6gL^{-1}$ (30wt%). As the $CMC_{SLS} = 2gL^{-1}$, the SLS was also involved in these systems as emulsifier. Therefore, the reactions

in this chapter although indicative of the behavior of ASR as stabilizer in emulsion polymerization are not completely conclusive. For that reason, a method to synthesize ASR that minimized the amount of SLS used will be presented in the following chapter.

2.4 Conclusions

In this chapter, the synthesis of MMA/BMA/MAA ASRs in emulsion polymerization was attempted. A first screening of the effect of the reaction conditions was carried out in batch finding that ASRs of the required molecular weight ($\bar{M}_n$~5000gmol^{-1}) able to become soluble upon increasing the pH to 10 can be obtained with 3wt% of oil-soluble CTA (1-Octanothiol). The concentration of SLS did not have any significant effect on the $\bar{M}_n$ of the ASR, but strongly affected particle size that in turn influenced the solubility of the ASR upon neutralization. 4wt% of SLS was needed to synthesize ASRs that become water-soluble rapidly.

Oil-soluble (1-Octanothiol) and water-soluble (2-Mercaptoethanol) CTAs were combined in an attempt to control the MWD of the polymer formed in both, polymer particles and aqueous phase. However, the effect of the water-soluble CTA on the whole MWD was small. Nevertheless, the effect on the CMC (lowering the CMC) and parking area (increasing a_s) was substantial.

The ASRs synthesized with (ASR_A) and without (ASR_B) CTA_{Water} were used as sole stabilizers in batch emulsion polymerization of styrene and methyl methacrylate. The reactions with MMA were too fast to allow drawing conclusions, but those carried out with S showed that the dependence of N_p on the concentration of ASR had exponents much higher than the 0.6 predicted for the Smith-Ewart theory [9] (1.7 for ASR_A and 2.4 for ASR_B), which was attributed to the solubilization of the ASRs in the monomer droplets. In addition, the polymerization rate per particle decreased with the concentration of ASR. Different possibilities were considered, but the topic is discussed in detail in Chapter 3.

2.5 References

1. Castan, P.; Switzerland, Z. Process of preparing synthetic resins. US 2324483 A, Castan, P., 1943.

2. Gandillon, C.; Castan, P. Process for the manufacture of synthetic resins obtained by condensation and esterification. US 3028348 A, Stella S. A., 1962.

3. Greenlee, S. O. Alkali soluble resins and compositions containing the same. US 2890189 A, Johnson & Son, Inc., Racine, Wis., 1959.

4. Stevens; Langers; Parry; Rollison. Alkali soluble resin polymer and method of preparing the same. GB 1107249 (A) Johnson & Son S. C., 1968.

5. Ballard, N.; Urrutia, J.; Eizagirre, S.; Schäfer, T.; Diaconu, G.; de la Cal, J. C.; Asua, J. M. *Langmuir* **2014,** 30, (30), 9053-9062.

6. Slawinski, M. Strategic Aspects of the Incorporation of Acrylic Acid in Emulsion Polymers. Ph.D. Thesis, Eindhoven University of Technology, 1999.

7. El-Aasser, M. S.; Ahmed, S. M.; Poehlein, G. W.; Vanderhoff, J. W.; Rovira, X.; Tabernero, J. I.; de La Morena, P., Application of the Serum Replacement Technique in the Characterization of an Ethyl Acrylate-Methyl Methacrylate Copolymer Latex. In *Polymer Colloids II*, Fitch, R. M., Ed. Springer USA, 1980; pp 361-377.

8. Roose, P.; De Doncker, P. *Journal of Applied Polymer Science* **2004,** 92, (5), 3226-3230.

9. Smith, W. V.; Ewart, R. H. *The Journal of Chemical Physics* **1948,** 16, (6), 592-599.

10. Nomura, M.; Tobita, H.; Suzuki, K., Emulsion polymerization: Kinetic and mechanistic aspects. In *Polymer particles*, Okubo, M., Ed. Springer Berlin Heidelberg, 2005; Vol. 175, p 33.

11. Coen, E. M.; Lyons, R. A.; Gilbert, R. G. *Macromolecules* **1996,** 29, (15), 5128-5135.

12. Lee, D. Y.; Kim, J. H. *Journal of Polymer Science Part A: Polymer Chemistry* **1998,** 36, (16), 2865-2872.

Chapter 3: Radical entry and exit in ASR stabilized latexes

Outline

3.1 Introduction

In Chapter 2, it was found that the polymerization rate did not correlate with the number of particles and that the polymerization rate per particle decreased with the concentration of ASR. This strongly suggested that the ASR hindered the entry of radicals into the polymer particles. Similar results have been reported in literature. Peck and Asua [1] studied the miniemulsion copolymerization of BA/MMA stabilized by a commercial ASR (styrene/alpha methyl styrene/acrilyc acid, S/AMS/AA) using two initiator systems TBHP/AsAc and KPS/NaBs, finding that the polymerization rate per particle was lower than that obtained in miniemulsion copolymerization of the same monomers, stabilized by a conventional surfactant. The effect was stronger for the initiator system giving charged radicals (KPS/NaBs), suggesting that electrostatic repulsion between the charged hairy layer of ASR and the radicals is at least partially responsible for the decrease in the entry rate. On the other hand, the fact that even the entry of non-charged radicals can be reduced suggests that diffusion through the hairy layer may also play a role. In addition, it has been proposed that the entering radicals can abstract hydrogens from the hairy layer, which would act as a radical sink lowering the net rate of radical entry [2-4]. However, the relative significance of diffusion, electrostatic repulsion and hydrogen abstraction has not been unambiguous determined.

This chapter is focused on shed light on the relative contribution of the three effects. For this, the miniemulsion polymerization of styrene and methyl

methacrylate with different ASRs and initiated by different initiator was investigated. Miniemulsion was used in an attempt to avoid the effect of the migration of the ASR on particle nucleation [5]. One of the ASRs contained labile hydrogens (from AA) and the other was devoid of easily abstractable hydrogens as it was synthesized using MAA. The amount of SLS used in the synthesis of these ASRs was minimized in an attempt to avoid the effect of the conventional surfactant on the outputs of this study. TBHP/AsAc that yields *tert*-butoxyl non-charged radicals and ammonium persulfate (APS) that yields charged sulfate ion radicals were used as water-soluble initiators. AIBN that yields non-charged radicals was also used as initiator. In addition, monomers of widely different water solubility were used.

3.2 Synthesis and properties of ASRs varying the acid monomer type

In this section, the synthesis of the ASRs containing either AA or MAA is presented. The results presented in Chapter 2 show that in order to obtain an easily dispersible ASR by emulsion polymerization, small particle size and good incorporation of the acidic monomer to the ASR are needed.

The small particle size and the minimization of the concentration of SLS to be used in the synthesis are conflicting requirements. Harada and Nomura [6] reported that below a certain monomer/surfactant ratio, the particle

size decreased as this ratio decreased. The reason for this behavior can be traced back to the classical equation of Smith-Ewart [7] for the effect of the process variables on the number of particles (N_p). In this equation, for constant temperature, initiator concentration and surfactant concentration, N_p increases as the rate of volumetric growth of the particles decreases. A decrease in the monomer concentration, for the rest of conditions constant, leads to a reduction on the particle growth rate and to a higher number of particles. This has been exploited to develop strategies leading to small particle sizes and relatively high solids content using small concentration of surfactant [8, 9]. The best strategy reported so far, comes from ours labs [8, 9] and basically consists in a semicontinuous emulsion polymerization in which all the surfactant is placed in the initial charge and the monomer is fed semicontinously under severe starved conditions. For the purposes of this chapter, such a process has the advantages of leading to small particles using modest amounts of surfactant and achieving a better distribution of the monomers in the backbone of the polymer chains.

The semi-continuous emulsion polymerizations were carried out using the formulation in Table 1 in a 1L jacketed glass reactor at 70ºC with an anchor stirrer at 214 rpm. The solids content was 30wt%. All the water, surfactant (SLS) and buffer ($NaHCO_4$) were placed as initial charge. When the reaction temperature was reached under nitrogen atmosphere, the APS was added as a shot and then, the mixture of the monomers and CTA was continuously fed into the reactor for 5 hours. The feeding rate was 0.9g min^{-1}; that led to starved conditions, avoiding the formation of a monomer layer on

the top of the reaction mixture. After the feeding, the reactor was maintained for 1 hour in batch.

Table 1: Formulation used in the synthesis of ASRs by semi-continuous emulsion polymerization

Ingredient	**Total charge (g)**	**Concentration**
MMA/BMA/MAA	255	30wt%
MMA/BMA/AA		
CTA_{Oil} (OcT)	Varying	
Buffer ($NaHCO_4$)	1.88	0.74wt%[a]
Emulsifier (SLS)	0.64	0.25wt%[a]
Initiator (APS)	2.55	1wt%[a]
Water	595	70wt%
(a) % with respect to monomers		

Technical grade monomers, methyl methacrylate (MMA, Quimidroga), butyl methacrylate (BMA, Aldrich), methacrylic acid (MAA, Aldrich) and acrylic acid (AA, Aldrich) were used as received. SLS (Aldrich), $NaHCO_4$ (Riedel-de Haën) and 1-Octanethiol (CTA_{Oil}, Aldrich) were used without purification as anionic surfactant, buffer and chain transfer agent, respectively.

Table 2 summarizes the ASRs prepared. Two different ASRs were synthesized varying the type of acidic monomer: MAA denoted as ASR_{MAA}, and AA denoted as ASR_{AA}. Preliminary reactions carried out with 14wt% of acidic monomer did not result in clear solutions after neutralization. Therefore, higher concentration (18, 20 and 22wt% with respect to the monomers) were

used. The MMA/BMA ratio was around 3/4. The values of the acid number (N_{Ac}) were calculated using the Equation 1 from Chapter 2. As shown in Table 2, only the ASRs containing 22wt% of acidic monomer gave a clear solution after neutralization. Thus, hereinafter only the ASRs obtained with 22wt% of acidic monomer, will be considered.

Table 2: ASRs synthesized with different amount of acid monomers using 3wt% of CTA_{Oil}

ASR	**Ratio (weight %)**				$\bar{M}_n$	D_p	N_{Ac}	**Final solution**
	MMA	**BMA**	**MAA**	**AA**	**(g/mol)**	**(nm)**	**(mg_{KOH}/g)**	
$18\%_{MAA}$	35	47	18	--	6000	100	117.2	No Clear
$18\%_{AA}$			--	18	5800	90	140.0	
$20\%_{MAA}$	34	46	20	--	5900	100	130.2	
$20\%_{AA}$			--	20	5600	95	155.6	
$22\%_{MAA}$	34	44	22	--	6000	104	143.3	Clear
$22\%_{AA}$			--	22	5700	98	171.1	

The CTA_{Oil} content was varied between 0.5-3wt% with respect to the monomers. The effect of the CTA_{Oil} concentration on $\bar{M}_n$ is presented in Figure 1. It can be seen that the choice of the acidic monomer had no effect on $\bar{M}_n$ and that using 3wt% of CTA_{Oil}, the molecular weight was around 5000g mol^{-1} that is close to the desirable value. Therefore, the 3wt% of CTA_{Oil} was chosen for the synthesis.

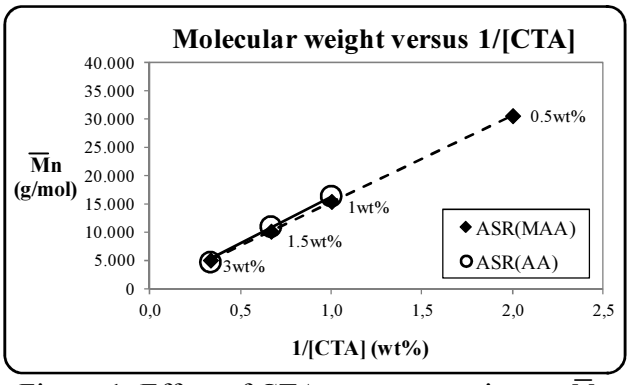

Figure 1: Effect of CTA_{Oil} concentration on $\overline{M}_n$ for the ASRs synthesized with 22wt% of acidic monomer

Figure 2 shows the evolution of the reactions in which ASR_{MAA} and ASR_{AA} were synthesized with 3wt% of CTA_{Oil}, 22wt% of acidic monomer, 34wt% of MMA and 44wt% of BMA. The evolution of the instantaneous and cumulative conversions shows that the reaction occurred under starved conditions, which favors the formation of rather homogeneous copolymers. Figure 2 also shows that the particle nucleation occurred in the first moments of the process and that a limited coagulation occurred during the major part of the semicontinuous process. Nevertheless, no macroscopic coagulation was observed and a clear solution was obtained by adjusting the pH to 10 using NH_4OH.

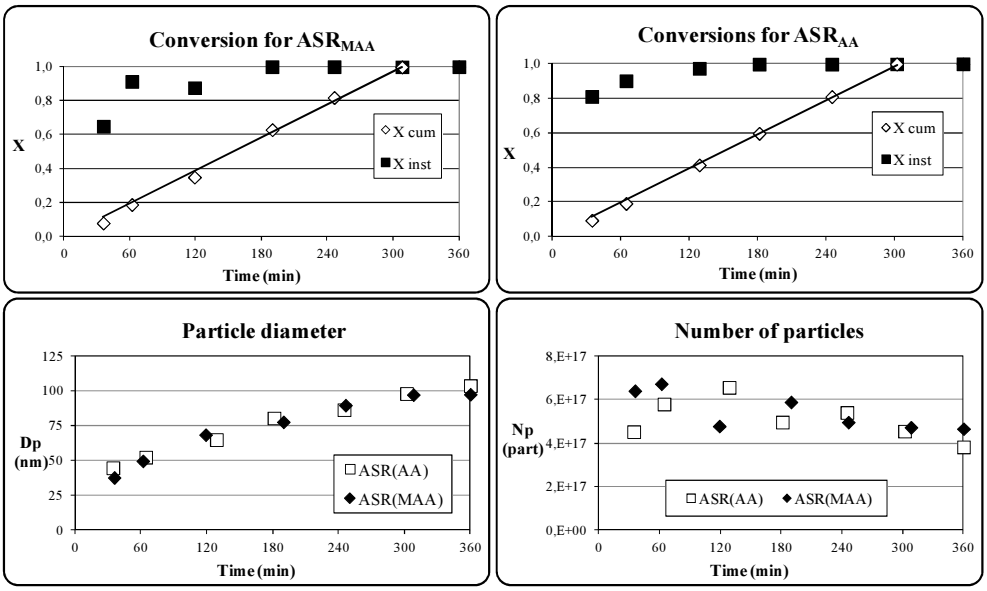

Figure 2: Evolution of the conversions, particle diameter and number of particles in the synthesis of ASRs with 3wt% of CTA_{Oil} and 22wt% of acidic monomer (AA or MAA)

The differences in water-solubility between AA and MAA are expected to have an effect on the amount of water soluble polymer formed in these reactions. Therefore, at the end of the reaction at pH=3, the serum was obtained by ultracentrifugation (20000 rpm during 1h at 20ºC) and then it was titrated using NaOH 0.1N as explained previously (Chapter 2, Section 2.2.2). The results are shown in Table 3. It can be seen that the amount of polymer in the serum for ASR_{AA} was higher than that of ASR_{MAA}, but they only represent a tiny fraction of the total acidic monomer. Comparison with the previous results obtained in batch in Chapter 2 shows that the strategy developed in this chapter led to more homogeneous copolymers.

Table 3: Amount of water soluble polymers in the serum

	Polymer content in the serum ($g\,mL^{-1}$)	Fraction of polymer in the serum with respect to the total acidic monomer
ASR_{MAA}	$1.6x10^{-4}$	0.17 wt%
ASR_{AA}	$2.5x10^{-4}$	0.27 wt%

The molecular weight distribution (MWD) of the two resins was measured at the end of the reaction by gel permeation chromatography (GPC, Waters) calibrated with PS standards at room temperature. The ASRs were dried at 60ºC in the presence of a highly hygroscopic salt ($CaCl_2$), and then dissolved in THF to which a very small amount of toluene was added to be used as reference peak.

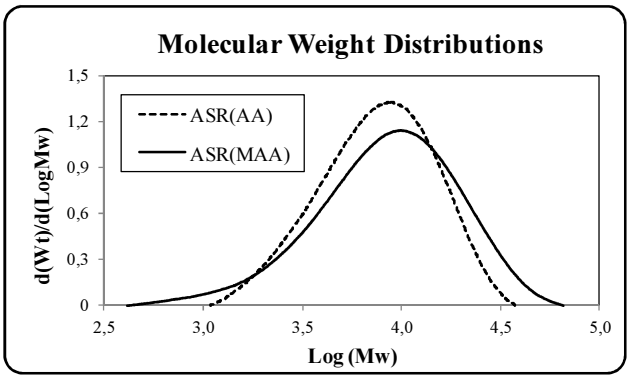

Figure 3: MWD of ASRs synthesized with 3wt% of CTA_{Oil} and 22wt% of acidic monomer

Figure 3 shows the MWD of the ASRs synthesized with 3wt% of CTA_{Oil} and 22wt% of acidic monomer. It can be seen that the acidic monomer had only a modest effect on the MWD. The number and weight average

molecular weights for ASR_{MAA} were $\overline{M}_n$=5700g mol^{-1} and $\overline{M}_w$=11300 g mol^{-1}; and for ASR_{AA} $\overline{M}_n$=6000g mol^{-1} and $\overline{M}_w$=9200g mol^{-1}.

If termination takes place by transfer to CTA_{Oil}, the dispersity must be 2. However, the dispersity for ASR_{AA} was 1.53, whereas for ASR_{MAA} was 1.98. Considering that chain transfer to CTA was the main termination event, it is surprising that dispersities lower than 2 were obtained. A possible reason for this observation is that small molecular weight polymer chains passed unnoticed through the GPC detectors.

The electrostatic stability provided by the ASR is related to the acid number (N_{Ac}) and the pH of the polymerization media. The acid number for both ASRs was determined by titration with NaOH (0.1N) using conductometric titration. The technique has been explained in Chapter 2 (Section 2.2.2). The results are shown in Table 4. The higher acid number of the ASR_{AA} is due to the lower molecular weight of AA as compared to MAA.

Table 4 shows that theoretical and calculated values are very close. Although in order to achieve good solubility in water, the concentration of the acidic monomer used in the synthesis was higher than originally planned, the acid numbers obtained were still similar or lower than the commercial ASRs [10, 11].

Table 4: Acid numbers of the ASRs synthesized with 3wt% of CTA_{Oil} and 22wt% of acidic monomer

	Measured acid number ($mg_{KOH}\ g_{ASR}^{-1}$)	**Theoretical acid number ($mg_{KOH}\ g_{ASR}^{-1}$)**
ASR_{MAA}	144	143
ASR_{AA}	171	171

Conventional surfactants are commonly characterized by the critical micellar concentration (CMC) which is the solubility of the surfactant in water. Above this value, micelles/aggregates are formed. The value of the CMC is determined by the hydrophilic and hydrophobic moieties of the surfactant. In the case of ASRs, the hydrophilic/hydrophobic balance depends on the pH, therefore, it is expected that the pH had a strong influence on the CMC. Consequently, the CMC of the ASRs were determined under two conditions of pH. In the first one, the pH of the water was increased to pH=10 with NH_4OH and the ASRs of pH=10 were added. In the second one, the ASRs (at pH=10) were added to pure water, and hence, during the experiment the pH increased from 7 to almost 10 (referred as pH=7-10).

Figure 4 presents the results obtained with the two ASRs. It can be seen that the surface tension measured for pH=7-10 was higher than for pH=10. This result was due to the fact that at low pH, a substantial fraction of the carboxyl groups were protonated reducing the amphiphilic characteristics of the ASRs and hence their adsorption at the air-water interface. The surface tension curves converged as the pH approached 10. The effect of the pH was smaller for AA than for MAA, probably due to the high number of carboxyl

groups in the ASR_{AA} (because of the differences in molecular weight between MAA and AA) and (less important) to the effect of the hydrophobic methyl group of the MAA. The different content of carboxyl groups had also an effect on the surface tension measured at pH=10 as it is shown in Figure 5 where the behavior of ASR_{AA} and ASR_{MAA} are compared.

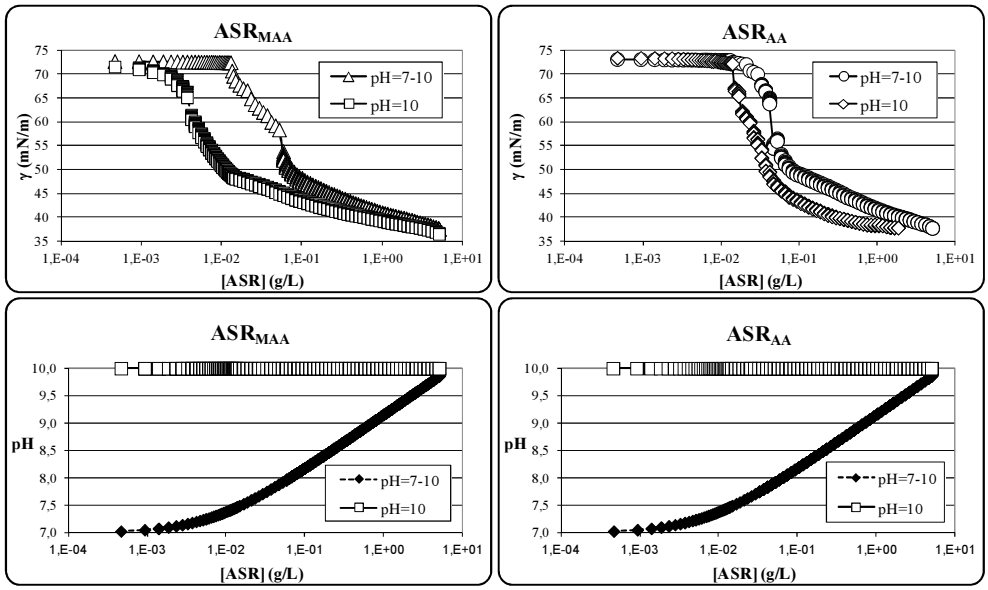

Figure 4: Evolution of surface tensions and pHs in the experiments aiming at determining the CMC of the ASRs obtained with 3wt% of CTA_{Oil} and 22wt% of acidic monomer

The experimental data showed that in all the cases the surface tension did not reach a constant value at high ASR concentrations. A possible reason was the exchange of the ASR chains adsorbed at the air-water interface by newly added acid-rich ASR chains. Apparent CMC values are presented in Table 5 where only the values at pH=10 are included.

Table 5: Apparent CMC values

	pH=10
ASR_{MAA}	0.015 g L^{-1}
ASR_{AA}	0.059 g L^{-1}

These results highlight the strong influence of the pH on the amphiphilic properties of the ASRs, which may be critical in polymerizations using initiators that modify the pH of the medium.

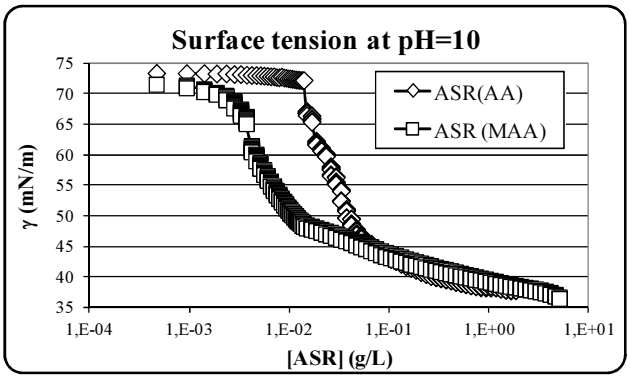

Figure 5: Surface tension for ASR_{MAA} and ASR_{AA} at pH=10

3.3 Radical entry and exit through ASR hairy layers

ASRs can be used in both emulsion and miniemulsion polymerization. In emulsion polymerization, compared to standard non-polymeric emulsifiers, ASRs are commonly used at high levels (>20% based on dry polymer).

Nevertheless, in miniemulsion polymerization, do Amaral and Asua [12] reported that high solids content latexes can be obtained using a substantially lower amount of ASR. The main difference between conventional emulsion and miniemulsion polymerization is the nucleation step; micellar and homogeneous for emulsion and droplet nucleation for miniemulsion polymerization (although in some cases, homogeneous nucleation cannot be avoided) [13]. Once the particles have been formed, the radical entry and exit mechanisms are expected to be similar in both processes.

In previous works [1, 14-17], using ASRs as emulsifier, it was proposed that the reduction in polymerization rate was caused by the reduction of the radical entry rate. Considering that the ASR is adsorbed on the particle surface forming a polymeric hairy layer that contains a high density of negative charges, the mechanisms proposed to justify the reduction of the radical entry are as follows:

1.-The hairy layer offers an additional resistance to the diffusion of the entering oligoradicals [18].
2.-The entering anionic oligoradicals are repelled by the negative charges in the hairy layer [19].
3.-The hairy layer acts as a radical sink, because the entering oligoradical abstract hydrogens from the ASR in the hairy layer leading to a tertiary radical [4].

Mechanism 1 may act on any type of entering oligomer, mechanism 2 can only affect charged oligoradicals and mechanism 3 would only be operative

for ASRs containing abstractable hydrogens. In this section, the relative importance contributions of the three mechanisms to the decrease of the radical entry rate have been studied.

ASR_{AA} containing acrylic acid may suffer hydrogen abstraction whereas ASR_{MAA} does not contain any easily abstractable hydrogen. Therefore, the differences in the kinetics using ASR_{MAA} or ASR_{AA} would provide proof of the hydrogen abstraction effect. Table 6 presents the initiators and the corresponding free radicals that were used: TBHP/AsAc, APS and AIBN. Two of them, TBHP/AsAc and APS, generate radicals in the aqueous phase. The THBP/AsAc yields oxygen centered radicals which are very efficient abstracting hydrogen, therefore a strong effect is expected. These radicals are hydrophobic enough to enter directly into the monomer droplets and polymer particles. The APS decomposition leads to water soluble oxygen centered anionic radicals that should react with monomer in the aqueous phase to become hydrophobic enough to be able to enter into the monomer droplets and polymer particles. AIBN is an oil-soluble initiator that produces non-charged carbon centered radicals in the oil phase. The carbon centered radicals are less efficient abstracting hydrogen.

Table 6: Radicals from initiators

Initiator	**Radical**
APS	$SO_4^{\bullet -}$
TBHP/AsAc	$(CH_3)_3CO^{\bullet}$
AIBN	$CN(CH_3)_2C^{\bullet}$

It is worth pointing out that TBHP partitions between the oil and the water phase. At 20ºC, the partition coefficient octane/water is P_{ow}=5. Therefore, if thermodynamic equilibrium is reached and if a polymer particle behaves as a pure oil phase, the concentration of TBHP in the oil phase will be 5 times that of the aqueous phase. On the other hand, ascorbic acid is soluble in the aqueous phase. Therefore, two sources of radicals are possible: thermal decomposition of the TBHP in the monomer droplets and redox reaction between TBHP and AsAc in the aqueous phase. At 60ºC, the thermal decomposition rate coefficient of the TBHP is about $5x10^{-11}s^{-1}$. For the sake of comparison, at 60ºC, the thermal decomposition rate coefficient of AIBN is $9x10^{-6}s^{-1}$, which is more than five orders of magnitude faster. Having in mind that AIBN is not a particularly fast initiator; this means that the rate of radical production by thermal decomposition of TBHP at 60ºC is negligible.

The effect of the type of ASR on the polymerization rate per particle achieved with TBHP/AsAc will give an indication of the relative effect of the hydrogen abstraction on entry rate as compared with diffusional limitation. On the other hand, the effect of the type of ASR on the polymerization rate per particle achieved with APS (which also gives oxygen centered radicals) will give an indication of the relative effect of the hydrogen abstraction on entry rate as compared with electrostatic repulsion and diffusional limitation. Also, the hydrophobicity of the monomer was varied to affect the composition of the oligomers growing in the aqueous phase. The effect of the ASR type on the polymerization rate per particle when using AIBN will give information about both radical entry and exit because desorption and reentry of initiator radicals

from droplets and particles is the key mechanism controlling the kinetics of miniemulsion polymerization and particle growth in emulsion polymerization. For these systems, the contribution of the fraction of the initiator dissolved in the aqueous phase is minor [20].

3.3.1 Styrene miniemulsion polymerization with TBHP/AsAc and APS

Miniemulsions were prepared by mixing the organic phase composed of the monomer (S) and the costabilizer (hexadecane) with the ASR aqueous solution and forming a coarse dispersion by magnetic stirring during 10 minutes. Then, the pH was measured and adjusted to 10 by NH_4OH addition. Immediately afterwards, the dispersion was sonicated in an ice bath. Sonication was carried out with a Branson Sonifier 450. The amplitude was set to 80% and the sonication time was 20 minutes. In order to avoid overheating, sonication was stopped every 54 seconds and the sample was kept at rest for 6 seconds. After sonication, the pH was measured again because of the overheating could provoke the NH_4OH loss. If this happen (it was unusual), the pH should be adjusted again. All miniemulsion polymerizations were carried out in a 500 mL glass jacketed reactor at 60°C and 220 rpm. The solids content was 32.4wt%. In all the cases, the amount of ASR was 8wt% with respect to the monomer.

Tables 7 and 8 show the formulations used for TBHP/AsAc and APS, respectively. The reactions were carried out during 5 hours.

Table 7: Miniemulsion polymerizations carried out with TBHP/AsAc as initiator

Component	**Initial charge (g)**	**Stream 1 (g)**	**Stream 2 (g)**
S	120		
Hexadecane	2.40		
ASR_{AA} or ASR_{MAA}	9.60		
TBHP			1.02
AsAc		2.16	
Water	178	42.84	43.98
Total	310	45	45

Table 8: Miniemulsion polymerizations carried out with APS as initiator

Component	**Initial charge (g)**	**Initiator added as a shot (g)**
S	120	
Hexadecane	2.40	
ASR_{AA} or ASR_{MAA}	9.60	
APS		1.20
Water	256.80	10
Total	388.80	11.20

When the redox system TBHP/AsAc was used, the components were added to the reactor in separate streams at a feed rate of $0.1875 g\,min^{-1}$ during 4 hours. Then, the system was maintained one additional hour in batch. When

thermal initiator was used (APS) the initiator solution was added as a shot at the beginning of the reaction. Both initiators created radicals in the aqueous phase.

Figures 6 and 7 present the kinetics of four miniemulsion polymerizations combining the two ASRs synthesized (ASR_{AA} and ASR_{MAA}) and two initiators (TBHP/AsAc and APS).

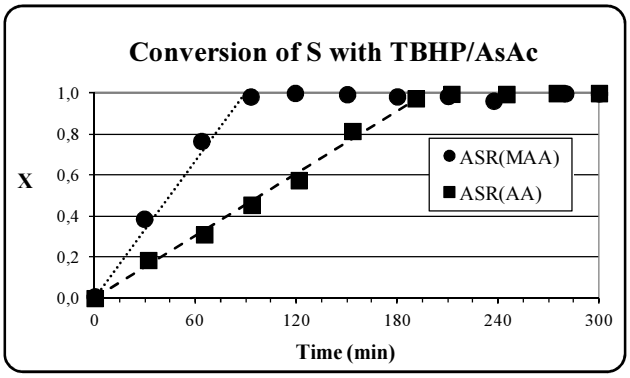

Figure 6: Effect of the ASR type on the kinetics of the styrene miniemulsion polymerization using TBHP/AsAc as initiator

It is worth pointing out that the weight of ASR used in each experiment was the same and that because AA and MAA had different molecular weights, the ratio between the number of acid groups in ASR_{AA} and ASR_{MAA} was 1.2, namely, ASR_{AA} had a slightly higher content of carboxylic groups.

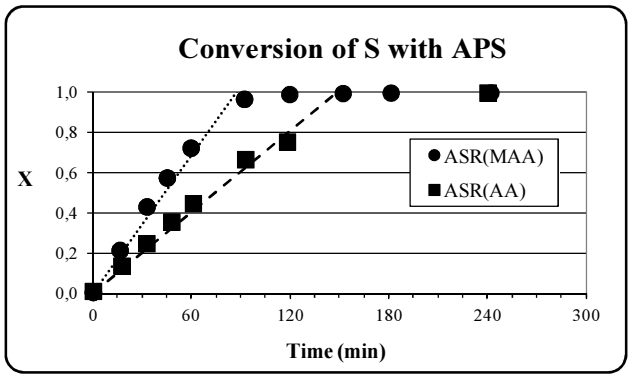

Figure 7: Effect of the ASR type on the kinetics of the styrene miniemulsion polymerization using APS as initiator

Polymerization rates (R_p) were calculated from the slope of the conversion-time curves shown in Figures 6 and 7. The number of polymer particles (N_p) was determined from the final particle size measured by light scattering. From R_p and N_p the polymerization rate per particle ($R_{pp}=R_p/N_p$) was calculated. The average number of radicals per particle ($\bar{n}$) was then obtained using the following equation:

$$\bar{n} = \frac{N_A}{k_p[M]_p} R_{pp} \qquad (1)$$

where N_A is the Avogadro's number, k_p (341 $Lmol^{-1}s^{-1}$) is the polymerization rate constant at 60ºC, and $[M]_p$ is the monomer concentration in the polymer particles. It was calculated assuming that the particles were at the maximum thermodynamic swelling.

Table 9: Main data for styrene polymerizations using TBHP/AsAc

	R_p (g $L^{-1}s^{-1}$)	D_p (nm)	N_p (part L^{-1})	R_{pp} (g $part^{-1}s^{-1}$)	$\bar{n}$
ASR_{MAA}	0.0561	439	$6.5x10^{15}$	$8.6x10^{-18}$	31
ASR_{AA}	0.0255	327	$15.6x10^{15}$	$1.6x10^{-18}$	5.7
$\frac{ASR_{MAA}}{ASR_{AA}}$	2.2	1.3	0.4	5.4	5.4

The most relevant data using TBHP/AsAc as initiator are listed in Table 9. It can be seen that the polymerization rate was higher for the reaction using ASR_{MAA} (Table 9 and Figure 6), even though the number of particles was greater for ASR_{AA} ($N_{p(MAA)}/N_{p(AA)} = 0.4$). Therefore, the polymerization rate per particle was significantly lower for ASR_{AA}, namely, for the alkali soluble resin that was prone to suffer hydrogen abstraction. This means that under the conditions used in these experiments, the radical entry rate was substantially reduced by the formation of tertiary radicals on the ASR backbone through hydrogen abstraction.

Table 9 shows that the average number of radicals per particle ($\bar{n}$) was well above 0.5, namely, the polymerizations occurred under pseudobulk conditions. Under these circumstances, the polymerization rate is proportional to the square root of the radical entry rate. Therefore, assuming that the three resistances (diffusion, electrostatic repulsion and hydrogen abstraction) are in series, the polymerization rate per particle should be inversely proportional to the square root of the overall resistance.

$$R_{pp} \propto \left(\frac{1}{R_1 + R_2 + R_3}\right)^{0.5} \quad (2)$$

where R_1 is the resistance to diffusion, R_2 that of the electrostatic repulsion and R_3 the hydrogen abstraction.

In the case of TBHP/AsAc, the electrical repulsion did not play any role and when using the ASR_{MAA}, the hydrogen abstraction was not a significant event. As a result, the polymerization rates per particle for the two ASRs were as follows:

$$(Rpp_{MAA})_{TBHP/AsAc} \propto \left(\frac{1}{R_1}\right)^{0.5} \quad (3)$$

$$(Rpp_{AA})_{TBHP/AsAc} \propto \left(\frac{1}{R_1 + R_3}\right)^{0.5} \quad (4)$$

Therefore, the ratio of polymerization rates per particle for the two ASRs was:

$$\left(\frac{Rpp_{MAA}}{Rpp_{AA}}\right)_{TBHP/AsAc} = \left(\frac{R_1 + R_3}{R_1}\right)^{0.5} \quad (5)$$

As the relationship between polymerization rates per particle was 5.4 (Table 9), R_3 was substantially bigger than R_1 ($R_3 = 28R_1$), which means that for TBHP/AsAc, the effect of hydrogen abstraction on the reduction of the radical entry rate was 28 times higher than that of the diffusion.

Figure 7 shows the effect of the type of ASR on the evolution of the monomer conversion in the experiments initiated with APS. The most relevant data for these reactions are listed in Table 10. It can be seen that the polymerization rate was higher for the reaction using ASR_{MAA}, even though the number of particles was greater for ASR_{AA} ($N_{p(MAA)}/N_{p(AA)} = 0.7$). The polymerization rate per particle was lower for ASR_{AA}, namely the radical entry rate was also lower for the ASR containing easily abstractable hydrogens. These results showed that hydrogen abstraction resulted in a decrease of the entry rate for both TBHP/AsAc and APS.

Table 10: Main data for styrene polymerizations using APS

	R_p (g $L^{-1}s^{-1}$)	D_p (nm)	N_p (part L^{-1})	R_{pp} (g $part^{-1}s^{-1}$)	$\bar{n}$
ASR_{MAA}	0.0575	522	$3.8x10^{15}$	$15.1x10^{-18}$	54
ASR_{AA}	0.0335	457	$5.7x10^{15}$	$5.9x10^{-18}$	21
$\frac{ASR_{MAA}}{ASR_{AA}}$	1.7	1.1	0.7	2.6	2.6

Tables 9 and 10 show that the ratio of the polymerization rates per particle (R_{pp}) for TBHP/AsAc was 5.4, whereas for APS was 2.6, namely that the effect was more accused for TBHP/AsAc. This indicates that the rate of entry into the particles of the anionic oligoradicals formed from the APS was lowered by both the negatively charged ASR and the hydrogen abstraction. Equation 3 applied to APS initiator should include the repulsion term (R_2) for the two ASRs. Consequently, the following equations could be obtained:

$$(\mathrm{Rpp_{MAA}})_{\mathrm{APS}} \propto \left(\frac{1}{\mathrm{R_1 + R_2}}\right)^{0.5} \quad (6)$$

$$(\mathrm{Rpp_{AA}})_{\mathrm{APS}} \propto \left(\frac{1}{\mathrm{R_1 + R_2 + R_3}}\right)^{0.5} \quad (7)$$

$$\left(\frac{\mathrm{Rpp_{MAA}}}{\mathrm{Rpp_{AA}}}\right)_{\mathrm{APS}} \propto \left(\frac{\mathrm{R_1 + R_2 + R_3}}{\mathrm{R_1 + R_2}}\right)^{0.5} \quad (8)$$

If it is assumed that the ratio between R_1 and R_3 of APS is similar than using TBHP/AsAc, it is possible to estimate the ratios between R_2 and R_1 (R_2=3.9R_1) and between R_3 and R_2 (R_3=7.2R_2). According to these values, the effect of electrostatic repulsion was 3.9 times greater than that of the diffusion and the resistance due to hydrogen abstraction was 7.2 times higher than that of the electrical repulsion.

The main conclusion of this section is that the hydrogen abstraction is the major factor to reduce the radical entry rate for styrene, and that electrostatic repulsion also reduces the entry of negatively charged radicals.

3.3.2 Methyl methacrylate miniemulsion polymerization with THBP/AsAc and APS

The oxygen centered radicals are more efficient for hydrogen abstraction than the carbon centered radicals. Therefore, a more hydrophilic monomer may reduce the probability of hydrogen abstraction because the oxygen centered radicals produced in the aqueous phase may more easily react

with the monomer giving carbon centered radicals. In order to check this idea, miniemulsion polymerizations using MMA as monomer were carried out under the same conditions as in Tables 7 and 8.

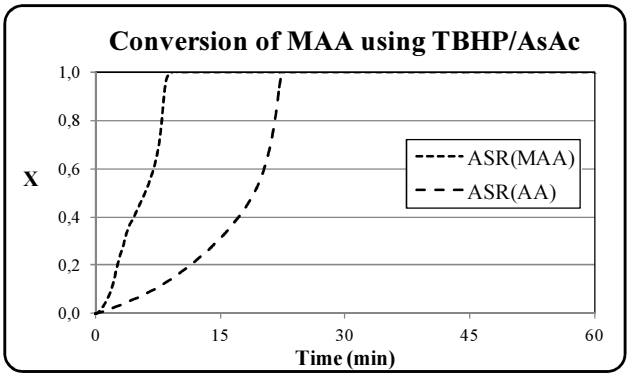

Figure 8: Effect of the ASR type on the kinetics of MMA miniemulsion polymerization using TBHP/AsAc as initiator

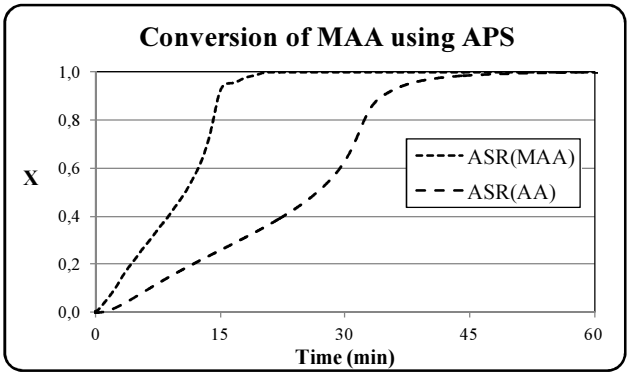

Figure 9: Effect of the ASR type on the kinetics of MMA miniemulsion polymerization using APS as initiator

The miniemulsion polymerizations of MMA were too fast to accurately measure the conversion evolution using gravimetry. Therefore, the reactions were carried out in a calorimeter reactor (Mettler, RC1). In this way, continuous data of conversion were obtained. Figures 8 and 9 show the results of these reactions. It can be seen that the polymerization rate was higher for the reaction using ASR_{MAA} for both TBHP/AsAc and APS.

The most relevant data of these reactions were listed in Table 11 for TBHP/AsAc and in Table 12 for APS. It can be seen that the polymerization rate per particle, for both cases, was lower for ASR_{AA}, so, the entry rate was lower for the ASR containing easily abstractable hydrogens.

Table 11: Main data for MMA polymerizations using TBHP/AsAc

	R_p (g $L^{-1}s^{-1}$)	D_p (nm)	N_p (part L^{-1})	R_{pp} (g $part^{-1}s^{-1}$)	$\bar{n}$
ASR_{MAA}	0.4080	333	$13.0x10^{15}$	$31.5x10^{-18}$	4.6
ASR_{AA}	0.0764	357	$10.5x10^{15}$	$7.3x10^{-18}$	10.8
$\frac{ASR_{MAA}}{ASR_{AA}}$	5.3	0.9	1.2	4.3	4.3

Using the same equations as for styrene, the different resistances (R_1, R_2, and R_3) were calculated. For TBHP/AsAc, $R_3 = 17.5R_1$. The hydrogen abstraction was the major factor in the reduction of radical entry rate, but the effect was less pronounced that when using styrene as monomer. This indicates that the amount of oxygen centered radicals was reduced by using a more water-soluble monomer.

On the other hand, for APS, the results were $R_2 = 39R_1$ and $R_3 = 0.45R_2$. Therefore, in this case, the main factor was repulsion, almost twice as high as that of hydrogen abstraction, which again shows the effect of reducing the concentration of oxygen centered sulfate ion radicals by reacting them with MMA.

Table 12: Main data for MMA polymerizations using APS

	R_p (g $L^{-1}s^{-1}$)	D_p (nm)	N_p (part L^{-1})	R_{pp} (g $part^{-1}s^{-1}$)	$\bar{n}$
ASR_{MAA}	0.2165	306	$16.7x10^{15}$	$12.9x10^{-18}$	19
ASR_{AA}	0.0880	392	$8.0x10^{15}$	$11.0x10^{-18}$	16
$\frac{ASR_{MAA}}{ASR_{AA}}$	2.5	0.8	2.1	1.2	1.2

The relative importance of the three mechanisms for the two monomers and the two initiators is presented in Figure 10. It can be seen that when APS was used as initiator, the behavior was strongly affected by the water solubility of the monomer. For styrene $R_3 = 7.2R_2$, that is, the effect of the abstraction of hydrogen was 7.2 times higher than that of the electrical repulsion. Conversely, for methyl methacrylate $R_3 = 0{,}45R_2$, namely, the effect of hydrogen abstraction was 2.2 times lower than that of the electrical repulsion. When TBHP/AcAc was used as initiator, the effect of the monomer hydrophilicity was much weaker.

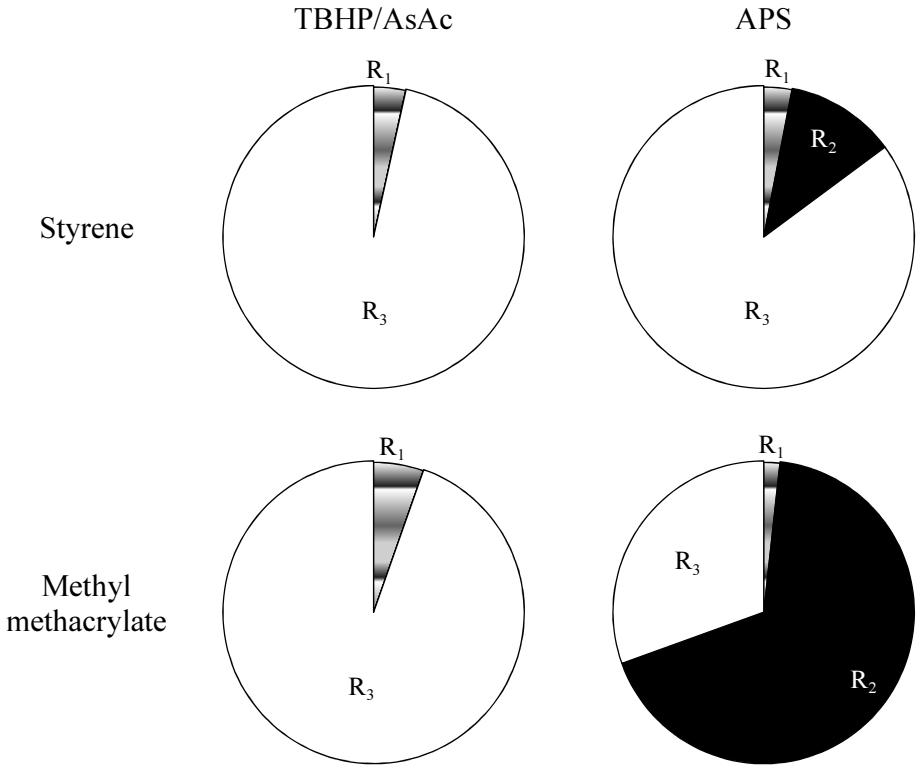

Figure 10: Relative importance of the different entry mechanisms
R_1: Diffusion, R_2: Electrical Repulsion, R_3: Hydrogen abstraction

These results may be explained as follows. When APS was used in the polymerization of styrene, the oxygen centered sulphate radicals which cannot enter into the polymer particles had a relative long life because the monomer concentration in the aqueous phase is very low. Therefore, they may approach the hairy layer abstracting hydrogens. In the polymerization of MMA, the concentration of the monomer in the aqueous phase was much higher, and therefore the life of the oxygen centered sulphate radicals was shorter.

Consequently, the rate of hydrogen abstraction was lower. The effect of the monomer concentration in the aqueous phase was modest for TBHP/AsAc because the *tert*-butoxy radicals can directly enter into the polymer particles.

3.3.3 Styrene miniemulsion polymerization with AIBN

In this section, the effect of using an oil soluble initiator (AIBN) that produce carbon centered radicals was investigated using the formulation given in Table 13.

Table 13: Miniemulsion polymerizations carried out with AIBN

Component	Initial charge (g)	Initiator solution as shot (g)
S	110	10
Hexadecane	2.40	
ASR_{AA} or ASR_{MAA}	9.60	
AIBN		1.20
Water	266.80	
Total	388.80	11.20

Figure 11 shows the effect of the ASR type on the monomer conversion for the experiments initiated with AIBN. Table 14 presents the most relevant data for these reactions. It can be seen that the polymerization rate was lower using ASR_{AA} than using ASR_{MAA}, even though the number of

particles was slightly higher for ASR_{AA} ($N_{p(MAA)}/N_{p(AA)} = 0.9$). However, the effect was lower than for the other initiators ($R_{pp(MAA)}/R_{pp(AA)} = 1.5$).

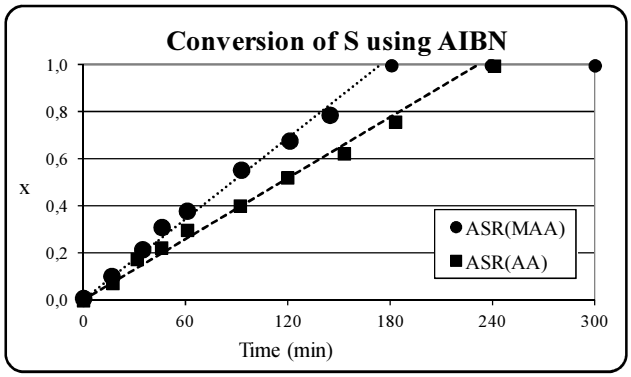

Figure 11: Effect of the ASR type on the kinetics of the styrene miniemulsion polymerization initiated with AIBN

Table 14: Main data for styrene miniemulsion polymerizations using AIBN as initiator

	R_p (g $L^{-1}s^{-1}$)	D_p (nm)	N_p (part L^{-1})	R_{pp} (g $part^{-1}s^{-1}$)	$\bar{n}$
ASR_{MAA}	0.0286	364	$1.13x10^{16}$	$2.5x10^{-18}$	8.9
ASR_{AA}	0.0210	352	$1.25x10^{16}$	$1.7x10^{-18}$	6.0
$\frac{ASR_{MAA}}{ASR_{AA}}$	1.4	1.03	0.9	1.5	1.5

The analysis of this system is more complex than for the previous cases. Figure 12 illustrates the radical fluxes in this system. Thermal decomposition of AIBN gives two radicals inside the polymer particles or droplets. In this case, electrical repulsion is not playing any role. Because

these radicals are confined in a very small volume, they terminate fast unless one of the radicals desorbs [20]. Therefore, the polymerization rate is only significant if one radical desorbs. The overall polymerization rate will be that due to the radicals which remains in the polymer particle plus the contribution of the radical that desorbs, provided that this one reabsorbs in another particle.

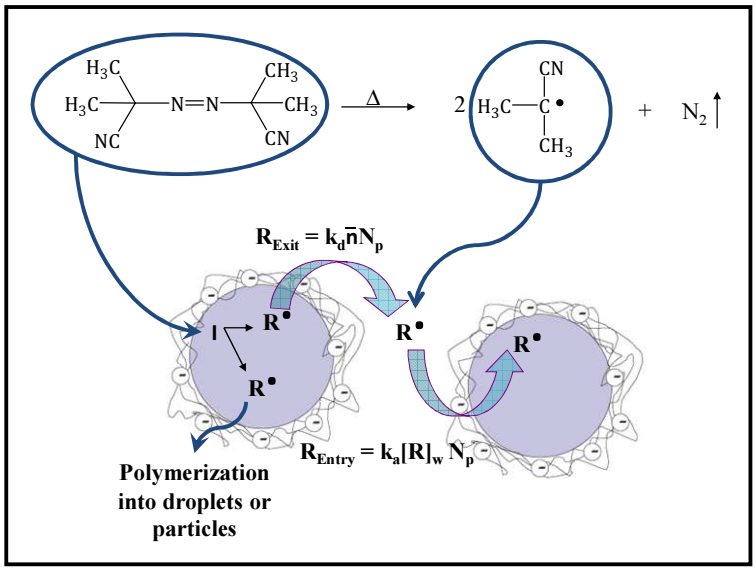

Figure 12: Behavior of AIBN in the reactions

The contribution of the desorbed radical will depend on the entry in other particles. Therefore, it should be inversely proportional to the resistance that has to overcome to enter in the particle. Thus, the polymerization rate per particle for the two ASRs can be written as follows:

$$(\mathrm{Rpp_{MAA}})_{\mathrm{AIBN}} = \mathrm{Rpp_1} + \mathrm{Rpp_2}^{\mathrm{MAA}} = \mathrm{Rpp_1} + \left(\frac{\mathrm{K}}{\mathrm{R_1}}\right)^{0.5} \quad (9)$$

$$(\mathrm{Rpp_{AA}})_{\mathrm{AIBN}} = \mathrm{Rpp_1} + \mathrm{Rpp_2}^{\mathrm{AA}} = \mathrm{Rpp_1} + \left(\frac{\mathrm{K}}{\mathrm{R_1} + \mathrm{R_3}}\right)^{0.5} \quad (10)$$

where R_{pp1} was the polymerization rate per particle of the radical that remains inside the particle, R_{pp2} the polymerization rate per particle of the reabsorbed radical, and K a proportionality coefficient. In this case, it is not possible to calculate the relative value between R_1 and R_3. Nevertheless, an estimation may be obtained from the mathematical modeling. It predicted that the contribution of the radicals that remained in the polymer particles was around 36% of the total polymerization rate [20]. Then, the following equation can be written:

$$\mathrm{Rpp_1} = 0.36\left(\mathrm{Rpp_1} + \left(\frac{\mathrm{k}}{\mathrm{R_1}}\right)^{0.5}\right) = \frac{9}{16}\left(\frac{\mathrm{k}}{\mathrm{R_1}}\right)^{0.5} \quad (11)$$

Therefore,

$$\left(\frac{\mathrm{Rpp_{MAA}}}{\mathrm{Rpp_{AA}}}\right)_{\mathrm{AIBN}} = \frac{25}{9 + 16\left(\frac{\mathrm{R_1}}{\mathrm{R_1} + \mathrm{R_3}}\right)^{0.5}} \quad (12)$$

Combining the Equation 12 and the value of $R_{pp(MAA)}/R_{pp(AA)}$ from Table 14 gave $R_3 = 3.3R_1$. Therefore, the resistance due to hydrogen abstraction was higher than that of the diffusion, but this value is much lower than the one found for TBHP/AsAc for styrene. The main reason for this

behavior is that AIBN gives carbon centered radicals that are less effective than oxygen centered radicals in the hydrogen abstraction from the polymeric chain.

3.4 Hydrogen abstraction from ASRs

The discussion on the mechanisms controlling radical entry in ASR stabilized miniemulsion polymerization was based on the relative polymerization rate per particle and it was concluded that chain transfer to ASR played a key role in the case of ASR_{AA}. Additional proof supporting this mechanism can be obtained analyzing the zone of the MWD corresponding to the ASR.

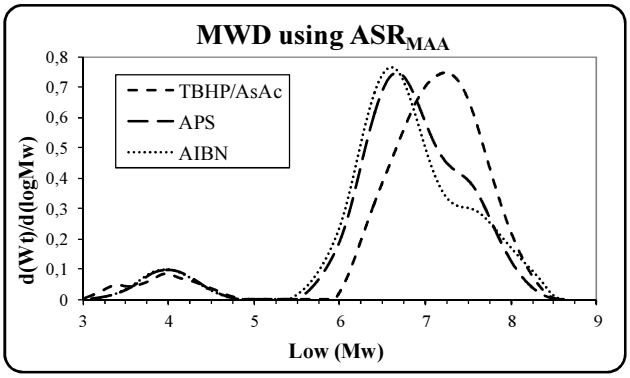

Figure 13: MWD of the final latexes obtained in the styrene miniemulsion polymerization stabilized with ASR_{MAA}

Figure 13 presents the MWD of the final latexes obtained in the styrene miniemulsion polymerizations stabilized with ASR_{MAA} and initiated with different initiators. It can be seen that a bimodal distribution was obtained. The high molecular weight peak corresponded to the main polymer and the low molecular weight one to the ASR.

Figure 14 presents the effect of the initiator on the small molecular weight peak for both, ASR_{MAA} and ASR_{AA}. The MWD of the pristine ASR was included as a reference. It can be seen that for ASR_{MAA} the low molecular weight peak closely corresponded to the MWD of the ASR.

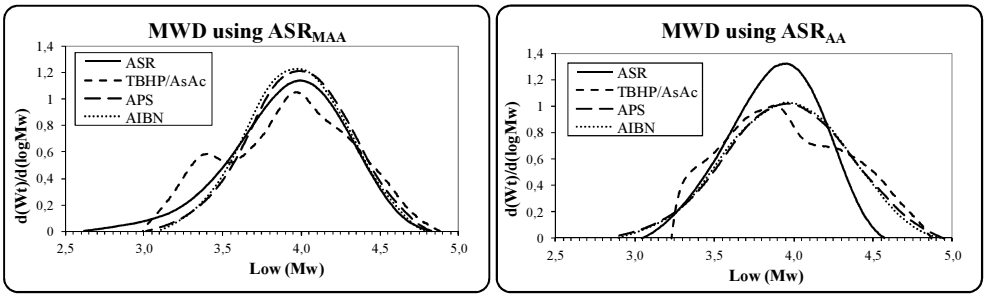

Figure 14: Effect of the initiator type on the small molecular peak (styrene miniemulsion polymerization). At left: ASR_{MAA}, and at right: ASR_{AA}

On the other hand, the MWD shifted to higher molecular weights for ASR_{AA} which proves that chain transfer to this ASR occurred. The shift seems to be higher for THBP/AsAc, but the differences are too small to be used as an additional proof for the higher abstraction activity of the *tert*-butoxyl radicals unveiled by the kinetic data.

3.5 Conclusions

A semi-continuos strategy for the synthesis of relatively homogeneous ASRs using a low concentration of SLS (0.25wt%) was developed. The molecular weight of the ASR was controlled by the oil-soluble chain transfer agent concentration. Almost complete incorporation of the acidic monomer (99.83wt% for MAA and 99.73wt% for AA) in the ASR was achieved. In order to achieve good water solubility at pH=10, the acid number of the ASRs were 143 $mg_{KOH}\,g_{ASR}^{-1}$ for ASR_{MAA} and 171 $mg_{KOH}\,g_{ASR}^{-1}$ for ASR_{AA}. The amphiphilic characteristics of the ASRs are strongly affected by the pH. CMC was determined at pH=10 finding that $CMC(ASR_{MAA})=0.015\ gL^{-1}$; and $CMC(ASR_{AA})=0.059\ gL^{-1}$, the difference likely due to higher content of carboxylic groups of the ASR_{AA}.

The relative significance of the three mechanisms proposed to justify the reduction of the radical entry in ASR-stabilized latexes was investigated. The three mechanisms considered were the resistance to radical diffusion, the charge repulsion, and the hydrogen abstraction. It was shown that the resistance to the radical entry depends on the type of ASR, the type of initiator, and the type of monomer used. Two monomers of different hydrophobicity (S, MMA), initiators producing different radicals in both aqueous and oil phases, and ASRs either prone or not prone to suffering hydrogen abstraction were used in several miniemulsion polymerizations.

For styrene (hydrophobic monomer), the polymerization rate when using APS (anionic hydrophilic radicals) was substantially reduced mainly because the ASR acted as a radical sink (due to hydrogen abstraction), but electrical repulsion was also important. For TBHP/AsAc (uncharged hydrophobic radicals), the effect was due to hydrogen abstraction and it was substantial.

For MMA (hydrophilic monomer), the effect of hydrogen abstraction was important (although slightly lower than for styrene) using THBP/AsAc. The effect of the monomer hydrophilicity was important when APS was used because the sulphate ion radicals must propagate in the aqueous phase before entering into the polymer particles. When the monomer concentration in the aqueous phase was very low (i.e., for S), the oxygen centered radical had a relative long life around the hairy layer, and hence they had the opportunity of abstracting hydrogens. When MMA, which has a relatively high concentration in the aqueous phase, was used, the life of the oxygen centered radical was shorter and the rate of hydrogen abstraction lower.

For the oil-soluble initiator (AIBN), the resistance due to hydrogen abstraction was higher than that of the radical diffusion. However, this value is much lower than that observed for TBHP/AsAc because carbon-centered radicals coming from AIBN are less effective than oxygen centered radicals in hydrogen abstraction.

The conclusions from the kinetic analysis were supported by the analysis of the MWD of the final latexes that showed that in the peak of the

ASR shifted to higher molecular weight for ASR_{AA} and remained unchanged for ASR_{MAA}.

3.6 References

1. Peck, A. N.; Asua, J. M. *Macromolecules* **2008,** 41, (21), 7928-7932.
2. Vorwerg, L.; Gilbert, R. G. *Macromolecules* **2000,** 33, (18), 6693-6703.
3. Thickett, S. C.; Gilbert, R. G. *Macromolecules* **2006,** 39, (6), 2081-2091.
4. Thickett, S. C.; Gilbert, R. G. *Macromolecules* **2006,** 39, (19), 6495-6504.
5. Ballard, N.; Urrutia, J.; Eizagirre, S.; Schäfer, T.; Diaconu, G.; de la Cal, J. C.; Asua, J. M. *Langmuir* **2014,** 30, (30), 9053-9062.
6. Nomura, M.; Harada, M., On the Optimal Reactor Type and Operation for Continuous Emulsion Polymerization. In *Emulsion Polymers and Emulsion Polymerization*, David R. Bassett, A. E. H., Ed. AMERICAN CHEMICAL SOCIETY: South Charleston, West Virginia, 1981; Vol. 165, pp 121-143.
7. Smith, W. V.; Ewart, R. H. *The Journal of Chemical Physics* **1948,** 16, (6), 592-599.
8. Nunes, J.; Asua, J. M. *Langmuir* **2012,** 28, (19), 7333-7342.

9. Nunes, J.; Asua, J. M. *Langmuir* **2013,** 29, (12), 3895-3902.

10. Greenlee, S. O. Alkali soluble resins and compositions containing the same. US 2890189 A, Johnson & Son, Inc., Racine, Wis., 1959.

11. Stevens; Langers; Parry; Rollison. Alkali soluble resin polymer and method of preparing the same. GB 1107249 (A) Johnson & Son S. C., 1968.

12. do Amaral, M.; Asua, J. M. *Macromolecular Rapid Communications* **2004,** 25, (22), 1883-1888.

13. Ugelstad, J.; El-Aasser, M.; Vanderhoff, J. *Journal of Polymer Science: Polymer Letters Edition* **1973,** 11, (8), 503-513.

14. Kato, S.; Sato, K.; Maeda, D.; Nomura, M. *Colloids and Surfaces A: Physicochemical and Engineering Aspects* **1999,** 153, (1), 127-131.

15. Hwu, H.-D.; Lee, Y.-D. *Journal of Polymer Research* **2000,** 7, (2), 115-123.

16. Wang, S.; Qiang, Y.; Zhang, Z.; Wang, X. *Colloids and Surfaces A: Physicochemical and Engineering Aspects* **2006,** 281, (1), 156-162.

17. Lee, D. Y.; Kim, J. H. *Journal of Applied Polymer Science* **1998,** 69, (3), 543-550.

18. Leemans, L.; Jérôme, R.; Teyssié, P. *Macromolecules* **1998,** 31, (17), 5565-5571.

19. Lee, D. Y.; Kim, J. H. *Journal of Polymer Science Part A: Polymer Chemistry* **1998,** 36, (16), 2865-2872.

20. Autran, C.; de La Cal, J. C.; Asua, J. M. *Macromolecules* **2007,** 40, (17), 6233-6238.

Chapter 4: Synthesis of electrosterically stabilized latexes using ASRs with acrylamide

Outline

4.1 Introduction

In the previous chapter, the radical entry and exit in ASR stabilized systems were analyzed. These ASRs had a high acid content to ensure their solubility in alkali media. The acid number depends on the acidic monomer amount. In order to reduce the content of the carboxyl groups, the hydrophobicity of the rest of the monomers should be reduced. This can be achieved by using more hydrophilic monomers such as acrylamide (AM). In this chapter, different ASRs containing MMA, BMA, MAA and AM were synthesized and characterized, and their effect on the polymerization in dispersed media was investigated.

4.2 Synthesis of ASRs using acrylamide

Technical grade monomers methyl methacrylate (MMA, Quimidroga), butyl methacrylate (BMA, Aldrich), methacrylic acid (MAA, Aldrich) and acrylamide (AM, Aldrich) were used as received. Sodium lauryl sulfate (SLS, Aldrich) and ammonium peroxodisulphate (APS, Panreac) were used as anionic surfactant and initiator, respectively. An oil-soluble chain transfer agent 1-Octanethiol (OcT, Aldrich), and three water-soluble chain transfer agents isopropanol (Is-P, Aldrich), 2-mercaptoethanol (M-Et, Aldrich) and formic acid (FA, Aldrich) were used. Ammonium hydroxide (NH_4OH, Fluka) was employed to neutralize the ASRs.

The synthesis of the ASR was carried out in a semi-continuous process already explained in Chapter 3 (Section 3.2). Almost all the water (5 ml was reserved to dissolve APS) and the total amount of emulsifier (SLS) were placed into the reactor as initial charge. When the reaction temperature (70ºC) was reached under nitrogen atmosphere and mechanical agitation (214 rpm), the initiator (APS) was added as a shot and the monomers and CTAs were fed for 5 hours. The monomers and CTAs were fed in two different streams, one with MMA, BMA, MAA and CTA_{Oil} (OcT) and other with AM and CTA_{Water} (Is-P, M-Et or FA). At the end of the feeding, the reaction was maintained for 1 hour in batch to maximize conversion. The reaction was carried out in a 1L jacketed reactor. The solids content was 30wt%. At the end of the polymerization, NH_4OH was added drop by drop in order to increase the pH up to 10 to obtain the ASR aqueous solution used later as emulsifier.

4.2.1 Acrylamide in the ASR backbone

To reduce the acid number of the ASRs, acrylamide (AM) was used. Water soluble acrylamide-based copolymers have proved to be very useful in a wide range of applications, from industrial and environmental fields [1,2].

In order to control the molecular weight in the particles and in the aqueous phase, CTA_{Oil} and CTA_{Water} were used. The oil phase composed by MMA, BMA and MAA had the same monomers than in the ASRs synthesized in Chapter 3 (Section 3.2); therefore, the same concentration of CTA_{Oil} (OcT,

3wt% with respect to the monomers) was employed. The CTA_{Water} (M-Et) concentration was varied from 1 to 12wt% with respect to the monomers. Unfortunately, massive coagulum was observed in all the cases using a low concentration (0.25wt%) of SLS. Probably the coagulation was due to the reaction of MAA with M-Et that reduced the amount of carboxyl groups available. This reaction was studied by Popovic et al.[3], who found that thio-esters are formed. In order to check the occurrence of this reaction, under the conditions employed in the synthesis, the mixture of MAA and M-Et was heated to 70ºC and a white dispersion was obtained, indicating that the reaction takes place.

A possible solution to avoid coagulation is to increase the concentration of SLS. This possibility was not considered to prevent the effect of SLS on the subsequent polymerizations that can mask the study of the performance of the ASR as emulsifier. Therefore, other CTA_{Water} [4,5] were tried. Formic acid (FA) prevented the formation of coagulum but the ASR did not dissolve after neutralization. Isopropanol (Is-P) allowed to obtaining stable latexes and also an easy dissolution after neutralization. For that reason, the Is-P was chosen as CTA_{Water}.

Several reactions were carried out varying the AM and Is-P concentrations with the minimum concentration of MAA (12wt%, $80 mg_{KOH} g_{ASR}^{-1}$) and 3wt% of CTA_{Oil} (that led to the adequate range of molecular weights in Chapters 2 and 3). It was found that 14wt% of AM and 3wt% of Is-P led to a transparent solution after neutralization. Figure 1

illustrates the effect of the AM concentration that gave a translucent solution with 6wt% and a nice transparent one with 14wt%.

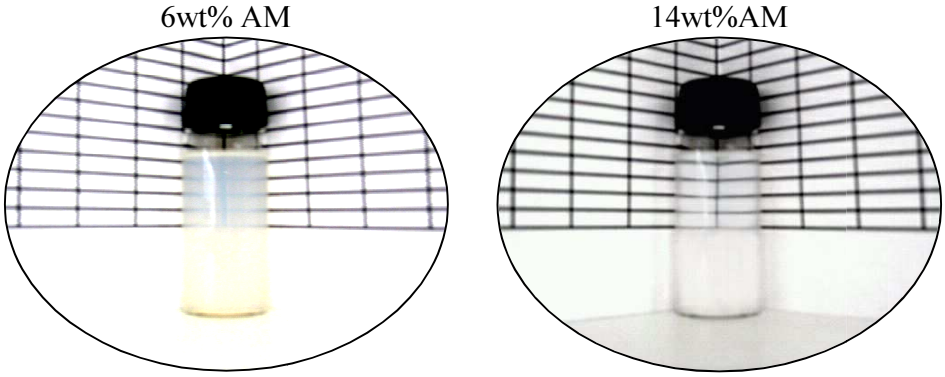

Figure 1: ASR solution after neutralization

Table 1: Formulation used for the synthesis of acrylamide containing ASRs

Ingredient	**Fraction (wt%)**	**Total charge (g)**
MMA/BMA/MAA/AM	30	255
CTA_{Water} (Is-P)	3[(a)]	7.65
CTA_{Oil} (OcT)	3[(a)]	7.65
SLS	0.25[(a)]	0.64
APS	1.5[(a)]	3.83
Water	68	575.23
Total	100	850
(a) wt% with respect to the monomer		

Table 1 summarizes the formulation used for the synthesis of AM containing ASRs. Using this formulation, the acid number (MAA

concentration) and the MMA/BMA ratio were varied as described in Table 2. Higher MMA/BMA ratios lead to more hydrophilic ASRs, which are expected to be solubilized easier. Therefore, a series of ASRs covering a broad range of hydrophilicity was synthesized. The hydrophilicity ranged as: ASR_5>ASR_3>ASR_2>ASR_4>ASR_1.

Table 2: Monomer ratio of the backbone of alkali soluble resins (ASR_1-ASR_5)

Name	**AM**	**MAA**	**MMA+BMA**	**MMA/BMA**
ASR_1	14wt%	12wt%	74wt%	3/4
ASR_2		14wt%	72wt%	
ASR_3		16wt%	70wt%	
ASR_4		12wt%	74wt%	1/1
ASR_5		16wt%	70wt%	

The evolution of conversion, particle size, number of particles and pH during the synthesis of these ASRs are shown in Figure 2. The conversion evolution (instantaneous as open symbols and cumulative as solid symbols) showed that the processes were conducted under rather starved conditions. The pH evolution increased from 2.5 to 4 for all the cases, likely due to the hydrolysis of the acrylamide. Finally, the evolution of particle size and the number of particles showed a limited coagulation. This behaviour can be attributed to the low concentration of emulsifier used (0.25wt% with respect to the monomers).

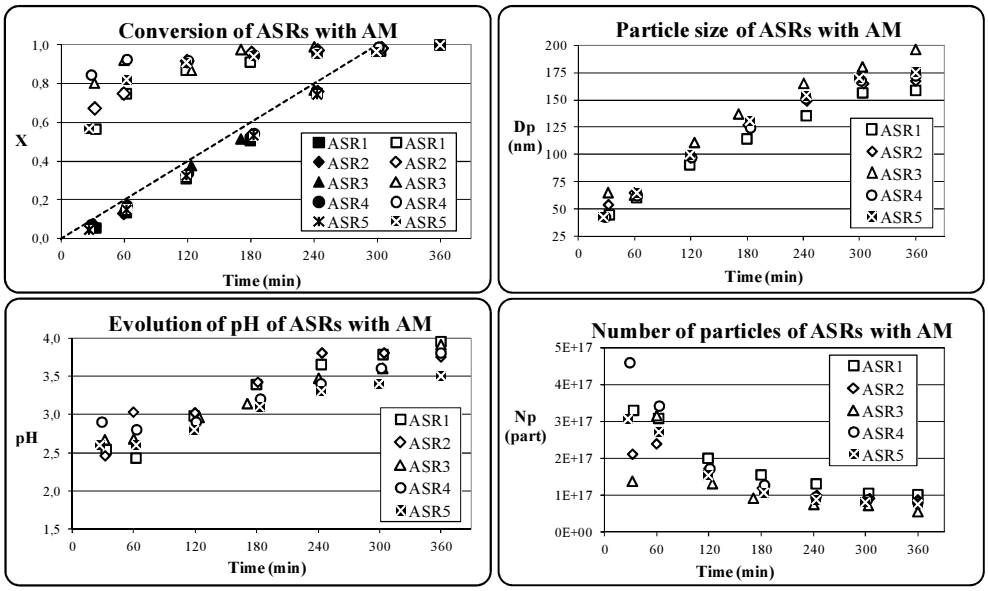

Figure 2: Evolution of conversion, particle size, pH and number of particles for the synthesis of different ASRs

4.3 Characterization of the ASRs

The intended use of the ASRs is as stabilizers in polymerization in dispersed media. Therefore, they should be efficient in both particle nucleation and stabilization. Ideally, the ASRs should form micelles at low concentration, diffuse fast, adsorb strongly on the polymer particles, have a faster adsorption-desorption equilibrium, provide good electrostatic or/and steric stabilization to the particles and be efficient at the reaction temperature. These properties are determined by the microstructure of the ASR. Therefore, in this section, the MWD, acid number and heterogeneity of the ASRs will be

determined first. Then, the colloidal properties (CMC, adsorption equilibrium and cloud point) will be determined.

4.3.1 ASRs Microstructure

4.3.1.1 Molecular weight distribution (MWD)

The most common method to measure the MWD is size exclusion chromatography (SEC), also referred as gel permeation chromatography (GPC). SEC is not an absolute method; as a result, it must be calibrated with PS standards. The sample preparation has been explained previously (see Chapter 3, section 3.2). One of the carriers more often employed in SEC was THF (that is almost a universal solvent for polymers). However, in the present case, the ASRs synthesized with AM were not fully soluble in this solvent.

The ASRs were subjected to shoxlet extraction with boiling THF to separate the soluble and insoluble parts. The insoluble fraction is shown in Table 3. It can be seen that a substantial insoluble fraction that increased with the MAA concentration was found. This strongly suggests that the insoluble fraction is related to the MAA-rich polymer produced in aqueous phase.

Table 3: Insoluble fraction of ASRs in THF

Insoluble fraction of ASR in THF (wt%)	**ASR_1**	**ASR_2**	**ASR_3**	**ASR_4**	**ASR_5**
	32.1	34.1	36.1	32.9	37.5

The MWDs of the soluble fractions are presented in Figure 3. It can be seen that the MWD was not affected by either the MAA content or the MMA/BMA ratio.

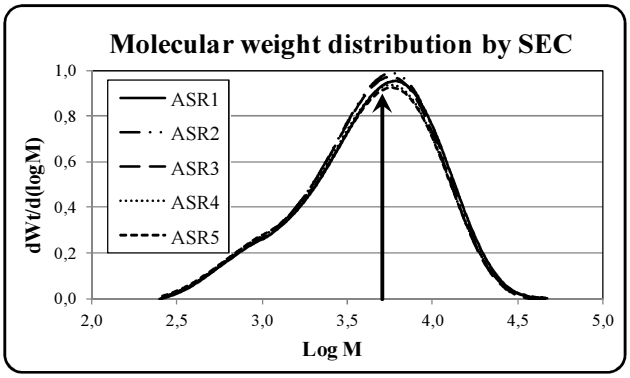

Figure 3: Molecular weight distribution of the part of the ASRs soluble in THF

The values of number and weight average molecular weights together with molar mass dispersity are presented in Table 4.

Table 4: $\overline{M}_n$ and $\overline{M}_w$ of soluble part of the ASRs using SEC

	ASR_1	**ASR_2**	**ASR_3**	**ASR_4**	**ASR_5**
$\overline{M}_n$ (g mol^{-1})	2170	2280	2120	2040	1910
$\overline{M}_w$ (g mol^{-1})	5740	5620	5480	5480	5390
Đ	2.6	2.5	2.6	2.7	2.8

In order to confirm that the insoluble polymer chains were mainly produced in the aqueous phase, new ASRs with the same overall composition than ASR_1 (12wt% of MAA, 14wt% AM and MMA/BMA=3/4) were

synthesized varying the concentrations of CTA_{Water} and CTA_{Oil} and their sol MWD measured by SEC. The results are presented in Figure 4. It can be seen that changes in CTA_{Water} did not produce any effect on the MWD, but the effect of CTA_{Oil} is clearly visible. Therefore, the fraction soluble in THF corresponded mainly to the oil phase polymerization, namely, to the fraction poor in MAA (and AM).

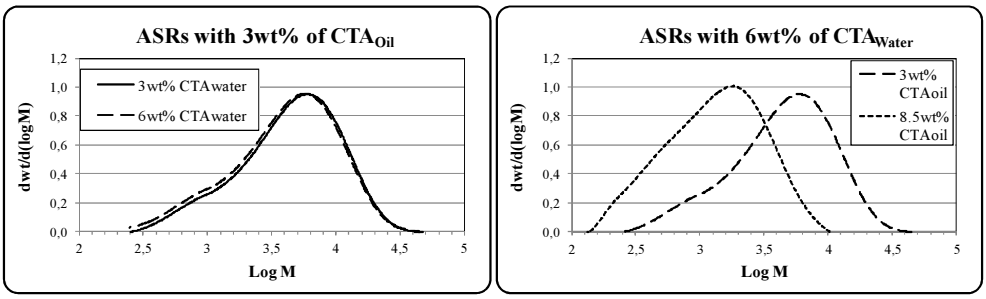

Figure 4: Molecular weight distributions of soluble part by SEC. At left, varying the CTA_{Water} amount, and at right, changing the CTA_{Oil} amount.

In an attempt to fully solubilize the ASRs, other solvents were used. Firstly, di-methyl sulfoxide (DMSO) was employed, but the problems of solubility persisted even at high temperature (close to 80ºC). Secondly, a SEC with an aqueous mobile phase (at basic pH adding NH_4OH) was utilized. In this case, the solubility was complete. However, the functional groups of the ASRs (COOH and $CONH_2$) interacted with the columns introducing artifacts in the measurement.

As it was not possible to obtain the whole MWD by SEC, attempts to determine the weight average molecular weight ($\bar{M}_w$) by means of Zimm [6]

plots (using a multi angle light scattering detector) were carried out using alkali medium (water with NH_4OH at pH=10) to solubilize the ASRs. Again, the results were unclear. The angular dependency of Zimm-plots fitted to curves instead of to straight lines. The curvature of the Zimm-plots is common in proteins and polyelectrolyte solutions and is indicative of association of macromolecules [7]. In our system, the formation of aggregates makes this technique not useful for measuring the absolute molecular weight of the ASRs.

Matrix-assisted laser desorption/ionization time of flight mass spectroscopy [8] (MALDI-TOF MS) was also used to determine the MWD. Mass spectroscopy is an absolute method to determine the molecular weight independently of their structure, using very low sample concentration and short analysis time. In this work, this technique can be employed to avoid the limitations observed for SEC and Zimm-plots.

Sample preparation for MALDI-TOF required an adequate matrix to embed the analyte (ASR). In this work, after testing different typical matrices and salts, the best results were obtained with sodium iodide (NaI) as salt and trans-2-[3-(4tertbutylphenyl)-2methyl-2propenylidene] malononitrile (DCTB) as matrix. The MWDs obtained for the ASRs are showed in Figure 5. It can be seen that the data lower than 1050Da are not observed owing to the matrix deflection used to avoid saturation of the detector signal. It can be seen that although the distribution were similar for molecular weights higher than 3000Da, substantial differences appeared for lower molecular weights. In particular, the relative fraction of smaller polymer chains increased with the

hydrohilicity of ASR (ASR_5>ASR_3>ASR_2>ASR_4>ASR_1). This suggests that the small molecular weights corresponded mainly to the polymer produced in the aqueous phase.

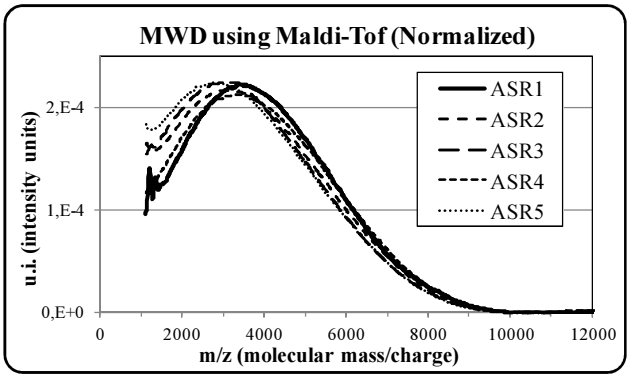

Figure 5: The MWD for ASRs using MALDI-TOF

The number average molecular weight ($\bar{M}_n$), weight average molecular weight ($\bar{M}_w$) and *Đ* ($\bar{M}_w/\bar{M}_n$) calculated from Figure 5 are presented in Table 5.

Table 5: $\bar{M}_n$ and $\bar{M}_w$ for ASRs using MALDI-TOF

	ASR_1	**ASR_2**	**ASR_3**	**ASR_4**	**ASR_5**
$\bar{M}_n$ (g mol^{-1})	3900	3700	3600	3900	3600
$\bar{M}_w$ (g mol^{-1})	4700	4600	4550	4800	4450
Đ	1.20	1.24	1.24	1.22	1.25

For all the ASRs, the dispersity is too low for a process in which termination is controlled by chain transfer to CTA, where the smallest possible value (corresponding to a polymerization in a single phase with a constant propagation transfer ratio) is equal to 2. Likely, the reason is that small

polymer chains were not observed. This means that $\overline{M}_n$ is overestimated, but likely the values of $\overline{M}_w$ had a lower error due to the higher contribution of high weight molecules.

Comparison between the results of SEC and MALDI-TOF shows that not very different $\overline{M}_w$ values were obtained in both cases. However, it may be surprising at first sight that the MWDs of the soluble part measured by SEC (Figure 3) show higher molecular weights. There are two reasons:

The first one is that a substantial part of the short chains are not soluble in THF, and hence the normalized MWD is shifted to higher molecular weights.

The second one is that a universal calibration based on polystyrene standards was used in the SEC measurements and as no values of Mark-Houwink constants for the ASRs were available, those of PS were used.

4.3.1.2 Acid number (N_{Ac})

The acid number was measured by conductometric titration [9] with NaOH (0.1N). The conductometric titration was explained previously (see Chapter 2, Section 2.2.2). The results are presented in Table 6.

Table 6: Comparison between theoretical and measured values of acid numbers

	MAA	**N_{Ac} (Theoretical)**	**N_{Ac} (Experimental)**
ASR_1	12 wt%	78	101
ASR_4			100
ASR_2	14 wt%	91	110
ASR_3	16wt%	104	113
ASR_5			113

It can be seen that the measured values were higher than the theoretical values. The reason may be due to the hydrolysis of the acrylamide units in alkaline medium [10,11] through the reaction presented in Figure 6. The extent of this reaction is limited when the ASR is neutralized by ammonia because for the case of the acrylamide (R'=H), the product of the reaction would be acrylic acid (AA) and ammonium hydroxide (NH_4OH). Therefore, the use of NH_4OH to increase the pH in the preparation of ASRs shifts the equilibrium to the left [11].

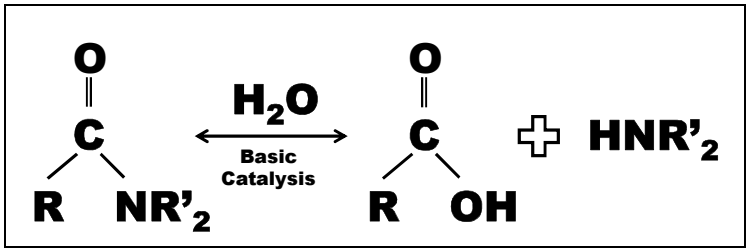

Figure 6: Hydrolysis suffered by amides under basic conditions such as those created by NaOH during the conductometric titration

The theoretical and experimental acid numbers of Table 6 are plotted in Figure 7 versus the MAA content.

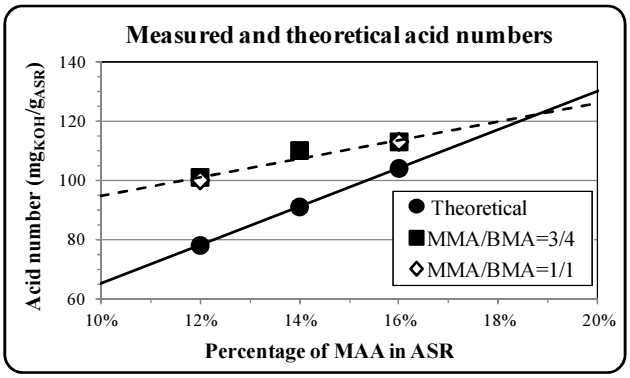

Figure 7: Measured and theoretical acid number versus MAA percentage

It can be seen that the MMA/BMA ratio does not seem to affect the AM hydrolysis. The fraction of AM hydrolyzed decreased when the concentration of MAA increased in the formulation. The reason for this behavior may be the repulsion between the negative charges formed that act against the hydrolysis [11]. As the fraction of acid units (from both initial MAA and formed AA) increases, the charge concentration present in the backbone increases reducing the probability of hydrolysis. A limited PAM hydrolysis of 70wt% was obtained by Kurenkov et al. [12] at basic conditions. The difference between the titrated carboxyl groups and those in the formulation provides an estimation of the extent of the hydrolysis. The values were 30wt% of hydrolysis for 12wt% of MAA, 21wt% for 14wt% of MAA and 9wt% for 16wt% of MAA.

4.3.1.3 Heterogeneity of the ASR chains

Emulsion polymerization is a heterogeneous reaction medium that due to several factors (reactivity ratios, partition coefficients, particle size distribution, etc) is prone to yield heterogeneous polymers in terms of both molecular weights and copolymer composition.

To measure the heterogeneity of the ASR's chains, a stock solution at pH=10 was evenly distributed in different vials. Afterwards, different quantities of hydrochloric acid (HCl) at 1M were added to each vial to vary the pH from 4 to 10. In order to maintain the solids content constant, the required amount of deionised water was added too. As a result, all the vials contained the same ASR concentration but the pH was different. Then, samples were stirred during one day in an orbital stirrer to reach equilibrium. Subsequently, the pH of every sample was measured again. These values were considered as actual values. After that, samples were centrifuged to separate aqueous and solid phase. For this purpose, an ultracentrifuge (Centrikon T2190) was used at 20,000rpm during 4hours at 20ºC. The aqueous phase (serum) contained the ASR chains soluble at the pH of the sample. The solid phase contained the insoluble fraction. It is important to ensure the absence of $ClNH_4$ precipitate that is produced by acid-base reaction between HCl and NH_4OH when the solubility limit is exceeded. Blank experiments without ASR were carried out and no evidence of $ClNH_4$ (which is able to precipitate as a white powder easily recognizable) was found.

The ASR chosen for this measurement was ASR_2 with 14wt% of MAA and MMA/BMA equal to 3/4. After centrifugation, the solids content and the amount of MAA in the serum were measured by gravimetry and conductometic titration respectively (Figure 8).

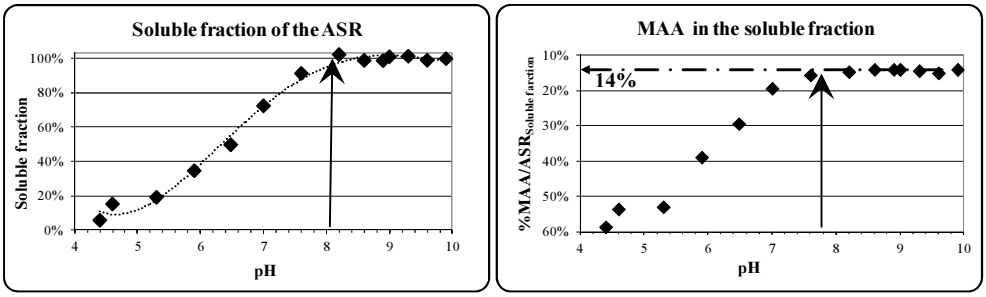

Figure 8: At left: soluble fraction of ASR_2 for different pH. At right: MAA percentage in the soluble fraction of the ASR_2 versus the pH

In the left part of the Figure 8, it can be seen that the fraction of ASR solubilized increased from about 10% at pH=4.5 to practically 100% at pH higher than 8.1 (arrow). The right part of the Figure 8 shows that at pH=4.5, the soluble part contained about 60% of MAA units. This fraction decreased as the pH increased and about pH=7.8 (arrow) the composition of the soluble part (which at this pH is close to 100%) approaches the value of the formulation (14wt%). These results indicated that heterogeneous ASRs were synthesized.

4.3.2 Colloidal properties

The presence of aggregates was studied first. Hence, the aggregate size distribution was measured using disc centrifuge photosedimentometer (DCP) at 14000 rpm at room temperature. The separation is based on the balance between centrifugal, viscous and buoyancy forces acting upon the particles that leads to an expression (Stokes law in integrate form) which gives the time, t, required for a particle of diameter, d, and density ρ_p to reach the detector position, R_d, from a starting position, R_i, in a fluid of density ρ_f and viscosity μ as:

$$t = \frac{18\mu \ln\left(\frac{R_d}{R_i}\right)}{\omega^2 d^2 (\rho_p - \rho_f)} \qquad (1)$$

where ω is the angular velocity of the disc.

Table 7 shows the number average ($D_{agg(n)}$) and volume average ($D_{agg(v)}$) diameters measured by DCP at pH=10.

Table 7: Average size of aggregates ($D_{agg(n)}$ and $D_{agg(v)}$)

	MMA/BMA	**%MAA**	**$D_{agg(n)}$ (nm)**	**$D_{agg(v)}$ (nm)**
ASR_1	3/4	12	36	53
ASR_2		14	36	53
ASR_3		16	36	55
ASR_4	1/1	12	34	54
ASR_5		16	29	47

It can be seen that the average values are similar for most of the ASRs. The more hydrophilic (ASRs) showed a slightly lower average diameter.

4.3.2.1 Critical micellar concentration (CMC)

Attempts to determine the CMC of the ASRs were carried out by measuring the surface tension of aqueous solutions at increasing ASR concentrations. As explained in Chapter 2 (Section 2.2.2.1) the surface tension gives a measure of the concentration of amphiphilic substances at the air-liquid interface. The results obtained at pH=10 using a SIGMA KSV70 tensiometer are presented in Figure 9. It can be seen that for all ASRs, the surface tension (γ) was not affected at low ASR concentrations (notice that a log scale is used in the x axis). At higher concentrations a sharp decrease of γ was observed and later the slope decreased but still was clearly negative. This behavior deviates from what is expected from a homogeneous surfactant that at a certain concentration saturates the air-liquid interface and no further decrease of γ is observed upon addition of more ASR. This critical concentration is the CMC and it is considered to be the concentration at which micelles are formed.

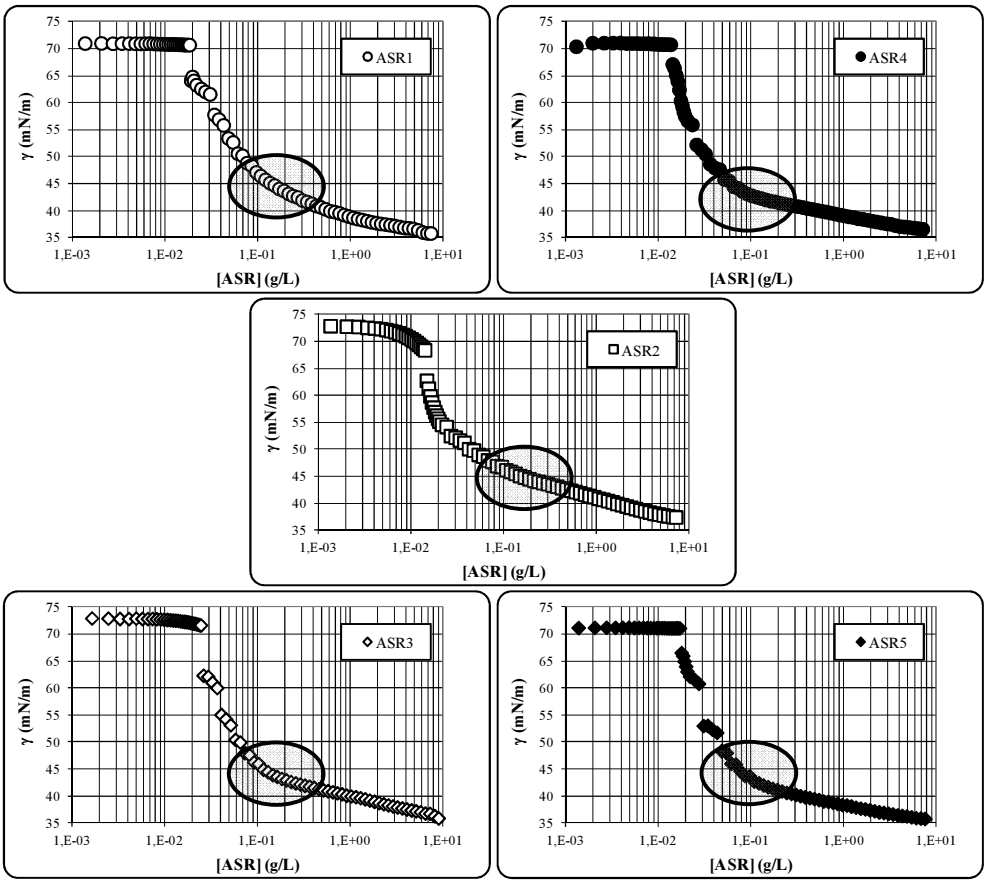

Figure 9: Variation of surface tension with the concentration of ASR

According the Gibb's equation [13] the continuous decrease of γ indicates that the concentration of amphiphilic substance at the air-liquid interface continuously increased. The reason likely was that the ASRs were composed by a broad range of species with different adsorption equilibria. At low concentration of ASR, all the species adsorb at the air-liquid interface according the individual adsorption equilibrium. The species with higher

adsorption constants become depleted in the aqueous phase. As they are not present in a high amount, they leave space for the adsorption of the other species. As the total concentration of ASR increases, the interface air-liquid becomes more crowded and the species with lower adsorptions constants are replaced by those with higher constants. This results in a continuous increase of the concentration of amphiphilic compounds at the interface air-liquid, and hence in a decrease of the surface tension.

Table 8: CMC of the ASRs from surface tension measurements

	MMA	**MMA/BMA**	**CMC (g/L)**
ASR_1	12%	3/4	0.05-0.5
ASR_2	14%		
ASR_3	16%		
ASR_4	12%	1/1	0.03-0.3
ASR_5	16%		

A consequence of the broad range of species contained in the ASRs is that the ASRs do not present clear CMCs. An estimation of the region where micelles (aggregates) can be formed may be obtained from the change in slope in the plots presented in Figure 9 (Table 8), but these are only crude estimates. Therefore, a method to detect the presence of aggregates based on the fluorescence of pyrene was used.

The fluorescence spectrum of pyrene shows strong solvent dependence [14-21]. Pyrene is a strongly hydrophobic compound and its

solubility in water is very low (2-3 μM). In presence of the micelles, pyrene is preferentially solubilised in the interior of the hydrophobic regions of these aggregates. As a result, the fluorescence spectrum of pyrene strongly changes as illustrated in Figure 10. This phenomenon has been used to detect the formation of micelles [17-21], which has been associated to changes in the ratio of the intensities of the first and third peaks [22].

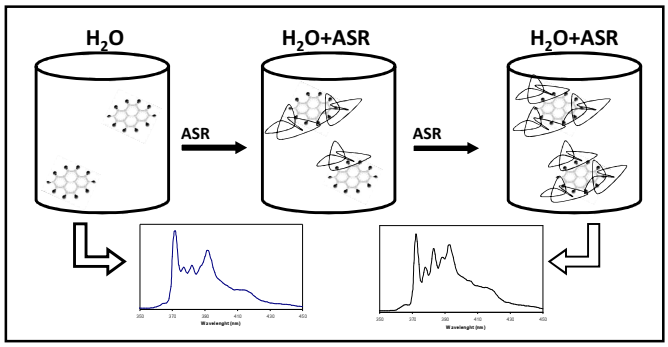

Figure 10: Scheme of pyrene behavior in presence of ASR aggregates and their emission spectra

For homogeneous surfactants this change is very sharp allowing an accurate estimation of the CMC. Using this method, Kalyanasundaran and Thomas [23] obtained an excellent agreement with the CMC values reported in the literature [24]. Furthermore, they said that the pyrene I_3/I_1 ratio was independent of the surface concentration and/or the presence of external additives such as electrolytes.

In the present work, the measurements were carried out in a FluoroMax-3, JOBIN YVON, Horiba (Japan) using pyrene as fluorescent

probe in a quartz cuvette. Before measurements, to obtain pyrene dissolved in water instead of fixed to the glass wall, the solution must be sonicated during 90 min. An excitation wavelength of 310 nm was used and the emission spectrum is recorded between 350-450 nm wavelength. The scan time was fixed at 2 seconds per nanometre of wavelength, namely, 200 seconds per scan. The slit width for excitation was fixed at 5 nm and for emission at 1 nm.

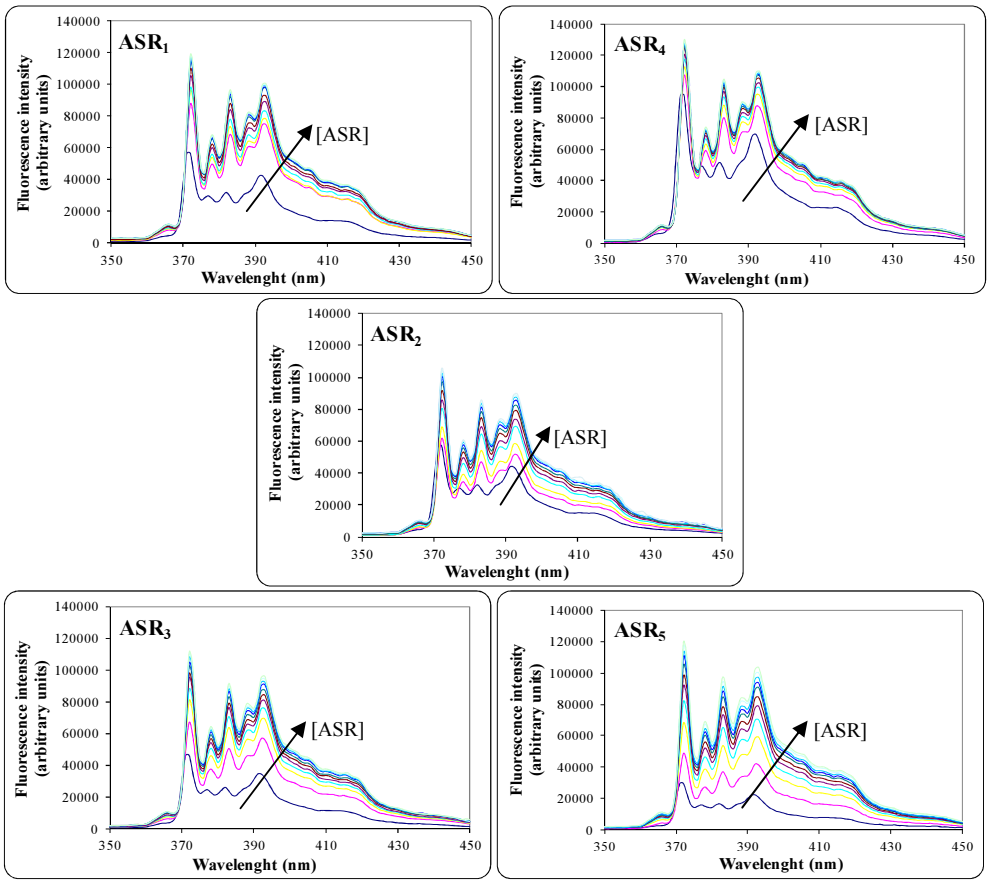

Figure 11: Pyrene emission spectrum in water at different ASR concentrations for ASR_1, ASR_2, ASR_3, ASR_4 and ASR_5

Figure 11 shows the effect of the addition of the ASR on the spectrum of emission of pyrene. All measurements were taken at 298±0.1ºK and pH=10. It can be seen that both the magnitude of the five characteristic peaks as well as their relative heights changed. Figure 12 shows the evolution of the ratio I_3/I_1 with the ASR concentration for the different ASRs. Throughout the experiment, the values of I_3/I_1 were in the range of polar solvents [23]. It can be seen that only a gradual increase of I_3/I_1 with increasing the ASR concentration was observed. Again, the reason was the heterogeneity of the ASRs in terms of composition (Figure 8) and also because of their broad molecular weight distribution (Figures 3 and 5).

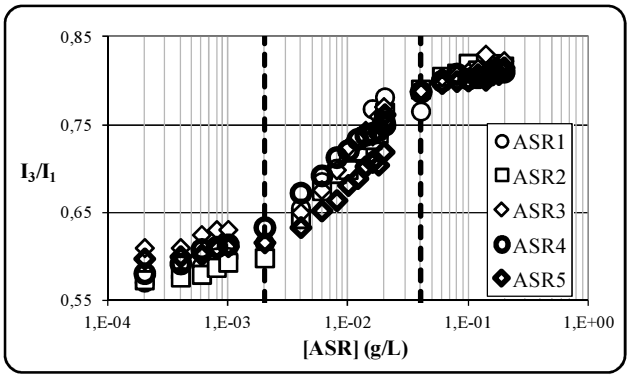

Figure 12: Ratio I_3/I_1 versus ASR concentration

The same behaviour was observed by the commercial ASR employed by Lee and Kim [25]. As a consequence, the CMC cannot be determined by this method. In any case, it seems that as it can be seen in Figure 12 the formation of aggregates takes places at very low ASRs concentrations (≈ 0.002g L^{-1}).

Figure 13 compares the evolution of the γ with that of I_3/I_1. It can be seen that the pyrene method was more sensitive at low ASR concentrations.

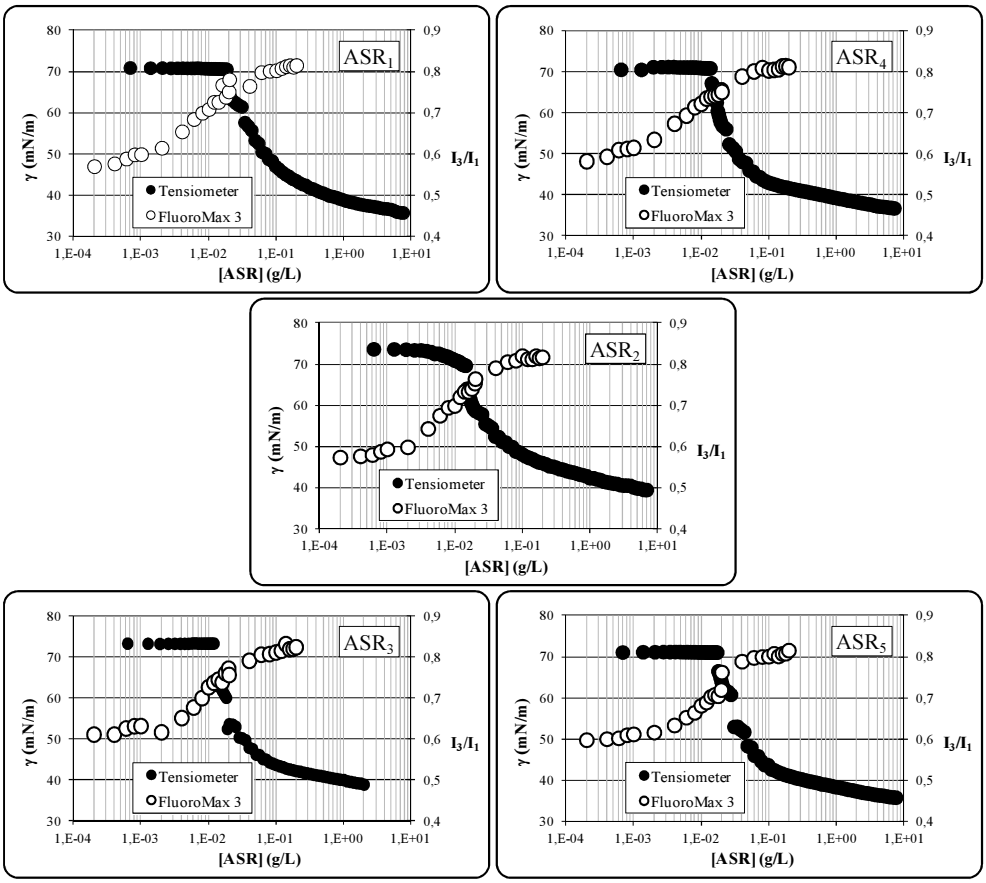

Figure 13: Comparison between both measurements; using Tensiometer (●) and using Espectrofluorimeter (○)

4.3.2.2 Adsorption of ASRs onto PMMA particles

The parking areas of the ASRs on poly(methyl methacrylate) were determined using the method explained in Chapter 2 (Section 2.2.2.2). Figure 14 presents the evolution of the surface tension in the presence and absence of cleaned PMMA particles for ASR_1, ASR_3, ASR_4 and ASR_5. All measurements were performed at pH=10 by adding NH_4OH.

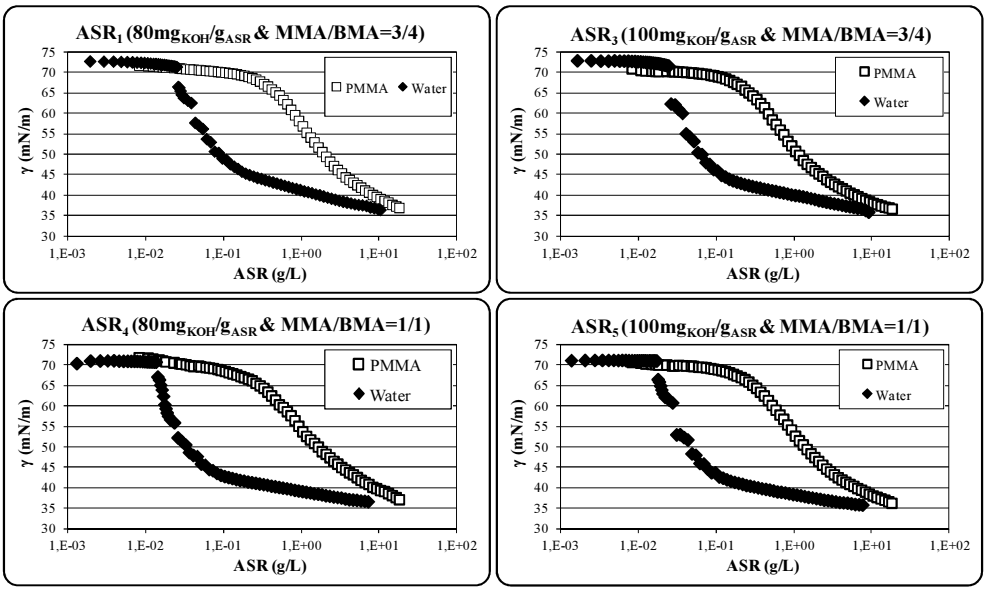

Figure 14: Surface tension versus ASR concentration in presence and absence of PMMA particles

At each value of γ, the difference between curves is a measure of the amount of ASR adsorbed on the polymer particles. Figure 15 shows the

amount of the ASR adsorbed onto the polymer particles versus the ASR concentration in water.

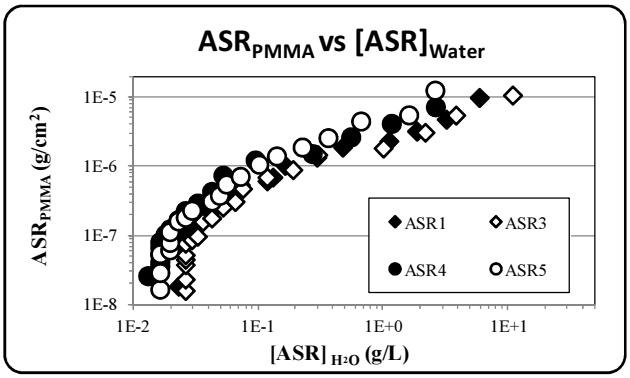

Figure 15: ASR onto PMMA particles versus ASR dissolved into water

Several mathematical models [26] have been developed to describe the adsorption isotherms. One of the most common is that of Langmuir [27]. This type of adsorption is valid only under certain restrictive conditions [28]: (i) the adsorbent is homogeneous; (ii) both solute and solvent have equal molar surface areas; (iii) both surface and bulk phases exhibit ideal behavior, namely, there are not interactions between adsorbed molecules; and (iv) the adsorption film is monomolecular. Many surfactant solutions show Langmuir-type behavior even when these restrictions are not strictly met.

Langmuir developed a simple model to predict the adsorption equilibrium. It is based on the idea that at equilibrium, adsorption and desorption rates are equal.

$$k_{ad}[ASR]_{H_2O}(S_0 - S_p) = k_{ds}S_p \quad (2)$$

where S_0 is the surface area of the particles (cm^2), S_p is the area of particles covered by the emulsifier (cm^2), $[ASR]_{H_2O}$ is the concentration of emulsifier in water (gL^{-1}), and k_{ad} and k_{ds} are the adsorption and desorption rate constants respectively. Equation 4 can be rewrite as follows:

$$\frac{S_p}{S_0} = \frac{b[ASR]_{H_2O}}{1 + b[ASR]_{H_2O}} \quad (3)$$

where $b=k_{ad}/k_{ds}$ in Lg^{-1} and the S_p/S_0 is the fraction of covered area. This fraction can be expressed in terms of the amount of ASR adsorbed onto the particles:

$$\frac{S_p}{S_0} = \frac{ASR_{PMMA}}{S_0} a_s \quad (4)$$

where ASR_{PMMA} is the amount of ASR adsorbed (g) and a_s is the parking area, which is defined as the area covered by one gram of ASR (in cm^2g^{-1}) at saturation conditions. Combination of equations 3 and 4; yields:

$$\frac{S_0}{ASR_{PMMA}} = a_s + \frac{a_s}{b}\frac{1}{[ASR]_{H_2O}} \quad (5)$$

Therefore, a_s and b can be obtained from the intercept and the slope of the S_0/ASR_{PMMA} vs $1/[ASR]_{H2O}$ plot.

Figure 16 compares the results for the ASRs with varying MMA/BMA ratios and acidic monomer amounts (12 and 16wt%).

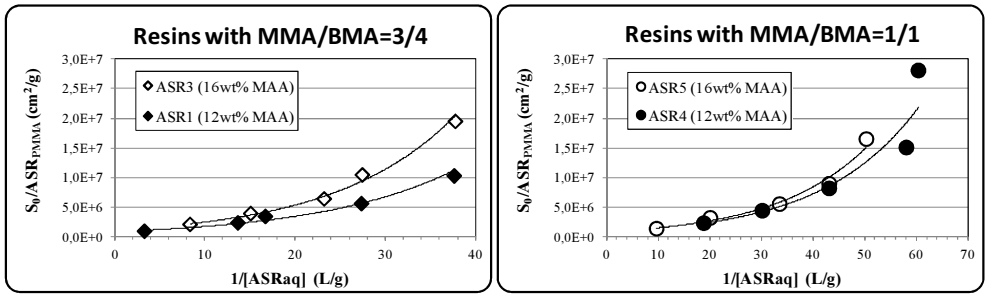

Figure 16: Langmuir adsorption isotherm for; (at left) resins with MMA/BMA=3/4 and (at right) resins with MMA/BMA=1/1

It can be seen that the adsorption behavior for all the ASRs does not correspond to a Langmuir isotherm since the experimental data points do not fit straight lines. In addition, the adsorption on the polymer particles increased with the hydrophobicity of the resin. This behavior was more evident for the resins with a MMA/BMA ratio of 3/4 (left of Figure 16). At higher MMA content (right of Figure 16), the differences in the amount of adsorbed ASR are less evident. It seems that for the greater MMA content, the effect of the acid amount becomes weaker. The better compatibility between the ASRs with higher MMA content and the PMMA polymer particles largely determines the adsorption equilibrium the hydrophilicity being a secondary factor.

In Figure 17, the adsorption of the ASRs with the same acid content (12wt% at left and 16wt% at right) but different MMA/BMA ratios is compared.

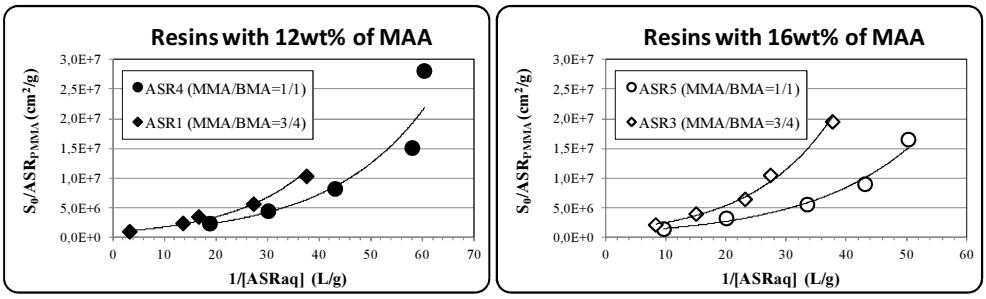

Figure 17: Langmuir adsorption isotherm for resins with 12 wt% of MAA at left and resins with 16 wt% of MAA at right

Figure 17 shows that for the same acid content, the ASRs with higher amount of MMA in the backbone exhibit a greater adsorption although they are more hydrophilic. Again, the compatibility with the polymer appears to be the determining factor in the adsorption equilibrium counteracting the effect of the increased hydrophilicity.

4.3.2.3 Cloud point of the ASRs

The cloud point is the temperature above which the non-ionic surfactant becomes insoluble in the medium leading to formation of large aggregates. These aggregates are much bigger than micelles and disperse light. Therefore, the solution becomes milky. Above the cloud point, the surfactant becomes inefficient. None of the ASRs (ASR_1-ASR_5) showed a cloud point from 20ºC to 90ºC.

4.4 ASRs as stabilizers in batch emulsion polymerization of MMA/BA

Most of the industrial emulsion polymerization processes are carried out in semi-continuous reactors [29] because these reactors allow a good control of temperature and polymer characteristics. In these processes, a relatively low solids content initial charge is often polymerized in batch and then the feeding of the monomers is started. The goal of the polymerization of the initial charge is to form the polymer particles, which are made to grow during the semi-continuous operation. Therefore, it is important to understand the behaviour of the ASRs in the batch polymerization of the initial charge.

Table 9: Formulation used in MMA/BA batch emulsion polymerization with different ASRs

Ingredients		**Total charge (g)**			**Concentration (wt%)**		
MMA		24	60		40	15	
BA		36			60		
APS		0.6			1[(a)]		
ASR_1	ASR_3	9	15	21	15[(a)]	25[(a)]	35[(a)]
ASR_4	ASR_5						
Water		340			85		
(a) % with respect to the monomer							

Batch emulsion polymerizations of butyl acrylate (BA) and methyl methacrylate (MMA) were carried out using technical grade monomers (from

Quimidroga). The 40/60 wt/wt MMA/BA reactions were carried out in batch emulsion polymerization during 1 hour. A pre-emulsion formed with water, ASR and the monomers was heated to 60ºC (reaction temperature) under nitrogen atmosphere and mechanical agitation with an anchor stirrer (~ 200 rpm). Then, ammonium persulfate (APS, Panreac) was added as a shot. The monomer/H_2O ratio was fixed at 15/85 and 15, 25 and 35wt% of ASR based on the monomers was used. As a result, the solids contents were 17.25, 18.25 and 20.25wt%, respectively. The formulation is summarized in Table 9.

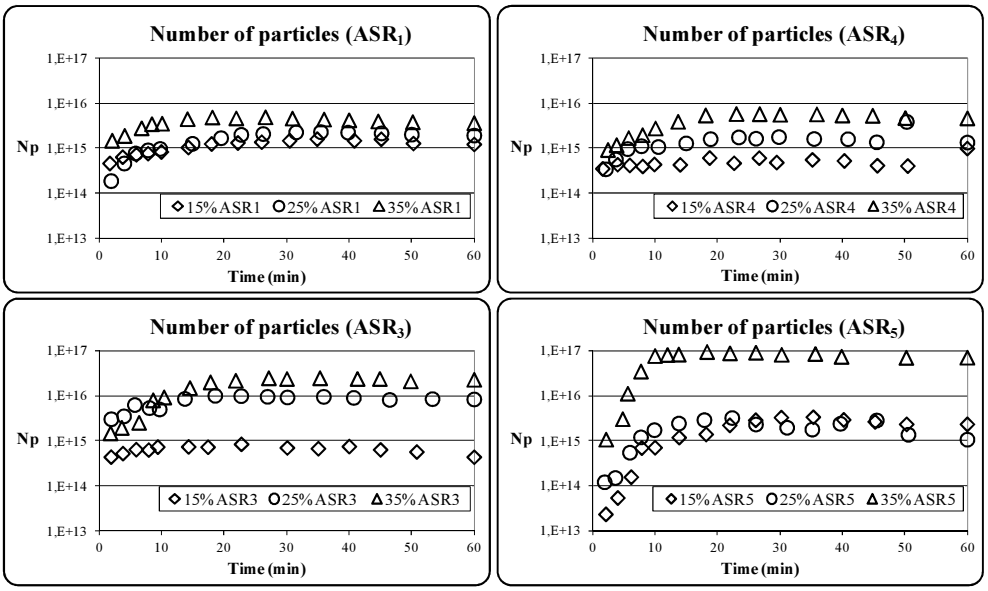

Figure 18: Number of particles obtained in batch emulsion polymerization at 60ºC using different types and concentrations of ASR

Is worth remembering that ASR_1 and ASR_4 contained 12wt% of MAA (N_{Ac}=80 mg_{KOH} g_{ASR}^{-1}), and ASR_3 and ASR_5 had 16wt% of MAA

(N_{Ac}=100 mg_{KOH} g_{ASR}^{-1}). In addition, for ASR_1 and ASR_3 MMA/BMA=3/4 whereas for ASR_4 and ASR_5 this ratio was 1/1. For all the ASRs, the AM amount was fixed in 14wt%.

Samples were withdrawn during the reaction and the conversion was measured by gravimetry and the particle size by dynamic light scattering (using water at pH=10). Figures 18 and 19 show the evolution of the number of particles (N_p) and monomer conversion in these reactions.

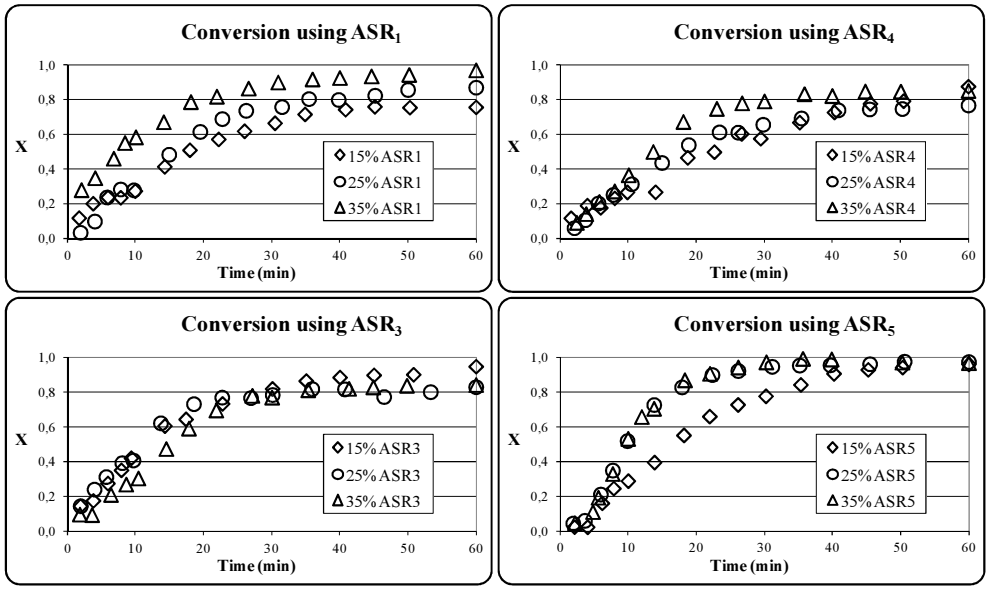

Figure 19: Evolution of the conversion in batch emulsion polymerization at 60ºC using different types and concentrations of ASR

For all ASRs, the number of particles increased with the ASR concentration and particle nucleation occurred during the first 10-15 min. This

corresponded to conversions in the range 40-60wt%, namely, particle nucleation occurred during a substantial part of the polymerization.

Figure 20 presents the effect of the ASRs concentration on the final number of particles for the different ASRs.

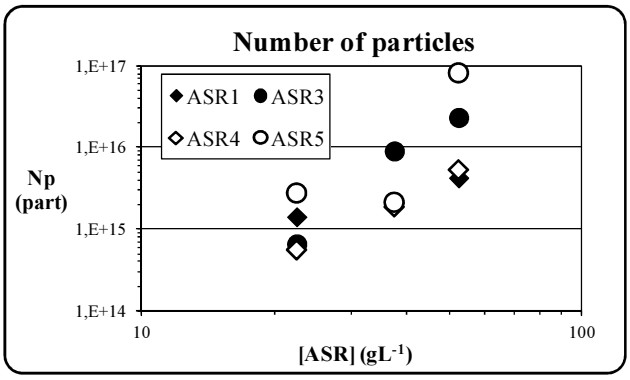

Figure 20: Influence of the ASR content on the number of particles

For conventional surfactants, Smith and Ewart [30] predicted that $N_p \div [S]^{0.6}$. Therefore, the present data have been fitted to $N_p \div [ASR]^Z$. The values of Z for the different ASRs are given in Table 10. It can be seen that for all the ASRs, Z was much larger than 0.6 and that Z substantially increased with acid content. This increase was more marked for the ASRs with lower ratio MMA/BMA.

The Smith-Ewart [30] theory was based on the assumptions that particles were formed by a micellar nucleation and that micelles disappear in the system before the monomer droplets. On the other hand, Harada and Nomura [31]

found that for a constant amount of surfactant, the number of particles increased when the amount of monomer was reduced in such a way that monomer droplets disappear before the micelles. This finding has been used to synthesize nanolatexes of relatively high solids content using a small surfactant/polymer ratio [32]. In these studies, it was found that particle nucleation extended beyond the depletion of micelles and that the extent of nucleation was higher for anionic than for non-ionic surfactants [33]. This was explained in terms of the faster diffusion of the smaller ionic surfactants that were able to reach the rapidly growing surface area of the particles of the particle precursors stabilizing them. However, recent results have demonstrated that the differences between ionic and non-ionic surfactants is not due to diffusion rates (which are quite similar), but to the slower desorption rate of the non ionic surfactants [34].

Table 10: Dependence of particle number with ASR's concentration for each system

	N_{Ac} (mg_{KOH} g_{ASR}^{-1})	MMA/BMA	$N_p \sim [ASR]^Z$
ASR_1	80	3/4	Z= 1.26
ASR_3	100		Z= 4.28
ASR_4	80	1/1	Z= 2.64
ASR_5	100		Z= 3.63

The application of these concepts to a system stabilized with heterogeneous ASRs is not straightforward, but they can shed some light on the process. In the present case, high ASR/monomer ratios were used (3/20; 5/20 and 7/20). Therefore, it is expected that monomer droplets were depleted

before the ASR micelles/aggregates. This would boost the number of particles generated yielding high values of Z. On the other hand, ASR_3 and ASR_5 had plenty of low molecular weight species (Figure 5) which were mainly formed in aqueous phase, namely they are rich in AM and MAA units. These species are expected to desorb more rapidly than the more hydrophobic ones and hence, they are able to stabilize the rapidly growing precursor particles, increasing the number of polymer particles, and consequently the values of Z (Table 10).

The polymerization rate (R_p) for all the emulsion polymerizations was calculated from the initial slope of the conversion-time curves (from Figure 19). Then, the polymerization rate per particle ($R_{pp} = R_p/N_p$) was also estimated. The N_p employed was the final value of N_p that remains constant for conversions higher than 40%. Both, R_p and R_{pp}, are presented versus N_p in Figure 21.

For the ASRs with lower N_{Ac} (ASR_1 and ASR_4) the polymerization rate (R_p) increased with N_p, namely, with the ASR concentration. However, using ASR_3 as stabilizer, the R_p did not increase with N_p and a slight decrease was observed for the 35wt% of ASR_3. A similar although less strong effect can be seen for ASR_5 where almost the same R_p was obtained using 25 and 35wt%, even though they had very different N_p. This suggests that entry rate into polymer particles of sulphate containing radicals was hindered by the charge repulsion, as explained in Chapter 3, Section 3.3.2.

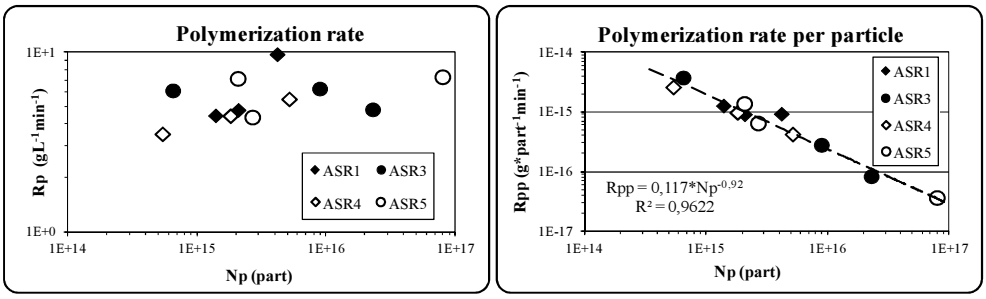

Figure 21: Influence of the number of particles (N_p) in the polymerization rate (R_p) at right, and on the polymerization rate per particle (R_{pp}) at left

It can be seen that in general, the polymerization rate was independent of the number of particles (N_p) and consequently the polymerization rate per particle (R_{pp}) was inversely proportional to N_p. The polymerization rate per particle depends on the propagation rate coefficient, the concentration of monomer in the particles and the average number of radicals per particle ($\bar{n}$). As the temperature used and the monomer concentration were the same, $\bar{n}$ was inversely proportional to the N_p as shown in Figure 22 that presents the values of $\bar{n}$ estimated from the experimental data.

According to the Smith-Ewart theory [30], $\bar{n}$ is inversely proportional to N_p when the system follows Cases 1 and 3 in the absence of termination in the aqueous phase. In addition, under Case 1 conditions, $\bar{n}$ is inversely proportional to N_p even in the presence of termination in the aqueous phase. It can be seen in Figure 22 that for most of the cases, $\bar{n}$ was much smaller than 0.5 (below the horizontal line). Therefore, the reactions proceeded under Smith-Ewart Case 1.

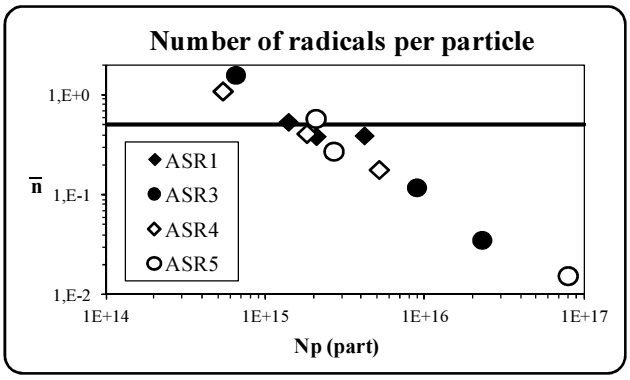

Figure 22: Average number of radicals per particle for four ASRs

4.5 Miniemulsion polymerization process stabilized by ASRs

In this section, the performance of the ASRs in batch miniemulsion polymerization was studied. The organic phase composed of the monomer (MMA or S) and the co-stabilizer (hexadecane) was mixed and stirred during 15-20min with the ASR aqueous solution forming a coarse dispersion. This dispersion was sonicated with a Branson Sonifier® 450 (400w; 20kHz). The amplitude was set to 80% and the sonication time was 20min. In order to avoid overheating, the dispersion was placed in an ice bath, sonication was stopped every 54 seconds and the sample was kept at rest for 6 seconds. The miniemulsion was introduced into a 0.5L glass jacketed reactor and heated until 60°C under 220rpm (anchor stirred) and nitrogen atmosphere. Then, the

initial pH was set equal to 10 by adding NH_4OH (if necessary). Finally, the initiator (APS) was added as a shot.

4.5.1 Miniemulsion polymerization of MMA

The formulation used in the miniemulsion polymerization is shown in Table 11. The MMA/H_2O ratio was fixed to 3/7 (30wt% of solids content) and the fraction of the rest of the components are given based on monomer. The concentration of the ASRs was varied between 4 and 8wt%. A 1wt% of APS and 2wt% of hexadecane were used.

Table 11: Formulation used in the MMA batch miniemulsion polymerization with different ASRs

Ingredients		**Total charge (g)**		**Concentration (wt%)**	
MMA		120		30	
Hexadecane		2.4		2[(a)]	
ASR_1	ASR_3	4.8	9.6	4[(a)]	8[(a)]
ASR_4	ASR_5				
APS		1.2		1[(a)]	
Water		280		70	
(a) % with respect to the monomer					

Table 12 presents the droplet diameters measured by DLS in a Coulter N_4^+ diluting the miniemulsion in a monomer saturated aqueous phase at pH=10. The number of droplets (N_d) was calculated assuming spherical

droplets. It can be seen that the number of droplets increases with the ASR concentration. ASRs with higher acid number (ASR_3 and ASR_5) yielded smaller droplet sizes (i.e., higher N_d). For the same acid content, the differences in droplet size were small, larger sizes were achieved for higher MMA/BMA ratios. These results seems be in agreement with the adsorption behavior of the ASRs onto PMMA polymer particles studied in Section 4.3.2.2. As a general rule, for the ASRs with the same MMA/BMA ratio, the adsorption is higher for the more hydrophobic ones leading to the higher droplets diameter (ASR_1>ASR_3 and ASR_4>ASR_5). On the other hand, for the same acid content, greater adsorption is obtained for the higher MMA/BMA ratio leading also to a larger droplet diameter (ASR_4>ASR_1 and ASR_5>ASR_3).

Table 12: MMA droplets formed by miniemulsion using 4wt% and 8wt% of ASRs varying their backbone

	4wt% ASRs		**8wt% ASRs**	
	D_d (nm)	**N_d (droplets)**	**D_d (nm)**	**N_d (droplets)**
ASR_1	389	$4.1*10^{15}$	242	$1.8*10^{16}$
ASR_3	180	$4.2*10^{16}$	99	$2.5*10^{17}$
ASR_4	384	$4.3*10^{15}$	267	$1.3*10^{16}$
ASR_5	206	$2.8*10^{16}$	126	$1.2*10^{17}$

The stability of these miniemulsions was checked using a Turbiscan Labexpert (Formulaction) at 60ºC that was the reaction temperature. The results are shown in Figures 23 and 24 for 4 and 8wt% of ASR, respectively.

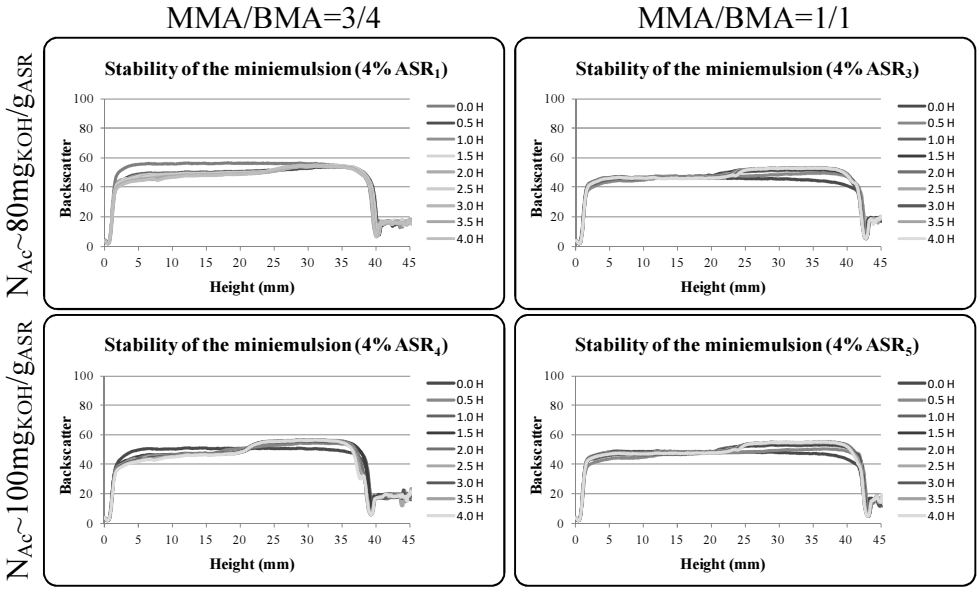

Figure 23: Stability of the miniemulsion using 4wt% of ASR

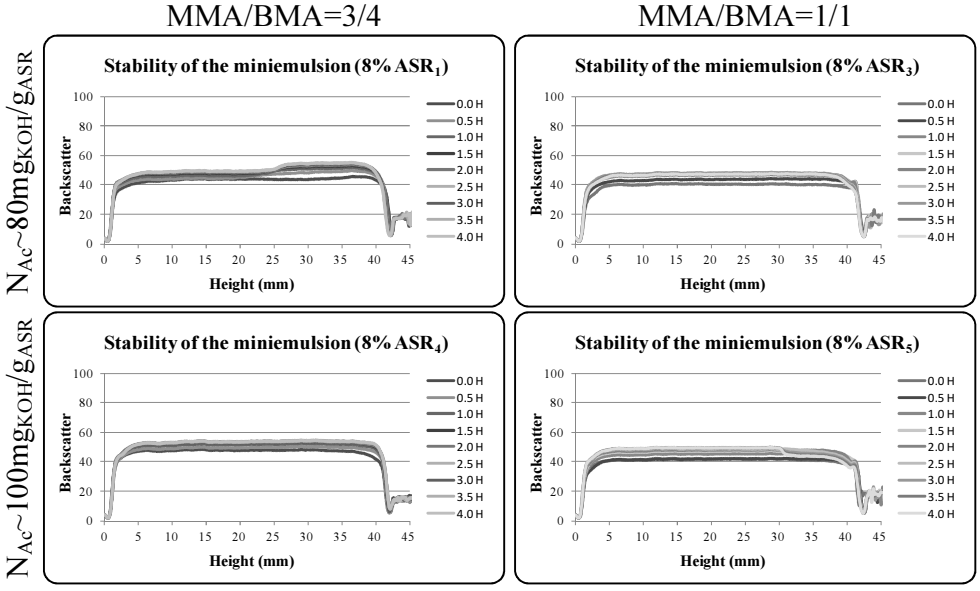

Figure 24: Stability of the miniemulsion using 8wt% of ASR

It can be seen that the miniemulsions were quite stable, although some creaming was observed with time. This effect was more remarkable using 4wt% of ASRs.

There are two possibilities for the degradation of a dispersion of monomer droplets [35]: (1) droplet coalescence, and (2) monomer diffusion (often referred as Ostwald ripening).

The first mechanism of degradation can be avoided by adding enough surfactant to the system. The second mechanism depends on monomer diffusion from small to large droplets across the continuous phase. The driving force for this process is the higher chemical potential of the monomer in the small droplets due to the contribution of the surface energy. Ostwald ripening can be reduced by using a costabilizer [34] (low molecular weight highly water insoluble compound, hexadecane in the present case). None of these degradation mechanisms can be disregarded in this case, but it seems that for 4wt% of ASRs, the droplet coalescence had a significant effect, because the stability of these miniemulsions is lower than those using 8wt% of ASR and the concentration of costabilizer is the same.

Figures 25 and 26 present the effect of ASR type and concentration on the evolution of the monomer conversion and Figure 27 shows the corresponding SEM images of the final dispersions. It can be seen that the particle size strongly decrease with the ASR concentration leading to a higher polymerization rate. In addition, a narrower particle size distribution was obtained with 8wt% of ASR. For 4wt% of ASR, the smallest size was

obtained with the most hydrophilic ASR (ASR_5) which resulted in a higher polymerization rate. For 8wt% the smallest size was also obtained with ASR_5. For this concentration, the polymerization rate was fast and the fact that a single sample was taken at intermediate conversions does not allow a round discussion of the effect of the particle size (number of particles) on polymerization rate.

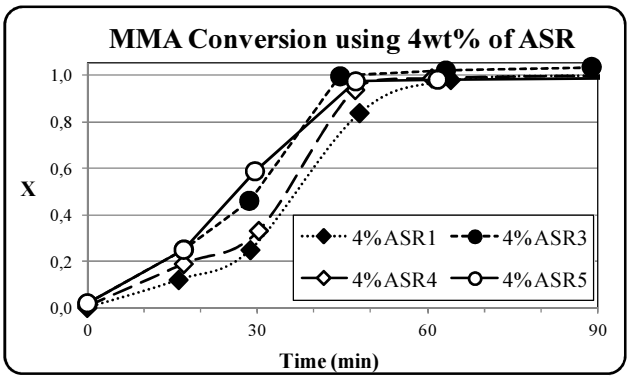

Figure 25: Evolution of conversion using 4% of ASRs

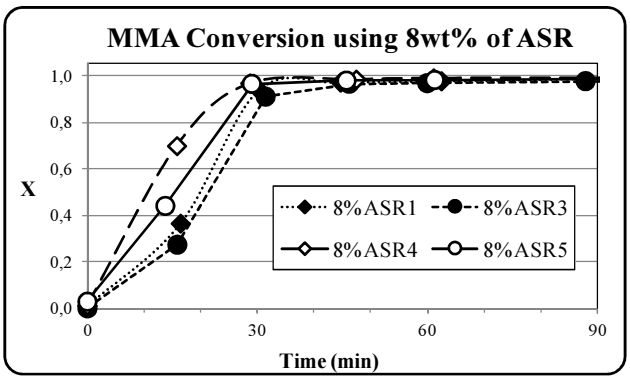

Figure 26: Evolution of the conversion using 8wt% of ASR

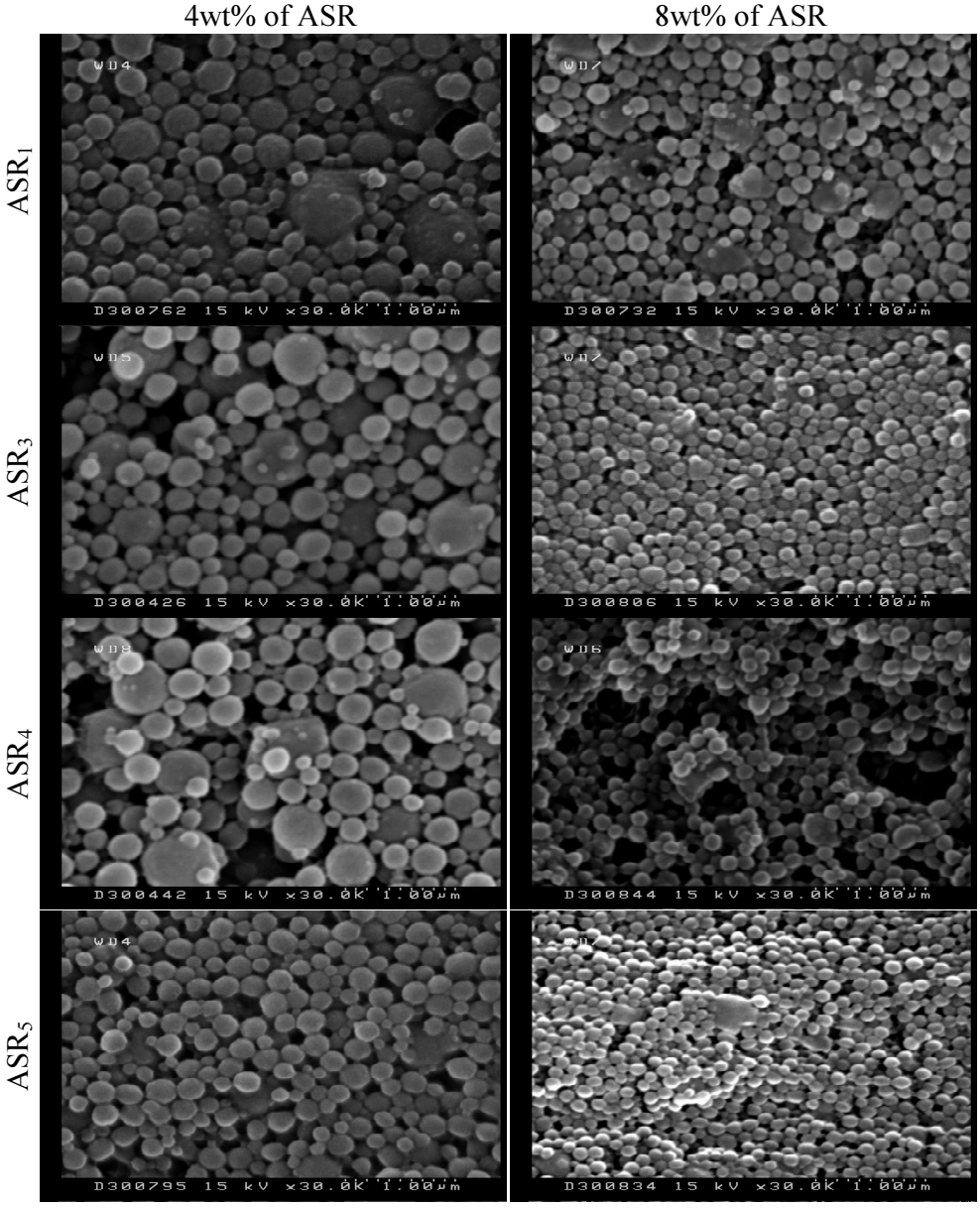

Figure 27: SEM images of the final latexes obtained in the MMA miniemulsion polymerization stabilized with different ASR type and concentration

4.5.2 Effect of monomer type (MMA, S)

Batch miniemulsion polymerizations of styrene were carried out with the formulation given in Table 11, but using S as monomer instead of MMA. In these reactions, only ASR_1 (N_{Ac}=80 mg_{KOH} g_{ASR}^{-1}; MMA/BMA=3/4) was employed. 4 and 8wt% of ASR_1 with respect to the monomer were used.

Figure 28 shows the stability of the miniemulsions at 60ºC. It can be seen that the styrene miniemulsions were more stable than those of MMA, likely due to the higher water solubility of MMA.

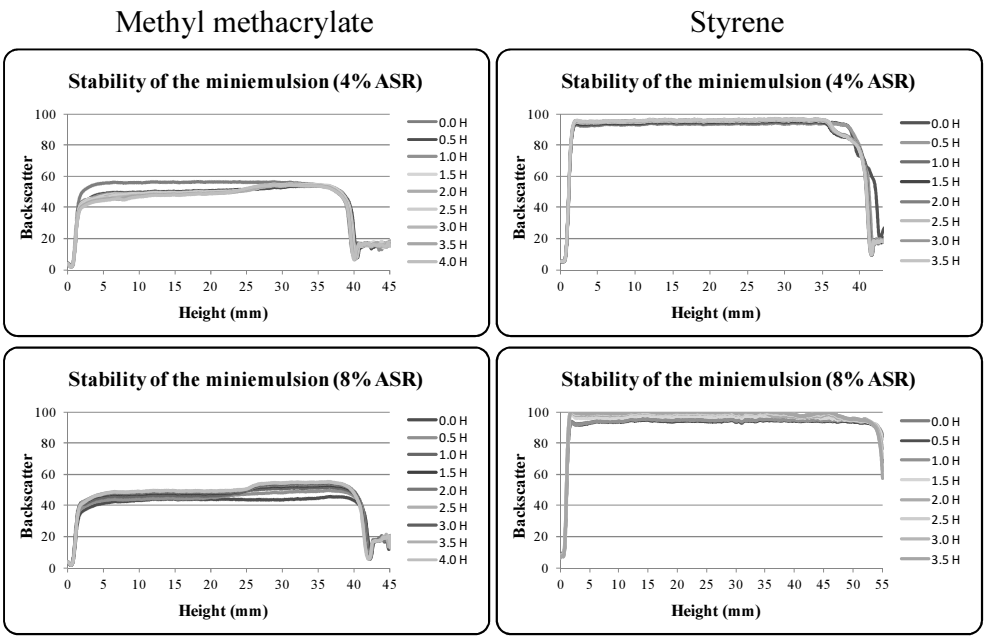

Figure 28: Stability of the miniemulsions for MMA and S

Figure 29 y 30 present the evolution of the monomer conversions and the SEM images of the final latexes. It can be seen that for both MMA and S particle size decreased with the ASR concentration and that smaller particles and narrower particle size distribution were obtained with MMA. The better compatibility of the ASR with the poly(methyl methacrylate) may be the reason for this behaviour.

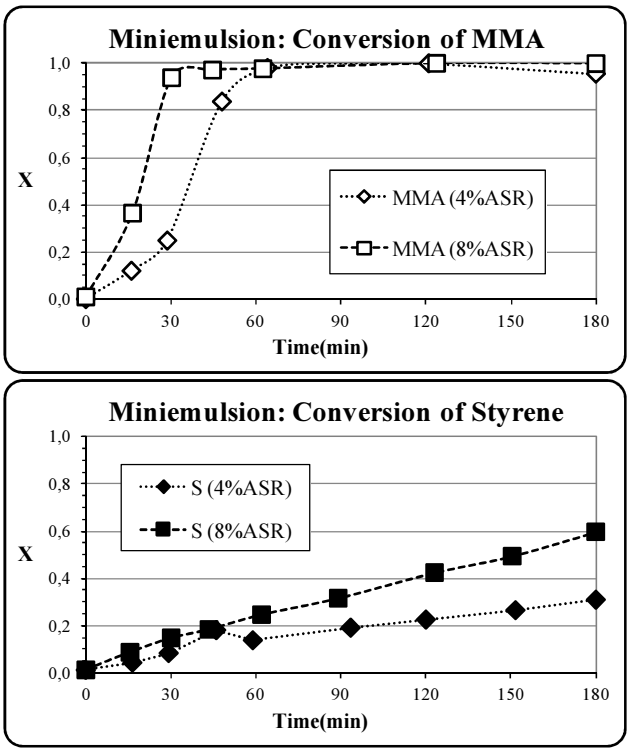

Figure 29: Evolution of the conversion for both systems, MMA and S

The increase in the number of particles with ASR concentration led to an increase in polymerization rate. On the other hand, the higher polymerization rates of the MMA were due to the combined effect of a higher propagation rate constant (833 molLs^{-1} for MMA [36] and 341 molLs^{-1} for S [37] at the polymerization temperature 60ºC) and the higher number of particles.

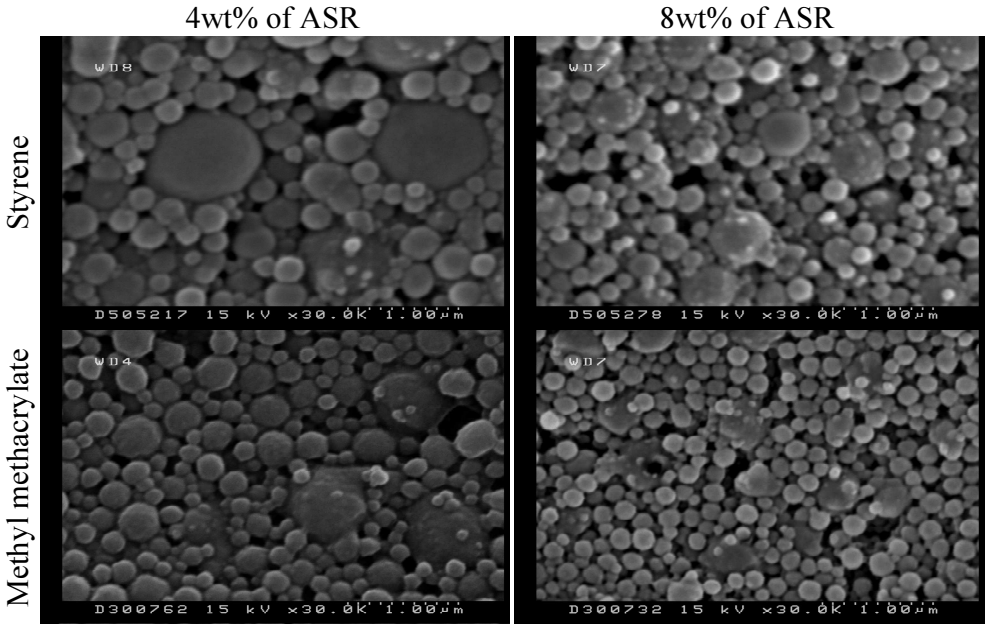

Figure 30: SEM micrographs of the final latexes obtained in the miniemulsion polymerizations of MMA and S with different contents of ASR_1

4.6 Conclusions

ASRs containing MMA, BMA, MAA and AM with different acid numbers (MAA content) and different MMA/BMA ratios were successfully

synthesized covering a certain range of hydrophilicity. These ASRs were characterized in terms of microstructure and colloidal properties.

Size exclusion chromatography using THF as mobile phase was used to determine the MWD of the soluble part of the polymer which is considered as the polymer produced mainly in the polymer particles. No significant differences were found in the average molecular weights ($\overline{M}n \sim 2100$; $\overline{M}w \sim 5500$) for all the ASRs regardless of their MMA content and MMA/BMA ratio. MALDI-TOF was used to measure the whole MWD of the ASRs. In this case the relative fraction of smaller molecular weights increased with the hydrophilicity of the ASR suggesting that low molecular weights were mainly produced in the aqueous phase. The $\overline{M}w$ measured by this technique (around 4600) was not affected by the ASR composition.

The acid numbers measured by conductometric titration indicate a certain degree of hydrolysis of AM that is increased for lower MAA contents.

The heterogeneity of the ASRs was verified measuring the fraction of the ASR solubilised at different pH values. From these experiments it can be concluded that the synthesized ASRs are rather heterogeneous in both, composition and molecular weights.

Despite the presence of ASR aggregates, no clear CMC values were obtained for the ASRs using surface tension measurements and fluorescence of pyrene. The reason seemed to be the heterogeneity of the ASR chains.

The adsorption of ASRs on PMMA particles did not follow a Langmuir isotherm. Adsorption measurements showed that the better compatibility between the ASRs with higher MMA content and the PMMA polymer particles largely determined the adsorption equilibrium the hydrophilicity being a secondary factor.

The ASRs synthesized were used as stabilizers in emulsion and miniemulsion polymerizations.

Bacth emulsion copolymerizations of BA/MMA were successfully carried out varying the ASR type and concentration. For all the ASRs, the number of particles increased with the ASR concentration. Fitting the data to a power function ($Np \div [ASR]^Z$), it was found that in all the cases the value of the exponent (Z) was much larger than that predicted by Smith-Ewart theory (Z=0.6). The reason could be the high ASR/monomer ratio used and the heterogeneity of the ASRs which include low molecular weight water soluble species that can desorb quickly being able to stabilize new precursor particles. Consequently, the more hydrophilic ASRs, resulted in higher exponent values. In addition, it was found that the polymerization rate was almost independent of the number of particles with together which the low values calculated for the average number of radicals per particle, suggest that the reactions proceeded under Smith-Ewart Case 1. In all the cases, no coagulum was observed.

Miniemulsion polymerizations of MMA were carried out using different types and concentration of ASRs. It was found that particle size

strongly decreased with the ASR concentration leading to higher polymerization rates. The smallest particle size was obtained with the most hydrophilic ASR (ASR_5). Comparison with styrene using ASR_1 showed that the smaller particle sizes and narrower particle size distributions were obtained with MMA, which might be due to the better compatibility of the ASR_1 with poly(methyl methacrylate).

4.7 References

1. El-Rehim, H. A. *Radiation Physics and Chemistry* **2005,** 74, (2), 111-117.

2. Pichot, C. *Current Opinion in Colloid & Interface Science* **2004,** 9, (3), 213-221.

3. Knežević, M.; Katsikas, L.; Popović, I. G. *Hemijska Industrija* **2005,** 59, (11-12), 321-323.

4. Blay, J. A.; Shahidi, I. K. Polyacrylic acid having high chelation value and its production. US 3904685, Celanese Corp, 1975.

5. Cramm, J. R.; Bailey, K. M. Water-absorbent acrylic acid polymer gels. US 4698404, Nalco Chemical Company, 1987.

6. Zimm, B. H. *The Journal of Chemical Physics* **1948,** 16, (12), 1093-1099.

7. Podzimek, S., Light Scattering. In *Light scattering, size exclusion chromatography and asymmetric flow field flow fractionation: powerful tools for the characterization of polymers, proteins and nanoparticles*, Podzimek, S., Ed. John Wiley & Sons: 2011; Vol. 1, pp 37-98.

8. Raeder, H.; Schrepp, W. *Acta Polymerica* **1998,** 49, (6), 272-293.

9. Labib, M. E.; Robertson, A. A. *Journal of Colloid and Interface Science* **1980,** 77, (1), 151-161.

10. Higuchi, M.; Senju, R. *Polymer Journal* **1972,** 3, (3), 370-377.

11. Kurenkov, V.; Hartan, H.-G.; Lobanov, F. *Russian Journal of Applied Chemistry* **2001,** 74, (4), 543-554.

12. Kudryavtsev, Y. V.; Litmanovich, A. D.; Platé, N. A. *Macromolecules* **1998,** 31, (14), 4642-4644.

13. Gibbs, J. W., *Collected Work of J.W. Gibbs*. Longman Green, New York: 1931; Vol. 1, p 219.

14. Azzi, A. *Quarterly Reviews of Biophysics* **1975,** 8, (02), 237-316.

15. Weber, G. *Annual Review of Biophysics and Bioengineering* **1972,** 1, (1), 553-570.

16. Radda, G. K.; Vanderkooi, J. *Biochimica et Biophysica Acta (BBA)-Reviews on Biomembranes* **1972,** 265, (4), 509-549.

17. Dorrance, R. C.; Hunter, T.-F. *Journal of the Chemical Society, Faraday Transactions 1: Physical Chemistry in Condensed Phases* **1972,** 68, 1312-1321.

18. Dorrance, R. C.; Hunter, T. F. *Journal of the Chemical Society, Faraday Transactions 1: Physical Chemistry in Condensed Phases* **1974,** 70, 1572-1580.

19. Hauser, M.; U, K. *Acta Physical Chemistry* **1973,** 19, 363.

20. Grätzel, M.; Thomas, J. *Journal of the American Chemical Society* **1973,** 95, (21), 6885-6889.

21. Kalyanasundaram, K.; Grätzel, M.; Thomas, J. *Journal of the American Chemical Society* **1975,** 97, (14), 3915-3922.

22. Ray, G. B.; Chakraborty, I.; Moulik, S. P. *Journal of Colloid and Interface Science* **2006,** 294, (1), 248-254.

23. Kalyanasundaram, K.; Thomas, J. *Journal of the American Chemical Society* **1977,** 99, (7), 2039-2044.

24. Mukerjee, P.; Mysels, K. J. *Critical micelle concentrations of aqueous surfactant systems*; DTIC Document: Natlional Standar Reference Data Service, 1971.

25. Lee, D. Y.; Kim, J. H. *Journal of Applied Polymer Science* **1998,** 69, (3), 543-550.

26. Rosen, M. J., Adsorption of Surface-Active Agents at Interfaces: The Electrical Double Layer. In *Surfactants and Interfacial Phenomena*, Rosen, M. J., Ed. John Wiley & Sons, Inc.: New York, 2004; Vol. 1, pp 34-104.

27. Langmuir, I. *Journal of the American Chemical Society* **1918,** 40, (9), 1361-1403.

28. Betts, J.; Pethica, B. *Transactions of the Faraday Society* **1960,** 56, 1515-1528.

29. Asua, J. M. *Progress in Polymer Science* **2014,** 39, (10), 1797-1826.

30. Smith, W. V.; Ewart, R. H. *The Journal of Chemical Physics* **1948,** 16, (6), 592-599.

31. Nomura, M.; Harada, M., On the Optimal Reactor Type and Operation for Continuous Emulsion Polymerization. In *Emulsion Polymers and Emulsion Polymerization*, David R. Bassett, A. E. H., Ed. AMERICAN CHEMICAL SOCIETY: South Charleston, West Virginia, 1981; Vol. 165, pp 121-143.

32. Nunes, J.; Asua, J. M. *Langmuir* **2012,** 28, (19), 7333-7342.

33. Nunes, J.; Asua, J. M. *Langmuir* **2013,** 29, (12), 3895-3902.

34. Ballard, N.; Urrutia, J.; Eizagirre, S.; Schäfer, T.; Diaconu, G.; de la Cal, J. C.; Asua, J. M. *Langmuir* **2014,** 30, (30), 9053-9062.

35. Asua, J. M. *Progress in Polymer Science* **2002,** 27, (7), 1283-1346.

36. Beuermann, S.; Buback, M.; Davis, T. P.; Gilbert, R. G.; Hutchinson, R. A.; Olaj, O. F.; Russell, G. T.; Schweer, J.; van Herk, A. M. *Macromolecular Chemistry and Physics* **1997,** 198, (5), 1545-1560.

37. Buback, M.; Gilbert, R. G.; Hutchinson, R. A.; Klumperman, B.; Kuchta, F.-D.; Manders, B. G.; O'Driscoll, K. F.; Russell, G. T.; Schweer, J. *Macromolecular Chemistry and Physics* **1995,** 196, (10), 3267-3280.

Chapter 5: High solids content latexes using ASRs as emulsifier in emulsion polymerization

Outline

5.1 Introduction

As explained in Chapter 1, ASRs are used because they improve the performance of the dispersed polymers in some applications. In the previous chapters, ASRs were designed to act as "conventional" surfactants, namely to stabilize particles formed by homogeneous and heterogeneous nucleation. In this chapter that was carried out at Nuplex-Resins labs in Wageningeng (Netherlands), a different strategy was used. Relatively hydrophobic ASRs that were able to form aggregates were synthesized and the aggregates were used as seeds for the synthesis of high solids content emulsion polymers. Therefore, low acid number ASR ($50 mg_{KOH}\, g_{ASR}^{-1}$) that corresponds to 8wt% of MAA was synthesized. Another important difference of the ASRs used in this chapter with respect to those used in Chapter 4 is that the acrylamide (AM) has been substituted by di-methyl acrylamide (DMAM). The main reason is to avoid the use of the highly toxic acrylamide. In addition, DMAM is not prone to suffer hydrolysis and hence allows better control of the acid number.

The chapter is organized in two parts. Firstly, the synthesis of an ASR of composition MMA/BMA/DMAM/MAA (at 67/15/10/8 wt/wt) was carried out and its capability to form aggregates in the absence and presence of different monomers (MMA, BMA and S) was checked. Then, it was used to synthesize high solids content latexes with different monomer systems (MMA, BA and MMA/BA). The second part, aimed at obtaining small particle size

high solids content latexes stabilized solely with ASRs. To achieve this goal the hydrophobicity of the ASR was increased by substituting part of the MMA by lauryl methacrylate (LMA).

5.2 High solids content latexes stabilized with a low acid number ASR

5.2.1 Synthesis of the low acid number ASR

Technical grade monomers methyl-methacrylate (MMA, Nuplex), butyl-methacrylate (BMA, Nuplex), methacrylic-acid (MAA, Nuplex) and N,N-dimethyl-acrylamide (DMAM, Aldrich) were used as monomers for the synthesis of the ASR. Ammonium persulphate (APS, Aldrich) was employed as initiator and sodium lauryl sulphate (SLS, Nuplex) as anionic surfactant. 1-Octanethiol (OcT, CTA_{Oil}, Aldrich) and 2-Mercaptoethanol (M-Et, CTA_{Water}, Aldrich) were used as chain transfer agents (CTAs). Ammonium hydroxide (NH_4OH, Acros) was employed to neutralize the ASRs. All the products were used as supplied.

A low acid number ($50mg_{KOH}\,g_{ASR}^{-1}$) was sought, which corresponds to 8wt% of MAA. In addition, a 15wt% of BMA, 67wt% of MMA and 10wt% of DMAM were used. The ASR was synthesized in semi-continuous using the formulation given in Table 1. The initial charge containing water and

surfactant (SLS) was heated to 70ºC under nitrogen atmosphere and mechanical agitation with anchor stirrer. Then, the initiator was added as a shot together with 5wt% of the pre-emulsion, and 10 min later the rest of the pre-emulsion was fed during 1 hour.

Table 1: Formulation used for the synthesis of the ASR

Ingredient	**Total charge (g)**	**Concentration (wt%)**	
MMA	180.90	30	67
BMA	40.50		15
MAA	21.60		8
DMAM	27.00		10
OcT	3.24	1.20 [(a)]	
M-Et	1.51	0.56 [(a)]	
SLS	2.70	1.00 [(a)]	
APS	4.05	1.50 [(a)]	
Water	618.50	68.72	
Total	900	100	
(a) wt% with respect to total amount of monomers			

Figure 1 presents the evolution of the monomer conversion, particle size and number of particles during the synthesis of the ASR. It can be seen that the instantaneous conversion was maintained higher than 0.8 during all the process, showing that the starved conditions had been achieved. Therefore, the homogeneity of the ASR chains was favoured. The evolution of the number of particles shows that nucleation occurred in the polymerization of

the initial charge. Afterwards, the number of particles decreased one order of magnitude during the semi-continuous operation.

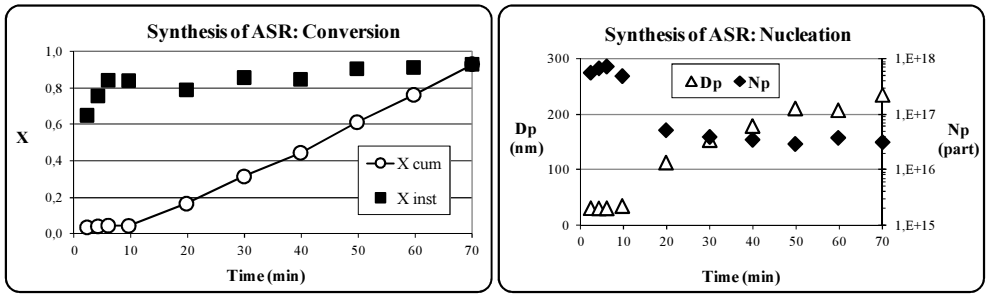

Figure 1: Evolution of conversion and number and diameter of particles during the synthesis of the ASR

5.2.2 Formation of aggregates

At the end of the reaction, NH_4OH was added dropwise at 70ºC until pH 8.5. Dynamic light scattering (Zetasizer Nano S90, Malvern Instruments) was used to determine the presence of aggregates. Figure 2 (size distribution by volume) shows that the ASR was indeed able to form aggregates with a broad size distribution and a Z-average value of 35nm. The broadness of the distribution suggests a heterogeneous ASR.

The existence of the large aggregates (Figure 2) opens the possibility to use them as seeds in emulsion polymerization, but for this it is necessary to check their behaviour in the presence of monomers. Therefore, the absorption of monomer in the aggregates was studied using three monomers of different

hydrophobicity; methyl methacrylate (MMA, water solubility 15gL^{-1}), butyl acrylate (BA, water solubility 2gL^{-1}) and styrene (S, water solubility 0.29gL^{-1}).

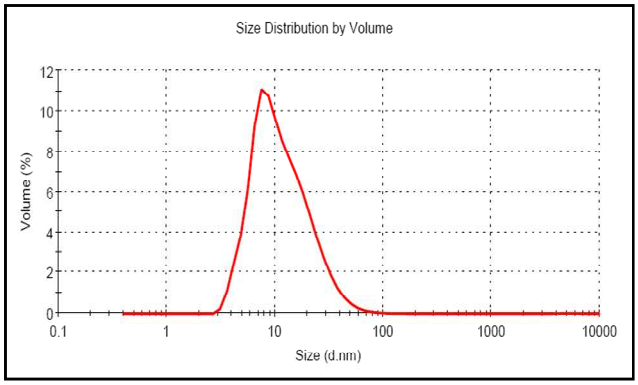

Figure 2: Aggregate size distribution of the ASR as measured by DLS

Table 2 shows the different amounts of monomers added to two ASR aqueous solutions (20 and 26wt% of ASR). Because of the different concentration of the ASR in the initial solution (based on water), the viscosity of the monomer swollen dispersion prepared with 26wt% of ASR was higher.

Figure 3 shows the aspect of the system after addition of the monomer and before shaking for the case of styrene. A clear phase separation can be observed. After shaking with a vortex shaker a fraction (or all) of the monomer layer disappeared because the monomer was absorbed in the aggregates. Then, the evolution of the monomer layer was monitored to get information about the stability of the monomer swollen ASR dispersions.

Table 2: Mixtures of the monomer and ASR (aqueous solution = 3g)

r_0 $\left(\frac{\text{Monomer}}{\text{ASR}}\right)$	**Low viscosity**			**High viscosity**		
	ASR (g)	**Monomer (g)**	**Monomer + ASR (wt%)**	**ASR (g)**	**Monomer (g)**	**Monomer + ASR (wt%)**
0.00	0.60	0.00	20	0.78	0.00	26
0.50		0.30	27		0.39	35
1.00		0.60	33		0.78	41
1.25		0.75	36		0.98	44
1.50		0.90	38		1.17	47
1.75		1.05	41		1.37	49
2.00		1.20	43		1.56	51

Figure 3: Styrene with ASR at 20wt% before shaking (S/ASR_{20})

In addition, the time evolution of the size of the monomer swollen aggregates was followed by DLS. Figures 4, 5 and 6 show the evolution of both the amount of monomer absorbed referred to the ASR content (r_t) and the size of the monomer swollen aggregates for the three monomers.

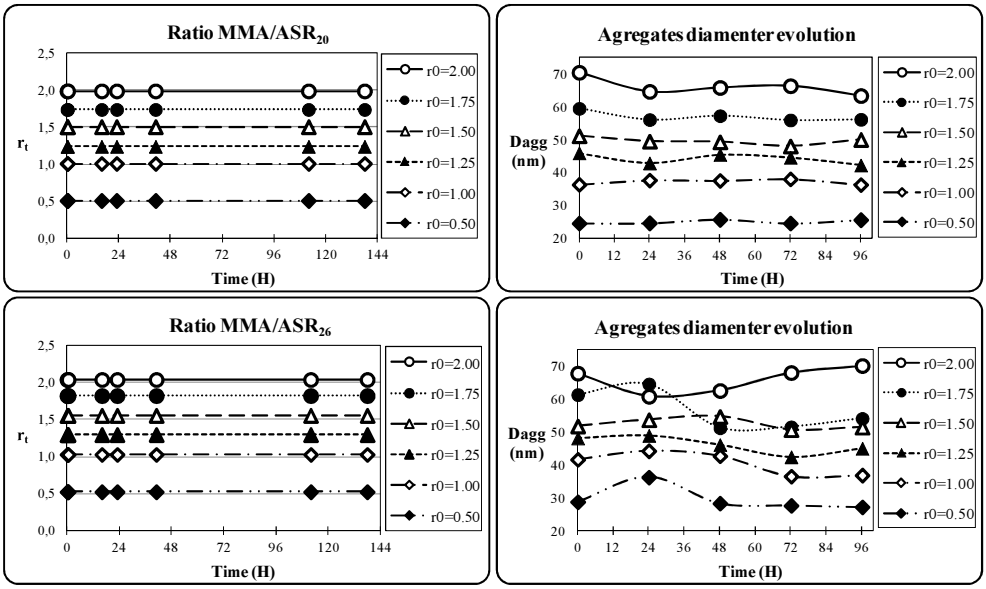

Figure 4: Evolution of the fraction of monomer absorbed, r_t, (left part) and aggregate diameters (right part) for the system MMA/ASR. 20 wt% of ASR (top); and 26wt% ASR (bottom)

r_t is calculated as follows:

$$r_t = r_0\left(1 - \frac{B}{A}\right) \qquad (1)$$

where r_0=monomer(g)/ASR(g); A the initial thickness of the monomer layer, and B the thickness at time t. Notice that when $r_t=r_0$ all the monomer is dispersed in the aqueous phase.

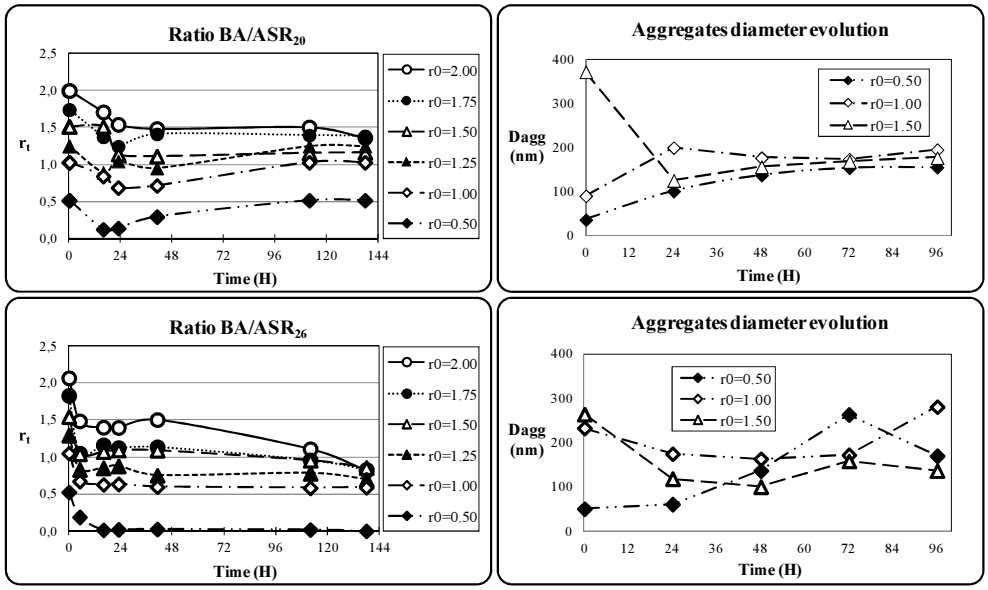

Figure 5: Evolution of the fraction of monomer absorbed, r_t, (left part) and aggregate diameters (right part) for the system BA/ASR.
20 wt% of ASR (top); and 26wt% ASR (bottom)

It can be seen that after shaking, the monomer layer disappeared in all cases ($r_t=r_0$) but the evolution with time was strongly affected by the monomer. For MMA, there was no layer of monomer 6 days after shaking; namely the monomer swollen aggregates were stable. However, for BA and S a severe destabilization that was faster and more pronounced for 26wt% of ASR was observed. Nevertheless, for 20wt% of ASR, BA yielded stable dispersions for $r_0 \leq 1.25$ and the dispersion of S was stable for $r_0=0.5$

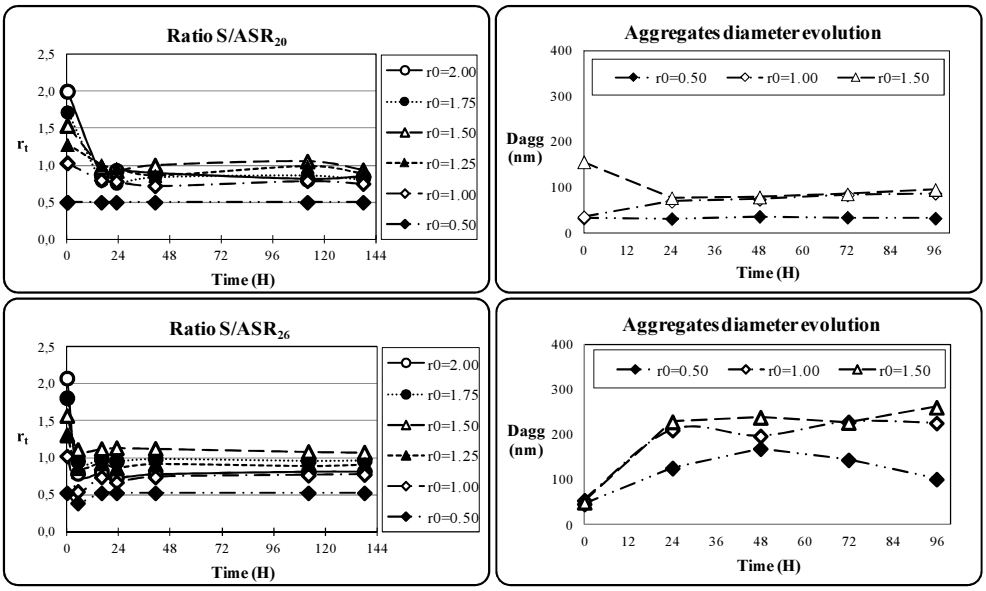

Figure 6: Evolution of the fraction of monomer absorbed, r_t, (left part) and aggregate diameters (right part) for the system S/ASR.
20 wt% of ASR (top); and 26wt% ASR (bottom)

For MMA, the size of aggregates increased with the monomer content (Figure 4, left) and was almost constant during 6 days. The increase in size and volume fraction led to translucent or opaque dispersions (Figure 7). The size of the aggregates containing BA and styrene were bigger than those of the MMA.

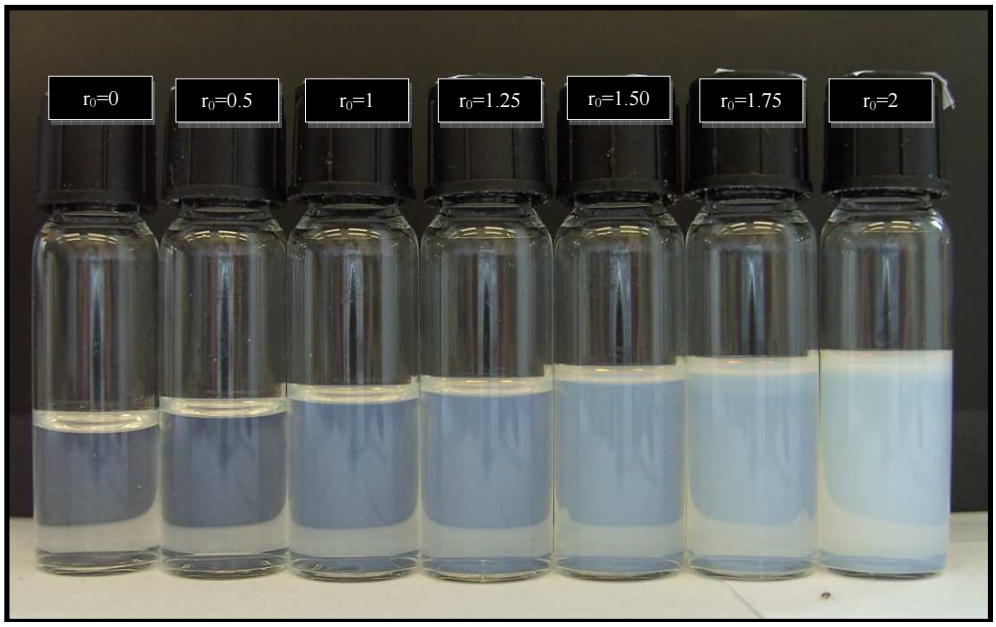

Figure 7: MMA containing ASR dispersions (20wt% system after 6 days)

5.2.3 High solids polymer dispersions

The latexes were synthesized in a two step process. In the first step, the aggregates of ASR were swollen with monomer using r_0=0.5 to ensure the stability of the aggregates, and then polymerized in batch. In the second step, the latex formed in the first step was swollen with more monomer (until r_0=1) and then polymerized in batch. In order to maximize the solids content, the 26wt% ASR aqueous solution was added. Polymerizations using MMA, BA and 50/50 wt/wt mixture of MMA and BA were carried out. The initiator system given in Table 3 was used. The oxidant/reductant (TBHP/AsAc) ratio

used was higher than the 2/1 (mol/mol) found optimal for this system [1] because the TBHP partitions preferently in the oil phase. Technical grade monomers were used as supplied.

Table 3: Initiator system

Initiator	**wt% with respect to the monomer**
Trigonox A-W70(*)	0.2200
Na_2-P (2Na EDTA)	0.0034
$FeSO_4$	0.0017
AsAc	0.1600
(*) *tert*-butyl hydroperoxide (TBHP)	

The aqueous solution of ASR (26wt%) was placed in the reactor and heated to 50ºC under nitrogen atmosphere and mechanical agitation with anchor stirrer (200 rpm). Afterwards, the necessary amount of monomer was added to reach r_0=0.5. After 30min, the redox initiator (TBHP (Trigonox A-W70) / AsAc) was added as a shot according to the formulation given in Table 3. The ferrous sulphate and chelating agent were employed to enhance the efficiency of the redox pair. The reaction time was 30min. At the end of this polymerization step, the solids content was estimated to be around 34.5wt%. After that, in the second step, the necessary amount of monomer to obtain a ratio $M_{(g)}/ASR_{(g)}$ equal to 1 was added. Again, after 30min, the same redox initiator system was added as a shot. The reaction time was fixed at 30min and the final solids content was estimated around 41.3wt%. Finally, an excess of AsAc was used to react the remaining TBHP (if any).

Before reaction, an important aspect to consider is the influence of the reaction conditions (50ºC and mechanical agitation) on the D_{agg} values that was not considered in the previous section. Table 4 shows the effect of these variables on D_{agg}. It can be seen that aggregates of adequate sizes are still obtained. In addition, it seems that temperature strongly affects the monomer-ASR interactions as for MMA D_{agg} increases and for BA decreases. However, no further study to clarify this effect was conducted.

Table 4: Swelling aggregates data for MMA, BA and mixture of both

	MMA	**MMA-BA**	**BA**
D_{agg} at room temperature without agitation	30nm	---	~200nm
D_{agg} at 50ºC under mechanical agitation	120nm	50nm	45nm

Figure 8 shows the evolution of conversion (left) and number of particles (right) during the first step for the three systems (MMA, BA and MMA/BA). It can be seen that the polymerizations were very fast due to the large number of particles and the use of a redox initiator. In addition, BA presented the highest R_p, followed by the MMA/BA mixture and the lowest R_p was for MMA. This was due to both the lower N_p obtained for MMA and the differences in propagation rate coefficients (k_p), whereas for BA [2] is 27700molLs^{-1}, for MMA [3] is 649molLs^{-1}; i.e. 42 times lower at reaction temperature, 50ºC. The final conversions (after 30min of polymerization) show that for BA and MMA/BA systems reached 90wt% conversion while for MMA it was only 65wt%. It is worth point out that this value is deceiving as due to the low value of r_0 (r_0=0.5), the monomer concentration corresponded

to a conversion of 97% in a regular emulsion polymerization. Nevertheless, it can be hypothesized that for BA and MMA/BA, the limiting conversion might be due to the depletion of at least one of the components of the redox pair. There are two possibilities. The first one is that as the AsAc was used in a fraction lower than the stoichiometric one (TBHP/AsAc=2/1) it was completely reacted. The second is that the TBHP dissolved in the aqueous phase was completely reacted and the fraction in the polymer particles diffused too slowly to the aqueous phase. For MMA, the limiting conversion may be due to the same effect although the occurrence of the glass effect, which strongly decreases propagation when the Tg (glass transition temperature) of the monomer-polymer system equals or exceeds the reaction temperature [4], may also play a role.

The right part of the Figure 8 shows that nucleation of new particles occurred during the first part of the process and that the number of particles was higher for BA and MMA/BA that presented the higher number of initial aggregates (Table 4). The nucleation of new particles was more pronounced for MMA, which is in agreement with its higher water solubility and lower number of initial aggregates that favor homogeneous nucleation.

Although the accuracy of the particle size distributions (PSD) provided by the DLS equipment is a matter of debate, it is worth to have a look to this information (Figure 9). It can be seen, that the PSD of the MMA latex presents a peak of large particles, that suggests the occurrence of particle-particle coagulation, although no macroscopic coagulum was observed. A possible

explanation is that a fraction of the particles created by homogeneous nucleation could not be stabilized by the ASR due to its limited mobility and coagulated between them yielding the large size peak observed in Figure 9.

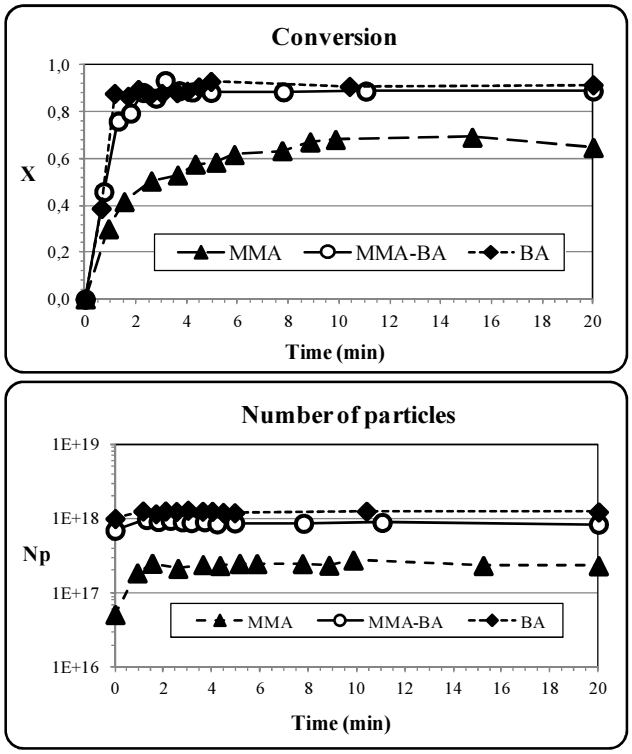

Figure 8: Evolution of monomer conversion (left) and number of particles (right) during the first polymerization step

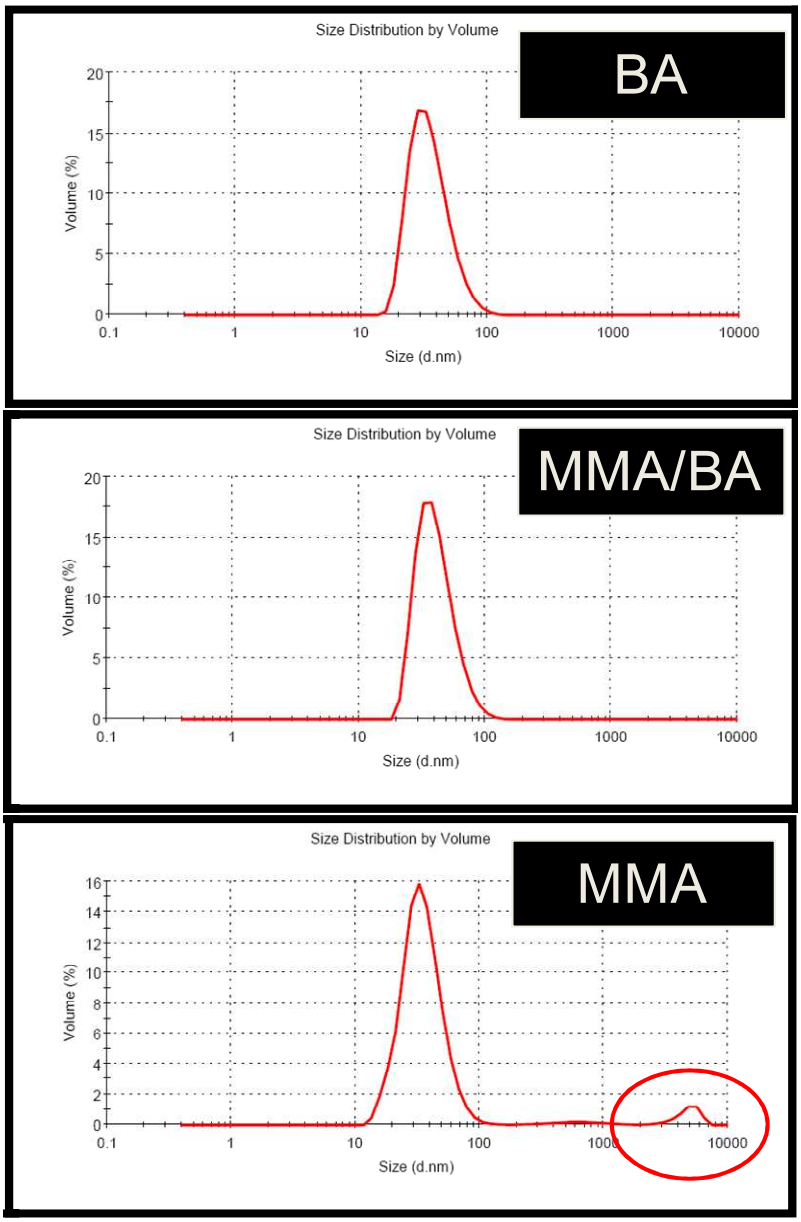

Figure 9: Volume particle size distributions measured by dynamic light scattering

The latexes from the first step were swollen at 50ºC under mechanical agitation (using anchor stirrer) with additional monomer until reaching r_0=1. The conversions and the particle sizes were measured before adding more initiator. Table 5 shows that whereas N_p was not significantly modified during the swelling process, the conversion measured was higher than the theoretical one calculated taking into account the conversion achieved in the first stage and the monomer added in the second step. This clearly shows that some initiator able to form radicals remained in the system, namely, that contrary to what was hypothesized, the limited conversion of BA and MMA/BA in step one was not due to the complete depletion of the initiators and it was due to the low concentration of monomer in the polymer particles.

Table 5: Theoretical and experimental number of particles and conversion after the second swelling process

	MMA		**MMA-BA**		**BA**	
	N_p (part)	**X**	**N_p (part)**	**X**	**N_p (part)**	**X**
Theoretical	$2.3*10^{17}$	0.33	$9.2*10^{17}$	0.45	$1.2*10^{18}$	0.45
Measured	$1.9*10^{17}$	0.48	$8.4*10^{17}$	0.65	$1.3*10^{18}$	0.62

Figure 10 presents the results obtained in the second step. It can be seen that also in this case a limiting conversion was observed for MMA. Although the conversion was higher than in the first step, the fraction of the unreacted monomer was similar (11wt% in the first step and 10wt% in the second). Therefore, the effective Tg should be similar in both cases, which seems to support the hypothesis of the glass effect. Higher conversions were

achieved for MMA/BA and BA, but due to the higher value of r_0 (r_0=1), the final monomer concentration were similar to those achieved in the first stage.

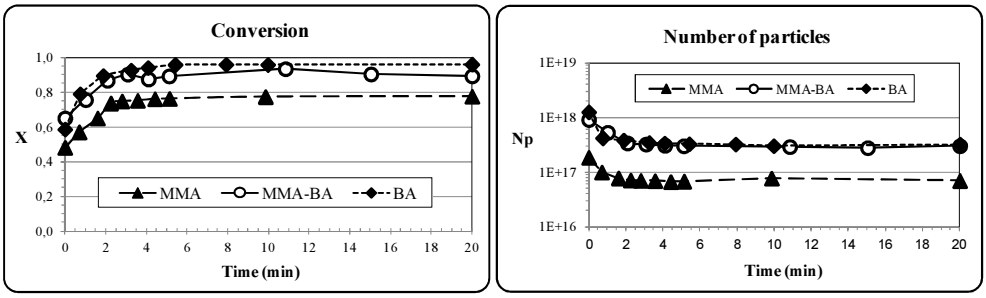

Figure 10: Evolution of monomer conversion (left) and number of particles (right) during the second step

Figure 10 also shows that the number of particles significantly decreased during the second step, although no macroscopic coagulum was produced. The reduction of the pH due to the addition of AsAc may be the reason for this limited coagulation.

Postpolymerization is often used to reduce the amount of residual monomer [1]. Taking into account that the amount of AsAc used was less than the stoichiometric one, a shot of AsAc (3.65 ml at 1.5wt%) was added to the final latexes and a substantial increase of the conversion was observed (Table 6).

The results presented in Table 6 show that the limiting conversion observed for MMA in Figures 8 and 10, was not only due to glass effect. The depletion of AsAc and/or slow diffusion of TBHP play also a role.

Table 6: Final parameters of the reactions

Polymer - ASR	Conversion	D_p (nm)	N_p ($partL^{-1}$)
PMMA - ASR	0.88	126	$6.9*10^{16}$
P(MMA/BA) - ASR	1.00	87	$2.8*10^{17}$
PBA - ASR	1.00	80	$3.1*10^{17}$

5.3 Small particle latexes

In order to synthesize small particle latexes, the size of the ASR aggregates should be reduced. To achieve this goal, the hydrophobicity of the ASR was varied by subtituting a fraction of the MMA by lauryl methacrylate (LMA). The ASRs summarized in Table 7 were synthesized in solution polymerization.

Table 7: ASRs with different amount of LMA

	DMAM	BMA	MAA	MMA	LMA
ASR	10 wt%	15wt%	8 wt%	67 wt%	0 wt%
5% LMA				62 wt%	5 wt%
10% LMA				57 wt%	10 wt%
20% LMA				47 wt%	20 wt%
40% LMA				27 wt%	40 wt%

At the end of the polymerization, the solvent (n-hexane) was evaporated under vacuum adding an alkali aqueous phase at the same time. Then, the sizes of the aggregates formed by these ASRs were determined by

DLS (Figure 11). It can be seen that the smallest sizes corresponded to the range of 5-20wt% of LMA (values highlighted in Figure 11).

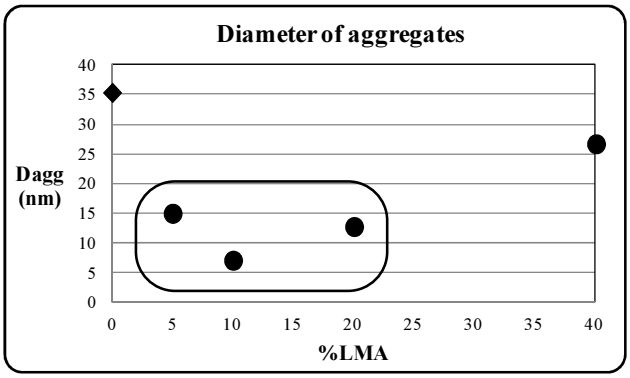

Figure 11: Effect of the LMA concentration on the diameter of the aggregates

Preliminary experiments were carried out to figure out a polymerization strategy able to give latexes with: (1) solids content higher than 35wt%; (2) good viscosity (able of being applied on a surface to give a film); (3) low particle size (D_p<60nm); and (4) $M_{(g)}/ASR_{(g)}$ ratio equal to 2.

Two polymerization methods (Table 8) were used with the 10%LMA ASR that gave smallest aggregate size. In both processes, the final solids content was 40wt% and a mixture of MMA/BA (40/60 wt/wt) was used.

The first method consisted in two shots of monomer (method used in the Section 5.2.3). The second method was a semi-continuous emulsion polymerization (0.3265 $gmin^{-1}$ feeding the monomers in 2 hours). The initiators used were TBHP/AsAc at 50ºC for the first method and APS at 80ºC

for second method. During the reaction using shots (first method), the viscosity of the medium increased too much making difficult the stirring. Therefore, the solids content of this process was lowered to 33wt%, but the final viscosity was still too high. Using the semi-continuous emulsion (second method), the solids content was 40wt% and the viscosity was good with a value of D_p within the desirable range. Therefore, this second method was used for the ASRs containing 5wt%, 10wt% and 20wt% of LMA.

Table 8: Formulations used for the MMA/BA polymerizations stabilized with ASR containing 10%LMA

Component	**First method**				**Second method**	
	Initial charge (g)	**1st shot (g)**	**2nd shot (g)**	**Final (g)**	**Initial charge (g)**	**Feed (g)**
MMA		8.00	8.00		0.82	15.18
BA		12.00	12.00			24.00
ASR (10%LMA)	20.00				20.00	
APS					0.32	
Trigonox A-W70		0.0176	0.0704			
Na_2-P (2Na EDTA)		0.0007	0.0007			
$FeSO_4$		0.0003	0.0003			
AsAc		0.0096	0.0096	0.0450		
Water	83.00	2.1218	2.6690	2.0550	89.68	0
Total	103.00	22.15	22.75	2.10	110.82	39.18
	150				150	

The results are presented in Figure 12. Complete conversion at the end of the process was achieved in all cases, although the polymerization rate using 5%LMA was slower. Monomer conversion was not sensitive to the number of particles, which indicates that polymerizations were under Smith-Ewart Case 1 or Case 3 conditions [5]. For these 3 reactions, $\bar{n}<<0.5$, which confirmed the Smith-Ewart Case 1 conditions. In any case, latexes fulfilling the requirements listed above were obtained.

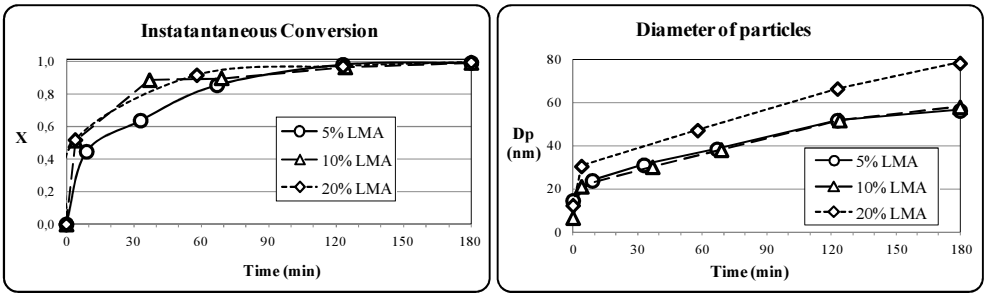

Figure 12: Evolution of conversion and particle diameter for the ASRs with different hydrophobicity

5.4 Conclusions

A low acid number ASR (~ $50 mg_{KOH} g_{ASR}^{-1}$) was synthesized by means of emulsion polymerization based on the system MMA/BMA/MAA/DMAM. This ASR produces small aggregates (d_{agg}=35nm) at pH=8.5.

The capability of the ASR aggregates to absorb monomers of different hydrophobicity (MMA, BA and S) was studied. For MMA, stable aggregates can be obtained even for high ratios (~ 2) of monomer/ASR. However, for BA

and S stable dispersions can only be obtained for lower ratios of monomer/ASR (1.25 for BA and 0.5 for S). These swollen aggregates were successfully polymerized to obtain high solids dispersions in a two steps emulsion polymerization process using MMA, BA and 50/50wt/wt mixture of MMA/BA.

In the first step, the aggregates of ASR were swollen with monomer using a monomer/ASR ratio equal to 0.5. Under reaction conditions the sizes of the aggregates were bigger for MMA than for MMA/BA and BA. The BA and MMA/BA showed high polymerization rates but MMA was slower due to the lower N_p and the low propagation rate constant of MMA. An equivalent conversion of about 97% was reached for BA and MMA/BA. For MMA, equivalent conversion was lower ($\approx$ 88%) in part due to the influence of the glass effect. In the second step, the latex formed in the first step was swollen with more monomer (until monomer/ASR ratio equal to 1) and then polymerized. The polymerization rate followed the same trend than in the first step. Polymerization of the residual monomer was achieved by adding a shot of AsAc. Stable and monodispersed latexes with particle diameters around 80-90nm were obtained for BA and MMA/BA. For MMA a large size peak is obtained in the PSD although macroscopic coagulum was not observed.

Small particles latexes of MMA/BA (40/60wt/wt) were synthesized using more hydrophobic ASRs substituting MMA by LMA in the backbone. It can be seen that the ASR with 5, 10 and 20wt% of LMA gave smallest size aggregates. Semi-continuous emulsion polymerizations were carried out at

80ºC using APS as initiator. Stable latex with 40% of solids content and particle size of about 60nm were successfully obtained.

5.5 References

1. Da Cunha, L.; Ilundain, P.; Salazar, R.; Alvarez, D.; Barandiaran, M. J.; Asua, J. M. *Polymer* **2001,** 42, (2), 391-395.

2. Asua, J. M.; Beuermann, S.; Buback, M.; Castignolles, P.; Charleux, B.; Gilbert, R. G.; Hutchinson, R. A.; Leiza, J. R.; Nikitin, A. N.; Vairon, J. P. *Macromolecular Chemistry and Physics* **2004,** 205, (16), 2151-2160.

3. Beuermann, S.; Buback, M.; Davis, T. P.; Gilbert, R. G.; Hutchinson, R. A.; Olaj, O. F.; Russell, G. T.; Schweer, J.; van Herk, A. M. *Macromolecular Chemistry and Physics* **1997,** 198, (5), 1545-1560.

4. Cowie, J. M. G.; Arrighi, V., Step-growth polymerization. In *Polymers: chemistry and physics of modern materials*, Cowie, J. M. G.; Arrighi, V., Eds. CRC Press: 2007; Vol. 1, pp 26-51.

5. Smith, W. V.; Ewart, R. H. *The Journal of Chemical Physics* **1948,** 16, (6), 592-599.

Chapter 6: Conclusions

The goal of this thesis is to gain understanding on the kinetics and nucleation mechanism in emulsion and miniemulsion polymerization stabilized with ASRs of low molecular weight (number average molecular weight around 5000 $gmol^{-1}$) and acid number lower than that of the commercial ASRs (which have values around 200 $mg_{KOH}\, g_{ASR}^{-1}$).

Firstly, the synthesis of MMA/BMA/MAA ASRs in emulsion polymerization using 1-Octanothiol as CTA and SLS as surfactant was explored. It was found that ASRs of the required molecular weight ($\overline{M}_n$~5000$gmol^{-1}$) able to become soluble in water at pH=10 can be obtained with 3wt% of oil-soluble CTA (1-Octanothiol). The concentration of SLS did not have any significant effect on the $\overline{M}_n$ of the ASR, but strongly affected particle size that in turn influenced the solubility of the ASR upon neutralization. 4wt% of SLS was needed to synthesize ASRs that become water-soluble rapidly. Oil-soluble (1-Octanothiol) and water-soluble (2-Mercaptoethanol) CTAs were combined in an attempt to control the MWD of the polymer formed in both, polymer particles and aqueous phase. However, the effect of the water-soluble CTA on the whole MWD was small.

Nevertheless, the effect on the CMC (lowering the CMC) and parking area (increasing a_s) was substantial.

The ASRs synthesized with (ASR_A) and without (ASR_B) water-soluble CTA (CTA_{Water}) were used as sole stabilizers in batch emulsion polymerization of styrene (S) and methyl methacrylate (MMA). The reactions with MMA were too fast to allow drawing conclusions, but those carried out with S showed that the dependence of N_p on the concentration of ASR had exponents much higher than the 0.6 predicted for the Smith-Ewart theory (1.7 for ASR_A and 2.4 for ASR_B), which was attributed to the solubilization of the ASRs in the monomer droplets. In addition, the polymerization rate per particle (R_{pp}) decreased with the concentration of ASR at the same time that the ASR amount around the particle increased. This suggested some resistance to radical diffusion through ASR. Nevertheless, these conclusions can be affected by a significant amount of SLS owing to it has used a 4wt% SLS in the synthesis of ASR.

A semi-continuos strategy for the synthesis of relatively homogeneous MMA/BMA/MAA ASR (ASR_{MAA}) and MMA/BMA/AA ASR (ASR_{AA}) using a low concentration of SLS (0.25wt%) was developed. The molecular weight of the ASR was controlled by the 3wt% of oil-soluble CTA (CTA_{Oil}). Almost complete incorporation of the acidic monomer (99.83wt% for MAA and 99.73wt% for AA) in the ASR was achieved. In order to achieve good water solubility at pH=10, the acid number of the ASRs were $143 mg_{KOH}\, g_{ASR}^{-1}$ for ASR_{MAA} and $171 mg_{KOH}\, g_{ASR}^{-1}$ for ASR_{AA}. The amphiphilic characteristics of

the ASRs are strongly affected by the pH. CMC was determined at pH=10 finding that CMC(ASR_{MAA})=0.015 gL^{-1}; and CMC(ASR_{AA})=0.059 gL^{-1}, the difference likely due to higher content of carboxylic groups of the ASR_{AA}.

The relative significance of the three mechanisms proposed to justify the reduction of the radical entry in ASR-stabilized latexes was investigated. The three mechanisms considered were the resistance to radical diffusion, the charge repulsion, and the hydrogen abstraction. It was shown that the resistance to the radical entry depends on the type of ASR, the type of initiator, and the type of monomer used. Two monomers of different hydrophobicity (S, MMA), initiators producing different radicals in both aqueous and oil phases (APS, TBHP/AsAc and AIBN), and ASRs either prone or not prone to suffering hydrogen abstraction (ASR_{MAA} and ASR_{AA}) were used in several miniemulsion polymerizations.

For styrene (hydrophobic monomer), the polymerization rate when using APS (anionic hydrophilic radicals) was substantially reduced mainly because the ASR acted as a radical sink (due to hydrogen abstraction), but electrical repulsion was also important. For TBHP/AsAc (uncharged hydrophobic radicals), the effect was due to hydrogen abstraction and it was substantial.

For MMA (hydrophilic monomer), the effect of hydrogen abstraction was important (although slightly lower than for styrene) using THBP/AsAc. The effect of the monomer hydrophilicity was important when APS was used because the sulphate ion radicals must propagate in the aqueous phase before

entering into the polymer particles. When the monomer concentration in the aqueous phase was very low (i.e., for S), the oxygen centered radical had a relative long life around the hairy layer, and hence they had the opportunity of abstracting hydrogens. When MMA, which has a relatively high concentration in the aqueous phase, was used, the life of the oxygen centered radical was shorter and the rate of hydrogen abstraction lower.

For the oil-soluble initiator (AIBN), the resistance due to hydrogen abstraction was higher than that of the radical diffusion. However, this value is much lower than that observed for TBHP/AsAc because carbon-centered radicals coming from AIBN are less effective than oxygen centered radicals in hydrogen abstraction.

The conclusions from the kinetic analysis were supported by the analysis of the MWD of the final latexes that showed that in the peak of the ASR shifted to higher molecular weight for ASR_{AA} and remained unchanged for ASR_{MAA}.

In order to reduce the acid number (N_{Ac}) of ASRs, a new family of ASRs was produced by adding a more hydrophilic monomer, acrylamide (AM). Therefore, ASRs containing MMA, BMA, MAA and AM with different acid numbers (MAA content) and different MMA/BMA ratios were successfully synthesized covering a certain range of hydrophilicity.

No significant differences were found in the average molecular weights ($\bar{M}n \sim 2100 gmol^{-1}$; $\bar{M}w \sim 5500 gmol^{-1}$) for all the ASRs regardless of their

MMA content and MMA/BMA ratio. MALDI-TOF was used to measure the whole MWD of the ASRs. In this case, the relative fraction of smaller molecular weights increased with the hydrophilicity of the ASR suggesting that low molecular weights were mainly produced in the aqueous phase. The $\overline{M}w$ measured by this technique (around 4600gmol^{-1}) was not affected by the ASR composition.

The acid numbers measured by conductometric titration indicated a certain degree of hydrolysis of AM that increased for lower MAA contents. The heterogeneity of the ASRs was verified measuring the fraction of the ASR solubilised in water at different pH values. From these experiments, it was concluded that the ASRs were rather heterogeneous in both, composition and molecular weights.

Despite the presence of ASR aggregates, no clear CMC values were obtained for the ASRs using surface tension measurements and fluorescence of pyrene. The reason seemed to be the heterogeneity of the ASR chains. The adsorption of ASRs on PMMA particles did not follow a Langmuir isotherm. Adsorption measurements showed that the better compatibility between the ASRs with higher MMA content and the PMMA polymer particles largely determined the adsorption equilibrium, the hydrophilicity being a secondary factor.

The MMA/BMA/MAA/AM ASRs synthesized were used as sole stabilizers in emulsion and miniemulsion polymerizations.

Batch emulsion copolymerizations of BA/MMA were successfully carried out varying the ASR type and concentration. For all the ASRs, the number of particles increased with the ASR concentration. Fitting the data to a power function ($Np \div [ASR]^Z$), it was found that in all the cases the value of the exponent (Z=1.3-4.3) was much larger than that predicted by Smith-Ewart theory (Z=0.6). The reason could be the high ASR/monomer ratio used and the heterogeneity of the ASRs which include low molecular weight water soluble species that can desorb quickly being able to stabilize new precursor particles. Consequently, the more hydrophilic ASRs resulted in higher exponent values. In addition, it was found that the polymerization rate was almost independent of the number of particles with together which the low values calculated for the average number of radicals per particle, proved that the reactions proceeded under Smith-Ewart Case 1. In all the cases, no coagulum was observed.

Miniemulsion polymerizations of MMA were carried out using different types and concentration of ASRs. It was found that particle size strongly decreased with the ASR concentration leading to higher polymerization rates. The smallest particle size was obtained with the most hydrophilic ASR (ASR_5). Comparison with styrene using a more hydrophobic ASR (ASR_1) showed that smaller particle sizes and narrower particle size distributions were obtained with MMA, which might be due to the better compatibility of the ASR_1 with poly(methyl methacrylate).

Finally, a low acid number ASR (~ 50$mg_{KOH}g_{ASR}^{-1}$) was synthesized substituting AM by dimethyl-acrylamide (DMAM) by means of emulsion polymerization based on the system MMA/BMA/MAA/DMAM. This ASR produces small aggregates (d_{agg}=35nm) at pH=8.5.

The capability of the ASR aggregates to absorb monomers of different hydrophobicity (MMA, BA and S) was studied. For MMA, stable aggregates can be obtained even for high ratios (~ 2) of monomer/ASR. However, for BA and S stable dispersions can only be obtained for lower ratios of monomer/ASR (1.25 for BA and 0.5 for S). These swollen aggregates were successfully polymerized to obtain high solids dispersions in a two steps emulsion polymerization process using MMA, BA and 50/50wt/wt mixture of MMA/BA.

In the first step, the aggregates of ASR were swollen with monomer using a monomer/ASR ratio equal to 0.5. Under reaction conditions the sizes of the aggregates were bigger for MMA than for MMA/BA and BA. The BA and MMA/BA showed high polymerization rates but MMA was slower due to the lower N_p and the low propagation rate constant of MMA. An equivalent conversion of about 97% was reached for BA and MMA/BA. For MMA, equivalent conversion was lower (≈ 88%) in part due to the influence of the glass effect. In the second step, the latex formed in the first step was swollen with more monomer (until monomer/ASR ratio equal to 1) and then polymerized. The polymerization rate followed the same trend than in the first step. Polymerization of the residual monomer was achieved by adding a shot

of AsAc. Stable and monodispersed latexes with particle diameters around 80-90nm were obtained for BA and MMA/BA. For MMA a large size peak is obtained in the PSD although macroscopic coagulum was not observed.

Small particles latexes of MMA/BA (40/60wt/wt) were synthesized using more hydrophobic ASRs substituting MMA by LMA in the backbone. It can be seen that the ASR with 5, 10 and 20wt% of LMA gave smallest size aggregates. Semi-continuous emulsion polymerizations were carried out at 80ºC using APS as initiator. Stable latex with 40% of solids content and particle size of about 60nm were successfully obtained.

Appendix I Emulsion polymerization

Outline

I.1 Introduction

Emulsion polymerization is a technique leading to colloidal polymer particles dispersed in a continuous medium [1], most often water. These polymeric dispersions are called latexes. The polymer particles are mostly spherical, but they often have a morphology that strongly affects application properties. The average diameter of the particles ranges from 50 to 1000 nm. This size range is more than one order of magnitude smaller than that of the particles obtained by suspension polymerization, and it is the result of a unique mechanism of particle formation. Emulsion polymers are produced by free-radical polymerization. The solids content (weight of solid material/weight of latex) of commercial latexes spans from 40 to 65 wt%, although for some applications higher solids contents are desirable.

Polymer dispersions include both synthetic polymer dispersions and natural rubber. Synthetic polymer dispersions are produced by emulsion polymerization. About half of these polymers are commercialized as water-borne dispersions. The main markets for these dispersions are paints and coatings (26%), paper coating (23%), adhesives (22%) and carpet backing (11%) [2]. Polymer dispersions have also found an interesting market niche in biomedical applications (diagnosis, drug delivery and treatment [3]).

I.2 Microstructural features and their effect on properties

The features of the emulsion polymers include copolymer composition, monomer sequence distribution (MSD), molecular weight distribution (MWD), polymer architecture (branching, grafting, crosslinking and gel content), particle surface functionality, particle morphology and particle size distribution (PSD).

Copolymer composition has a direct effect on the Tg of the polymer, which determines the minimum film forming temperature (MFFT) of the latex and the application. Thus, a 95/5wt/wt butyl acrylate/methyl methacrylate is an adhesive, whereas a 50/50 copolymer of the same monomers is a binder for paints. Copolymer composition affects properties such as resistance to hydrolysis and weatherability.

Molecular weight distribution strongly affects application properties. For example, in papers coated with styrene-acrylate copolymers, the dry pick strength increases and the blister resistance decreases as the molecular weight of the polymer [2] increases.

The application properties of many latexes are strongly affected by the chemistry of the surface of the polymer particles. Relatively small amounts (1–2 wt% based on monomers) of acidic monomers (e.g., acrylic acid, AA) are frequently used in the manufacture of latexes. Because this monomer is

water-soluble, upon polymerization, most of the AA-rich polymer chains are located at the surface of the polymer particles. The presence of AA at the surface of the polymer particles is beneficial for both the stability of the latex [4] and the application properties (e.g., both the shear strength of the adhesives and the pick strength of coated paper increase with the AA content). In addition, the type and amount of surfactant affects application properties such as colloidal stability and water sensitivity of the film.

Particle size distribution (PSD) and the particle surface functionality determine the rheology of the latex [5]. Rheology is critical during emulsion polymerization because it controls mixing and heat transfer. Rheology also determines the maximum solids content achievable and plays a crucial role in the applications of the polymeric dispersion [1]. On the other hand, the quality of the film improves when particle size decreases.

I.3 Description of emulsion polymerization

Commercial implementation of emulsion polymerization is mostly carried out in stirred tank reactors operated semicontinuously. Continuous stirred tank reactors (CSTRs) are used for the production of some high tonnage emulsion polymers. Batch processes are only used to polymerize monomers with similar reactivities and low heat generation rate. In the semicontinuous process, the reactor is initially charged with a fraction of the formulation (monomers, emulsifiers, initiator and water). The initial charge is

polymerized in batch for some time and then the rest of the formulation is added over a certain period of time. The monomers can be fed either as an aqueous pre-emulsion stabilized with some emulsifier or as neat monomers. The initiator is fed in a separate stream. The goal of the batch polymerization of the initial charge is to nucleate the desired number of polymer particles. Because particle nucleation is prone to suffer run-to-run irreproducibility, seeded semicontinuous emulsion polymerization is often used to overcome this problem.

I.3.1 Emulsion polymerization process

In batch, the monomers are dispersed in water in the presence of surfactants. The surfactants adsorb on the surface of the monomer droplets stabilizing them. Ionic surfactant stabilizes the droplets by electrostatic repulsion, whereas non-ionic surfactants provide steric stabilization [6]. In most formulations, the amount of surfactant exceeds that needed to completely cover the monomer droplets and saturate the aqueous phase. The excess of surfactant forms micelles that are swollen with monomer.

Thermal initiators are used when the process is carried out at elevated temperatures, and redox systems are used for lower temperatures and when a high rate of initiation is needed. Most initiators are water-soluble, therefore the radicals are formed in the aqueous phase. These radicals are often too hydrophilic to directly enter into the organic phases. Therefore, they react with

the monomer dissolved in the aqueous phase, forming oligoradicals that grow slowly because of the low concentration of monomer in the aqueous phase. After adding some monomer units, the oligoradicals become hydrophobic enough to be able to enter into the organic phases of the system. Because the total area of the micelles is about three orders of magnitude greater than that of the droplets, entry of radicals into the micelles is more likely. The entering oligoradicals find a monomer-rich environment within the micelle, and hence they grow fast forming a polymer chain. The new species formed upon entry of a radical into a micelle is considered to be a polymer particle. The process of formation of polymer particles by entry of radicals into micelles is called *heterogeneous nucleation*. Polymer particles can also be formed when the oligoradicals grow in the aqueous phase beyond the length at which they are still soluble in water and precipitate. The precipitated polymer chain is stabilized by the emulsifier present in the aqueous phase, and monomer diffuses into the new organic phase, which allows a fast growth of the polymer chain. The process of formation of polymer particles by precipitation of oligoradicals is called *homogeneous nucleation*. Both homogeneous and heterogeneous nucleation may be operative in a given system. In general, homogeneous nucleation is predominant for monomers of relatively high water-solubility and heterogeneous nucleation is predominant for water-insoluble monomers.

Irrespective of the mechanism of particle nucleation (heterogeneous or homogeneous), the newly formed particles are very small and suffer a tremendous increase in surface area upon particle growth. It is arguable that

the emulsifier molecules may diffuse fast enough to the surface of these fast growing particles to stabilize them. Therefore, the species formed by entry of radicals in micelles and by precipitation of growing radicals in the aqueous phase may be regarded as precursor particles that only become stable particles upon growth by coagulation and polymerization. This combined process is sometimes called *coagulative nucleation*.

The classical Harkins theory[7] of emulsion polymerization is illustrated in Figure 1. During nucleation, monomer droplets, monomer swollen micelles and monomer swollen polymer particles coexist in the batch reactor (Interval I). Polymer particles efficiently compete for radicals and as their number increases, they become the main polymerization loci. The monomer that is consumed by free-radical polymerization in the polymer particles is replaced by monomer that diffuses from the monomer droplets through the aqueous phase. Therefore, the size of the particles increases and that of the monomer droplets decreases. The number of micelles decreases because they become polymer particles upon entry of a radical, and also because they are destroyed to provide surfactant to stabilize both the polymer chains that precipitate in the aqueous phase and the increasing surface area of the growing polymer particles. After some time, all micelles disappear. This is considered to be the end of the nucleation and only limited formation of new particles may occur after this point because heterogeneous nucleation is not possible and there is no free surfactant available in the system to stabilize the particles formed by homogeneous nucleation. The stage of the batch emulsion polymerization in which particle nucleation occurs is called Interval I. Unless

coagulation occurs, the number of particles remains constant during the rest of the batch process.

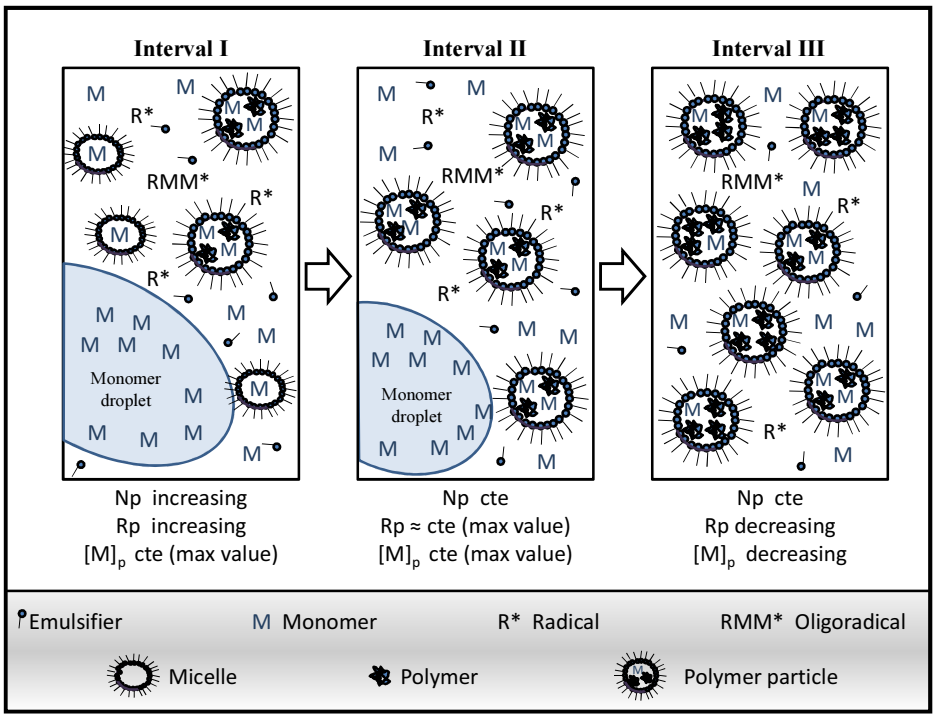

Figure 1: The classical Harkins Theory

In Interval II, the system is composed of monomer droplets and polymer particles. The monomer consumed by polymerization in the polymer particles is replaced by monomer that diffuses from the monomer droplets through the aqueous phase. The mass transfer rate of monomers is in most cases higher than the polymerization rate, and hence monomer partitions between the different phases of the system according to thermodynamic equilibrium. In the presence of monomer droplets, the concentration of the

monomer in the polymer particles reaches a maximum value that is roughly constant during Interval II. The transport of reactants with low water solubility may be diffusionally limited. The polymer particles grow in size and after some time, the monomer droplets disappear, marking the end of Interval II. The monomer conversion at which Interval II ends depends on the extent in which the polymer particles are swollen by the monomer. The higher the maximum swelling, the earlier the monomer droplets disappear. In general, the more water-soluble the monomer the higher the maximum swelling, and hence the lower the monomer conversion at the end of Interval II. Most of the monomer polymerizes during Interval III. In this interval, the monomer concentration in the polymer particles decreases continuously.

In semicontinuous reactors, monomers, surfactant, initiator and water are continuously fed into the reactor. In CSTRs, the whole formulation is continuously fed into the reactor and the product continuously withdrawn. In these systems, emulsion polymerization does not follow the sequence of events described earlier. Nevertheless the underlying processes are the same.

I.3.2 Mechanisms of emulsion polymerization

Figure 2 illustrates the mechanisms involved in emulsion polymerization. Radicals formed in the aqueous phase from water-soluble initiators, react with the monomer dissolved in the aqueous phase forming oligoradicals. These oligoradicals may (1) enter into the polymer particles, (2)

enter into the micelles (heterogeneous nucleation), (3) propagate in the aqueous phase until they become insoluble and precipitate forming new polymer particles (homogeneous nucleation) and (4) terminate with other radicals in the aqueous phase.

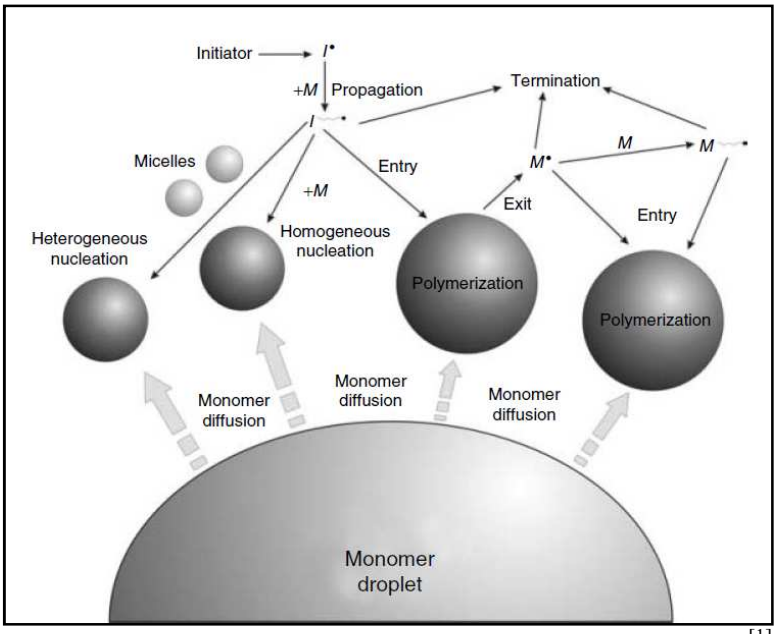

Figure 2: Mechanisms involved in emulsion polymerization [1].

The likelihood of each of these events depends on the particular conditions of the system. Within the polymer particles, polymerization follows the same mechanisms as in bulk free-radical polymerization. These mechanisms involve chain transfer to small molecules (e.g., monomers and CTAs), that yield small radicals. These small radicals may exit the polymer particles diffusing into the aqueous phase.

I.3.3 Radical compartmentalization

In an emulsion polymerization system, radicals are distributed among the polymer particles. The size of these particles is so small that there are only a small number of radicals per particle, as an average less than one radical per particle in many cases of practical interest. The compartmentalization of radicals among the particles is the most distinctive kinetic feature of emulsion polymerization and has profound implications in both the polymerization rate and polymer microstructure. Radicals in different particles cannot terminate by bimolecular termination. Consequently; the overall radical concentration in emulsion polymerization is higher than in bulk polymerization. This means that the polymerization rate in emulsion polymerization is significantly higher than in bulk polymerization. In a latex, the overall concentration of radicals increases. This gives a further way of increasing polymerization rate.

Radical compartmentalization also results in longer life-time of the radicals, which leads to higher molecular weights. For the system described above, a polymer chain grows until a second radical enters into the polymer particle and terminates with the growing one. Therefore, the chain length is inversely proportional to the entry frequency. For a given concentration of initiator, the frequency of radical entry decreases with the number of particles, therefore the molecular weight increases. Consequently, in emulsion polymerization it is possible to simultaneously increase the polymerization rate and the molecular weight by simply increasing the number of particles.

This is not possible in any other free-radical polymerization technique (bulk, solution, suspension).

I.4 Emulsion polymerization kinetics

The main equations governing the kinetics of emulsion polymerization are reviewed below. The polymerization rate expression and the variables needed to compute it, will be analyzed.

I.4.1 Polymerization rate

The rate of polymerization per unit volume of monomer swollen polymer particle (R_p^* in mol $L^{-1}s^{-1}$) is:

$$R_p^* = k_p[M]_p[P_{tot}]_p \quad (1)$$

where k_p is the propagation rate constant (L $mol^{-1}s^{-1}$), $[M]_p$ the concentration of monomer in the polymer particles (mol L^{-1}) and $[P_{tot}]_p$ the concentration of radicals in the polymer particles (mol L^{-1}).

An emulsion polymerization system is composed of particles of different sizes. Because of the stochastic entry and exit of radicals, the concentration of radicals in a given particle varies randomly with time, and

particles with the same size have a different concentration of radicals. Although there are ways to model such a complex system, for most practical applications the polymerization rate is accurately estimated by considering that the system is represented by a population of particles of an average size. Under these circumstances, $[P_{tot}]_p$ can be expressed in terms of the average number of radicals per particle, $\bar{n}$, in such a way that the polymerization rate per unit volume of the reactor, R_p, is given by:

$$R_p = k_p [M]_p \frac{\bar{n}}{N_A} \frac{N_p}{V} \tag{2}$$

where N_A is the Avogadro's number, N_p the number of polymer particles in the reactor and V the volume of the reactor. In order to calculate the polymerization rate, $\bar{n}$, N_p and $[M]_p$, should be available.

I.4.2 Average number of radicals per particle

The average number of radicals per particle is defined as follows:

$$\bar{n} = \frac{\sum_{n=0}^{n=\infty} n N_{p(n)}}{\sum_{n=0}^{n=\infty} N_{p(n)}} \tag{3}$$

where $N_{p(n)}$ is the number of particles with n radicals, which depends on the relative rates of radical entry, termination and exit. First principles equations for the rate of radical entry have been derived. However, these equations

contained parameters difficult to estimate and are strongly influenced by the mechanistic assumptions used in their derivations. A pragmatic way of expressing the rate for radical entry (radicals particle^{-1}s^{-1}) is as follows:

$$\text{Rate of entry} = k_a[P_{tot}]_w \tag{4}$$

where k_a is the entry rate coefficient (L mol^{-1}s^{-1}), which should be estimated for each system and $[P_{tot}]_w$ the concentration of radicals in the aqueous phase (mol L^{-1}). It is worth pointing out that $[P_{tot}]_w$ includes radicals of any length.

The rate of radical termination (radicals particle^{-1}s^{-1}) in the polymer particles with n radicals is:

$$\text{Rate of termination} = \frac{k_t}{v_p N_A}\, n(n-1) = 2cn(n-1) \tag{5}$$

where k_t is the termination rate constant (L mol^{-1}s^{-1}), v_p is the volume of a monomer swollen polymer particle, and the pseudo-first order rate coefficient for termination in the polymer particles is:

$$c = \frac{k_t}{2v_p N_A} \tag{6}$$

Radical exit occurs by chain transfer to a small molecule followed by diffusion of the small radical to the aqueous phase. The rate of radical desorption or exit (radicals particle^{-1}s^{-1}) from a particle with n radicals is:

$$\text{Rate of exit} = k_d n \tag{7}$$

where k_d (s^{-1}) is the average desorption rate coefficient.

The population balance of particles with n radicals is:

$$\begin{aligned}\frac{dN_{p(n)}}{dt} = {} & k_a[P_{tot}]_w N_{p(n-1)} + k_d(n+1)N_{p(n+1)} \\ & + c(n+2)(n+1)N_{p(n+2)} - k_a[P_{tot}]_w N_{p(n)} \\ & - k_d n N_{p(n)} - cn(n-1)N_{p(n)} \\ & n = 0; 1; 2; 3 \ldots\end{aligned} \tag{8}$$

Equation 8 includes the concentration of radicals in the aqueous phase. This concentration can be calculated by means of the following material balance:

$$\frac{d[P_{tot}]_w}{dt} = 2fk_I[I]_w + K_d\bar{n}\frac{N_p}{N_A V_w} - k_{tw}[P_{tot}]_w^2 - k_a[P_{tot}]_w\frac{N_p}{N_A V_w} \tag{9}$$

where radical formation from a thermal water-soluble initiator is considered and f is the efficiency factor of the initiator radicals, k_I the rate coefficient for initiator decomposition (s^{-1}), $[I]_w$ the concentration of the thermal initiator in the aqueous phase (mol L^{-1}) and k_{tw} the termination rate in the aqueous phase (L $mol^{-1}s^{-1}$).

For most practical cases, the pseudo-steady-state assumption can be applied to the radicals in the polymer particles and in the aqueous phase. Therefore, Equations 8 and 9 are converted in algebraic equations by making the left-hand side equal to zero. Under pseudo-steady-state conditions the exact solution for $\bar{n}$ is available in terms of Bessel functions, but it is not easy to use. A simpler and accurate equation for $\bar{n}$ is as follows:

$$\bar{n}=\frac{2k_a[P_{tot}]_w}{k_d+(k_d{}^2+4k_a[P_{tot}]_w c\Psi)^{0.5}} \tag{10}$$

$$\Psi=\frac{2(2k_a[P_{tot}]_w+k_d)}{2k_a[P_{tot}]_w+k_d+c} \tag{11}$$

Equations 10 and 11 should be solved together with Equation 9. The solution of this system of algebraic equations includes the three limiting cases of the pioneering work of Smith and Ewart [8] summarized in Table 1. For Case 1, $\bar{n} << 0.5$, and it corresponds to a system in which the radical desorption rate is much faster than the rate of radical entry. In Case 2, $\bar{n} = 0.5$ corresponding to a system in which the radical desorption rate is zero, and instantaneous termination occurs when a radical enters a polymer particle already containing one radical. In Case 3, the concentration of radicals in the polymer particle approaches that of bulk polymerization ($\bar{n} >> 0.5$).

Table 1: Smith-Ewart limiting cases

Smith and Ewart limiting case	**Experimental conditions**	$\bar{n}$	**Equation to calculate $\bar{n}$**
Case 1	(1) Small particles (d_p<100 nm) (2) Relatively water-soluble monomers or relatively water-soluble CTAs (3) Low rate of generation of radicals from the initiator (4) Large number of particles	$\bar{n} << 0.5$	$\bar{n} = \frac{k_a[R]_w}{2k_a[R]_w + k_d}$
Case 2	(1) No chain transfer to small molecules (i.e., monomers and CTAs) or these small molecules are highly water insoluble (2) Fast bimolecular termination rate (3) The polymer particles are relatively small (typically d_p<200nm)	$\bar{n} = 0.5$	$\bar{n} = 0.5$
Case 3	(1) Large particles (d_p>200nm) (2) High initiator concentrations or redox initiators (3) Slow termination rates (gel effect)	$\bar{n} >> 0.5$	$\bar{n} = \left(\frac{k_a[R]_w}{2c}\right)^{0.5}$

For Case 2, the polymerization rate is proportional to the number of particles and the molecular weight also increases with N_p. For Cases 1 and 3 the polymerization rate is independent of the number of polymer particles if radical termination in the aqueous phase is negligible, and increases with N_p when it is significant. In Case 1, the molecular weights are determined by chain transfer, and in Case 3, the molecular weights are similar to those in bulk.

I.5 References

1. Barandiaran, M. J.; de la Cal, J. C.; Asua, J. M., Emulsion polymerization. In *Polymer reaction engineering*, Asua, J. M., Ed. John Wiley & Sons: 2008; pp 233-272.

2. Schmidt-Thümmes, J.; Schwarzenbach, E.; Lee, D. I., Applications in the paper industry. In *Polymer dispersions and their industrial applications*, Urban, D.; Takamura, K., Eds. Wiley-VCH Weinheim: 2002; pp 75-101.

3. Delair, T., Applications biomédicales des latex synthétiques. In *Les Latex Synthétiques. Élaboration, Propriétés, Applications*, Daniel, J. C.; Pichot, C., Eds. Lavoisier: Paris, 2006; pp 699-718.

4. Waters, J. A., Latex paint formulations. In *Polymeric dispersions: principles and applications*, Asua, J. M., Ed. Kluwer Academic Publishers: Netherlands, 1997; Vol. 335, pp 421-433.

5. Arevalillo, A.; do Amaral, M.; Asua, J. M. *Industrial & Engineering Chemistry Research* **2006,** 45, (9), 3280-3286.

6. Ottewill, R. H., Scattering techniques-fundamentals. In *Polymeric dispersions: principles and applications*, Asua, J. M., Ed. Kluwer Academic Publishers: Netherlands, 1997; Vol. 335, pp 217-228.

7. Harkins, W. D. *Journal of the American Chemical Society* **1947,** 69, (6), 1428-1444.

8. Smith, W. V.; Ewart, R. H. *The Journal of Chemical Physics* **1948,** 16, (6), 592-599.

Appendix II Miniemulsion Polymerization

Outline

II.1 Introduction

In emulsion polymerization, the polymer particles can be formed by entry of radicals into the micelles (heterogeneous nucleation), or by precipitation of growing oligomers in the aqueous phase (homogeneous nucleation). Monomer droplets are relatively large compared to monomer swollen micelles and consequently the probability for a radical to enter into droplets is very low.

Once the polymer particles are formed, the monomer must be transported from the monomer droplets by diffusion trough the aqueous phase. In some cases, this represents a severe limitation of the conventional emulsion polymerization. Nevertheless, the need of mass transport of the monomer through the aqueous phase would be greatly diminished if all or a large fraction of monomer droplets were nucleated. Prevalent droplet nucleation can only occur if the surface area of the monomer droplets is large in comparison with that of the micelles, and this requires submicron droplet sizes. Miniemulsions are submicron oil-in-water dispersions that are stable for a period ranging from hours to months.

In miniemulsion polymerization [1, 2], nucleation takes place preferently by entry of radicals into monomer droplets (droplet nucleation). Thereby, the monomer diffusion through the aqueous phase is not required, allowing by this technique the synthesis of polymeric dispersions from water insoluble monomers.

Miniemulsion polymerization [1, 2] seems to be the perfect technique to synthesize complex materials that cannot be produced otherwise. The performance of the materials is determined by the characteristics of the particles:

particle size and particle size distribution; polymer functionality and architecture; molecular weight distribution (MWD); number, type and relative amount of the phases; particle composition distribution; and particle morphology (including the characteristics of the surface of the particles). These materials are "products-by-process" and hence their characteristics are attained in the reactor, namely, they depend on the way in which the process is conducted.

II.2 Miniemulsification

Miniemulsification adds complexity and cost to the process. Therefore, phase inversion emulsification is an attractive way to produce miniemulsions as it does not involve the use any special emulsification device and the energy consumption is modest. Transitional phase inversion involves an induced change of the surfactant affinity.

Another way of preparing miniemulsions is to subject the coarse emulsion produced by conventional agitation to a high energy source in order to break the composite droplets up to the submicron size (80-200nm), if possible, with a narrow droplet size distribution. In order to break-up the droplets, the disruptive energy should overcome the surface energy and the viscoelastic energy of the dispersed (organic) phase. Surface energy depends on the interfacial tension, which is substantially reduced by the presence of surfactant. Several devices can be used to provide the disruptive energy including sonicators, rotor-stators, membranes, static mixers and high pressure

homogenizers. Sonication is very efficient at lab scale, but it is very difficult to scale-up. On the other hand, small droplet size and high solids contents may not be prepared with the use of membranes.

Static mixers are very attractive because the energy consumption is low as compared with rotor-stators and high pressure homogenizers. The results available show that a relatively high number of passes through the static mixer (40-300) are necessary to form the miniemulsion.

Rotor-stators can produce 50 wt% solids content miniemulsions using reasonable concentrations of surfactant, although the droplet size seems to be quite sensitive to the viscosity of the dispersed phase.

High pressure homogenization facilitates the preparation of high solids content dispersions of nanodroplets even for systems dealing with highly viscous organic phases. In these systems, the coarse emulsion is passed through the narrow gap of a valve. This process results in a tremendous increase of the surface area of the droplets that if it is not rapidly covered by the surfactant leads to droplet coagulation. A consequence of the droplet break-up and coagulation processes is that both the size and the broadness of the droplet size distribution decrease with the number of passes. Therefore, several passes are often needed to achieve small droplets sizes. High pressure homogenizers (HPHs) seem to be a promising choice for industrial scale as large capacity HPHs are available. The use of two or more HPHs in series would likely lead to small droplet sizes in shorter times, but this option substantially increases the investment.

In-situ formation of the surfactant by neutralizing an oil-soluble carboxylic acid with an alkali aqueous solution may be a way to further reduce the time required for the miniemulsification. However, there is some confusion about this process. Thus, it has been claimed that the in-situ formed surfactant reduces the interfacial tension to much lower values than the pre-synthesized surfactant of the same composition [2] making easier the emulsification. The resulting emulsion was reported to be 5-10 times more stable than that prepared with the pre-synthesized surfactant. However, more recent studies have shown that the emulsions formed with in-situ and pre-synthesized surfactants were similarly unstable.

Irrespective of the method used to perform the miniemulsification, the miniemulsion should be colloidally stable and stable against Oswald ripening at least for the time needed to perform the polymerization. Colloidal stability is provided by the use of the adequate type and concentration of surfactant(s). Oswald ripening refers to the degradation of the dispersion because of the diffusion of the components of the organic phase from small to large droplets. The driving force for this diffusion is the higher chemical potential of the monomer in the small droplets as compared to the monomer in the large ones, which is caused by the contribution of the surface energy to the chemical potential. The effect of the Oswald ripening can be limited by using a costabilizer that is a highly water insoluble compound of low molecular weight. The costabilizer provokes the super-swelling of the droplets by the monomers. Hexadecane is the costabilizer most often used in the open literature, but it causes environmental concerns in application because it

remains unreacted in the final dispersion. In order to overcome this problem, highly water insoluble monomers, chain transfer agents and initiators have been used as costabilizers. However, this is not free from problems.

Polymers, often referred as hydrophobes, have also been used to limit the Oswald ripening, but because their high molecular weight, they are less efficient than costabilizers[1]. The stability of the miniemulsion can be conveniently assessed by measuring the backscattered light over time. It is good practice to perform this test at the reaction temperature because the stability of the miniemulsions decreases as temperature increases.

II.3 Droplet nucleation

For most formulations, the miniemulsion consists of a dispersion of composite droplets colloidally stabilized by surfactants. The objective in miniemulsion polymerization is to transform the composite droplets into composite polymer particles minimizing the heterogeneity in particle composition. The challenges strongly depend on the process used: batch or semicontinuous.

In batch reactors, under some conditions, the size of polymer particles was similar to that of the miniemulsion droplets measured by dynamic light scattering (DLS) and this is often taken as proof of a complete nucleation of the miniemulsion droplets. The mechanisms involved in the nucleation process

elucidates the conditions for a successful miniemulsion polymerization: (i) a very stable miniemulsion under polymerization conditions to avoid the lost of droplets, (ii) a fast nucleation rate to minimize the mass transfer of monomer from droplets to particles, and (iii) absence of homogeneous nucleation to avoid the formation of particles that do not contain the water insoluble compounds of the formulation.

High stability of the miniemulsion is a necessary condition for an efficient particle nucleation. In apparently well stabilized systems, it has been demonstrated that collision represents a significant contribution to mass transport among droplets and particles. The same mechanism seems to be operative in emulsion polymerization. Fast nucleation involves a rapid generation of radicals, which when water-soluble initiators are used, should be captured by the existing droplets/particles to avoid homogeneous nucleation. Radical capture is maximized by increasing the high solids contents and reducing the droplet size. The use of water-soluble initiators that yield uncharged radicals able to enter directly into droplets and particles may reduce the occurrence of homogeneous nucleation while still maintaining a fast droplet nucleation rate. Oil-soluble initiators, produce radicals in pairs within droplets and particles and although desorption of initiator radicals is a key aspect for the efficiency of these initiators [3], the probability of forming oligoradicals that upon precipitation form new particles is substantially reduced. However, because of the extensive radical termination, the rate of droplet nucleation is low.

A way in which homogeneous nucleation may be limited is controlling the availability of the surfactant to stabilize the precipitated oligoradicals. This can be achieved by limiting the total amount of surfactant in the formulation and by using surfactants that strongly adsorb on the droplet/particle surface.

In semicontinuous reactors, there are two ways in which miniemulsion polymerization can be implemented. One approach is to use a miniemulsion containing all the water and the insoluble compounds as initial charge, polymerize it and then feed semicontinuously the components of the formulation that can be transported through the aqueous phase (monomers, CTA, crosslinking agent). In the second approach, a fraction of the whole miniemulsion is used as initial charge, polymerized in batch and then the rest of the miniemulsion is fed semicontinuously.

In order to obtain particles with a narrow composition distribution, in the first approach, the goal is to nucleate the miniemulsion droplets of the initial charge avoiding both homogeneous nucleation and coagulations during the polymerization. Therefore, the challenges in the polymerization of the initial charge are similar to those discussed for the batch process.

II.4 Miniemulsion kinetics

In order to use miniemulsion polymerization for the commercial production of free radical polymers that can be produced by conventional

emulsion polymerization, the polymer obtained by miniemulsion polymerization must present substantial advantages in properties to overcome the additional investments and operational costs associated to miniemulsification.

In batch miniemulsion copolymerization, the incorporation of the less water soluble monomer to the copolymer is higher than in emulsion polymerization. The reason is that in miniemulsion polymerization, both monomers are from the beginning in the polymerization loci, whereas in emulsion polymerization the monomers should be transported from large droplets to growing particles and this transport is slower for the less water soluble monomers. In semicontinuous miniemulsion polymerization with a neat monomer feed, the copolymer was substantially richer in the more water-soluble monomer than what was predicted by the Mayo-Lewis equation. However, the use of a miniemulsion feed significantly improved the incorporation of the less water soluble monomer into the copolymer, likely due to polymerization in the entering droplets.

On the other hand, miniemulsion polymerization is the best way to synthesize polymers from very water-insoluble monomers such as the long chain fluorinated acrylates used for textile applications. Due to the droplet nucleation mechanism and to the limited monomer diffusion between droplets and particles, the evolution of polymerization rate in miniemulsion polymerization differs from that observed in emulsion.

A typical styrene miniemulsion polymerization process (using cetyl alcohol (CA) or hexadecane (HD) as costabilizers) does not show a constant reaction rate period. As a result, it can be divided in four major regions based on the polymerization rate versus monomer conversion curve; as explained broadly in "Principles and applications of emulsion polymerization" [4]. Firstly, the rate of miniemulsion polymerization increases rapidly to a primary maximum and then decreases with increasing monomer conversion. This is followed by the increase of polymerization rate to a secondary maximum. After the secondary maximum is achieved, the rate of polymerization then decreases rapidly toward the end of polymerization [5].

The first maximal polymerization rate is attributed to the continuous formation of latex particles. Formation of latex particles originating from the submicron monomer droplets primarily occurs in Interval I, and the polymerization rate increase with increasing monomer conversion. According to the Smith-Ewart [6] Case 2, both the number of latex particles and the concentration of monomer in the particles contribute to the changed rate of polymerization with monomer conversion. The larger the number of particles and the concentration of monomer into the particles, the faster the polymerization rate. Therefore, the primary maximal polymerization rate does not necessarily correspond to the end of particle nucleation. Particle nuclei may be generated continuously in Interval II, but this effect may be outweighed by the decreasing polymerization rate due to the reduced concentration of monomer in the latex particles. This unique feature is illustrated by the experimental results of Miller et al. [7]. They showed that the

styrene miniemulsion polymerization using cetyl alcohol as the costabilizer exhibits a long and slow particle nucleation. Once a significant concentration of latex particles is generated, the particle nucleation process is greatly retarded because most of the oligomeric radicals are captured by the monomer-swollen particles. In addition, the average number of free radicals per particle can be bellow 0.5, and it increases slowly with increasing monomer conversion in Interval I. This can be attributed to the slow absorption of oligomeric radicals by the monomer droplets.

During Interval II, the concentration of monomer in the polymer particles continues to decrease, and hence the rate of polymerization decreases with increasing monomer conversion. The average number of free radicals per particle ($\bar{n}$) is equal to 0.5 during this interval, which is similar to the Smith-Ewart [6] Case 2 kinetics involved in conventional emulsion polymerization. It is also interesting to note that the concentration of monomer and the average number of free radicals in the polymer particles originating from monomer droplet nucleation should be different from those in the water-borne particles. This is due to the presence of these highly costabilizer in the nucleated monomer droplets and the large size of these highly monomer-swollen particles compared to the water-borne particles.

Beyond Interval II, the second maximal polymerization rate can be attributed to the gel effect. The bimolecular termination reaction becomes diffusion controlled in the latex particles and the average number of radicals per particle ($\bar{n}$) increases significantly in the latter stage of polymerization,

leading to an acceleration of the free radical polymerization. The rate of polymerization then decreases continuously toward the end of polymerization due to the depletion of monomer.

As expected, the rate of polymerization in common miniemulsion polymerization systems increases with increasing concentration of surfactant and/or initiator. As to the influence of the concentration of costabilizer on the miniemulsion polymerization kinetics, the experimental results reported in the literature are not conclusive. The rate of polymerization may decrease with increasing concentration of hexadecane (costabilizer) or this effect may be insignificant in miniemulsion polymerization. These conflicting observations can be attributed to the different concentrations of monomer in the monomer droplets and the varying droplet sizes when the level of hexadecane is varied. On the other hand, all the particle nucleation mechanisms, coalescence of monomer droplets and flocculation of latex particles can appear simultaneously.

In general, conventional emulsion polymerization is faster in comparison with the miniemulsion polymerization because more latex particles are nucleated and the rate of polymerization is linearly proportional to the number of latex particles per unit volume of water. Nevertheless, the rate of polymerization per particle is larger for miniemulsion polymerization, as evidenced by the higher concentrations of free radicals and monomer in the latex particles.

II.5 References

1. Asua, J. M. *Progress in Polymer Science* **2002,** 27, (7), 1283-1346.

2. Asua, J. M. *Progress in Polymer Science* **2014,** 39, (10), 1797-1826.

3. Autran, C.; de La Cal, J. C.; Asua, J. M. *Macromolecules* **2007,** 40, (17), 6233-6238.

4. Chern, C.-S., Miniemulsion polymerization mechanisms and kinetics: Polymerization Kinetics. In *Principles and applications of emulsion polymerization*, Chern, C.-S., Ed. John Wiley & Sons: 2008; pp 142-145.

5. Capek, I.; Chern, C.-S., Radical polymerization in direct mini-emulsion systems. In *New Polymerization Techniques and Synthetic Methodologies*, Abe, A.; Joanny, J.-F.; Albertsson, A.-C.; Kausch, H.-H.; Cantow, H.-J.; Kobayashi, T.; Dusek, K.; Lee, K.-S.; Edwards, S.; McGrath, J. E.; Höcker, H.; Monnerie, L.; Stupp, S. I.; Wegner, G.; Suter, U. W.; Young, R. J., Eds. Springer: Verlag Berlin Heidelberg, 2001; Vol. 155, pp 101-165.

6. Smith, W. V.; Ewart, R. H. *The Journal of Chemical Physics* **1948,** 16, (6), 592-599.

7. Miller, C. M.; Sudol, E. D.; Silebi, C. A.; El-Aasser, M. S. *Journal of Polymer Science Part A: Polymer Chemistry* **1995,** 33, (8), 1391-1408.

Resumen

Las resinas álcali solubles (ASRs) son copolímeros de bajo peso molecular compuestos por al menos un monómero con grupos ácidos. Estos copolímeros son capaces de agregarse y actuar como emulsificantes bajo condiciones alcalinas (normalmente a pH>8). En esta tesis, se han sintetizado distintas familias de ASRs usando acrilatos y metacrilatos como monómeros no ácidos y ácido acrílico y metacrílico como monómeros ácidos. La síntesis se ha llevado a cabo mediante polimerización en emulsión ya que es un método muy respetuoso con el medio ambiente y permite un mejor control de la temperatura de reacción evitando disparos térmicos. Las resinas sintetizadas se han caracterizado convenientemente y posteriormente se han empleado como únicos emulsificantes en diversas polimerizaciones tanto en emulsión como en miniemulsión estudiando su cinética y nucleación en profundidad.

Inicialmente se han sintetizado dos ASRs (ASR_A y ASR_B) compuestas por metil metacrilato, butil metacrilato y ácido metacrílico (MMA/BMA/MAA). En ambos casos se ha empleado un 4% de SLS para obtener un tamaño de partícula suficientemente pequeño que permita una buena disolución de las ASRs al utilizarlas como emulsificantes. La resina ASR_A se ha sintezado con un 3% en peso de 1-octanotiol con respecto a la cantidad de monómero. Se trata de un agente de transferencia (CTA) soluble

en fase orgánica utilizado para controlar el peso molecular del polímero formado en las partículas. La resina ASR_B se ha sintetizadocon un 3% en peso de 1-octanotiol y además con el 1% en peso de 2-mercaptoetanol con respecto a los monómeros que es un CTA soluble en agua y se ha utilizado para controlar el peso molecular del polímero formado en la fase acuosa. Aunque el efecto del CTA soluble en agua en la distribución del pesos moleculares no sea significativo, su efecto en la concentración micelar crítica (CMC) y en el área específico de recubrimiento(a_s) es importante. La CMC de la ASR_B es menor que la de la ASR_A por lo que la formación de agregados tiene lugar a menor concentración (compuesto más hidrófobo). Por otro lado, el área específica (a_s) de ASR_B es mayor que la de ASR_A con lo que la cantidad de emulsificante por unidad de área de partícula es mayor, es decir, las partículas estan más recubiertas.

Se han llevado a cabo diversas polimerizaciones en emusión de metil metacrilato (MMA) y estireno (S) usando ASR_A y ASR_B como únicos emulsificantes al 10, 20 y 30% en peso con respecto al monómero. Las reacciones con MMA fueron demasiado rápidas como para dar unas conclusiones fiables. Por el contrario, usando S se observó que la dependencia del número de partículas (N_p) con la concentración de ASR es mayor que la que predice la teoría de Smith-Ewart para polimerizaciones en emulsión. Este aumento se atribuye a la solubilidad de la ASR en el monómero lo que impulsa la creación de partículas a lo largo de la polimerización. Por otro lado, la velocidad de polimerización por partícula (R_{pp}) disminuye con la concentración de ASRs al mismo tiempo que el recubrimiento aumenta, por

ello, se deduce que las ASRs generan cierta resistencia en la entrada de radicales. Este efecto es más acusado en el ASR_B dando una menor R_{PP} y un mayor recubrimiento.

La entrada de radicales hacia el interior de las partículas de polímero se ha estudiado en base a un mecanismo que incluye tres resistencias en serie (abstracción de hidrógeno, difusión y repulsión electrostática). Para evitar interferencias, la cantidad de SLS se ha reducido a un 0,25% en peso debido al desarrollo de un nuevo método de síntesis en semicontinuo. Con este método se han sintetizado dos nuevas resinas (una con ácido metacrílico: MAA y otra con ácido acrílico:AA), la ASR_{MAA} con MMA/BMA/MAA y la ASR_{AA} con MMA/BMA/AA. La ASR_{AA} es propensa a sufrir abstracción de hidrógeno y la ASR_{MAA} no. La resistencia que sufren los radicales por difusión siempre está presente, sin embargo la repulsión electrostatica sólo se da con radicales cargados.

Con este nuevo método de síntesis la incorporacíon del monómero ácido a las partículas es casi completa (99,83% para MAA y 99,73% para AA) por lo que sólo se ha empleado un 3% en peso con respecto a los monómeros del CTA soluble en fase orgánica. Para favorecer la solubilidad a pH=10, se aumento el contenido en ácido de las resinas sintetizadas.

Se llevaron a cabo diversas reacciones de polimerización en minimeulsión usando ASR_{MAA} y ASR_{AA} como emulsificantes utilizando monómeros de distinta hidrofobicidad (S y MMA) y diferentes iniciadores

(APS, TBHP/AsAc y AIBN) solubles en ambos medios que produces radicales con y sin carga.

Usando iniciadores solubes en agua (APS y el sistema TBHP/AsAc), para S (monómero hidrófobo) se ha observado que la velocidad de polimerización se reduce fundamentalmente debido al efecto de la abstarcción de hidrógeno aunque en el caso de utilizar APS (radicales cargados) el efecto de la repulsión es también importante. Para el MMA (monómero hidrofílico) el efecto de la abstracción de hidrógeno es importante para el sistema TBHP/AsAc (radicales no cargados) aunque relativamente menor que para el S. Sin embargo, el efecto de la hidrofilicidad del momómero se observa fundamentalmente al utilizar APS como iniciador ya que los radicales generados deben propagar en la fase acuosa entes de entrar en las partícula. Dado que la concentración de MMA en la fase acuosa es relativamente alta, el tiempo que permanecen los radicales en la fase acuosa es menor que en el caso del estireno disminuyendo con ello el efecto de la abstracción de hidrógeno. En este caso la repulsión electrostática es la principal causante de la disminución de la velocidad de polimerización.

. Usando un iniciador soluble en fase orgánica (AIBN) que da radicales no cargados y generados en el interior de la partículas se observó que la resistencia debida a la abstración de hidrógeno es mayor que la debida a la difusión. Sin embargo, su importancia relativa es menor que el observada cuando se utiliza el sistema THBP/AsAc ya que los radicales centrados en carbono que se generan a partir del AIBN son mucho menos effectivos

abstrayendo hidrógeno que los centrados en oxígeno. La existencia de la abstracción de hidrógeno fue demostrada para los tres iniciadores analizando mediante medidas de GPC la zona de la distribución de pesos moleculares correspondiente a las ASRs. Se observa un desplazamiento a mayores pesos moleculares para la ASR_{AA} mientras que el peso molecular permanece invariable para la ASR_{MAA}.

Con el fin de reducir el contenido en ácido, se sintetizó una nueva familia de ASRs utilizando un monómero más hidrofílico: la acrilamida (AM). Se han producido diferentes ASRs (MMA/BMA/MAA/AM) con distintas cantidades de MAA (12%-14%) y diferente relación MMA/BMA (3/4 y 1/1) para cubrir un amplio rango de hidrofilicidad.

El análisis del peso molecular de estas resinas muestra que las cadenas de más bajo peso molecular corresponden fundamentalmente a las cadenas producidas en la fase acuosa (MALDI-TOF). Esto supone una cierta heterogeneidad de las ASRs que ha sido comprobada midiendo su solubilidad a distintos pH.

Si bien la formación de agregados parece evidente, no se ha obtenido un valor bien definido para la concentración micelar crítica (CMC) de las resinas sintetizadas ni utilizando medidas de tensión superficial ni mediante espectrofluorometría. Esta falta de definición de la CMC se puede atribuir a la heterogeneidad de las cadenas tanto en composición como en el peso molecular. Por otro lado, aunque la adsorción de las ASRs sobre partículas de polimetilmetacrilato (PMMA) no siguen una isoterma de Langmuir, estas

medidas mostraron una mayor adsorción al aumentar la relación MMA/BMA (probablemente debido a una mayor compatibilidad con el polímero) ,y en menor medida un incremento de la adsorción al disminuir el contenido de ácido (mayor hidrofobicidad).

Variando la hidrofobicidad y la concentración de estas nuevas ASRs se han llevado a cabo de manera satisfactoria diferentes reacciones de copolimerización en emulsión (BA/MMA) en discontinuo. Nuevamente y para todos las ASRs utilizadas, el valor del exponente correspondiente a la dependencia del número de partículas con la concentración de ASR es mucho mayor que el predicho por la teoría de Smith-Ewart. El motivo puede ser las altas relaciones ASR/monómero que junto a la gran heterogeneidad de las ASRs, hace que puedan desorberse rapidamente para estabilizar nuevos precursores o partículas. Por otro lado, las velocidades de polimerización (R_p) son independientes del número de partículas (N_p) lo que junto a los bajos valores del número de radicales promedio por partícula, sugiere que las reacciones se dan bajo las condiciones del Caso 1 de Smith-Ewart.

En polimerizaciones en miniemulsión de MMA en discontinuo con distintas concentraciones y tipos de estas nuevas ASRs se observó una disminución del tamaño de partícula con el aumento de la concentración de ASR dando lugar a un mayor número de partículas y una mayor velocidad de polimerización. Los menores tamaños de particula se han obtenido para la ASR más hidrofílica (16% de MAA y MMA/BMA=1). Los tamaños de partícula son mayores y las distribuciones de tamaño más anchas al utilizar

estireno en lugar de metil metacrilato. Este resultado puede ser debido a una mayor compatibilidad de las resinas sintetizadas con el polimetilmetacrilato que con el poliestireno.

Finalmente una nueva ASR con un contenido en ácido mucho menor se ha sintetizado en polimerización en emulsión sustituyendo la AM (debido a su alta toxicidad) por dimetil acrilamida (DMAM). La capacidad de absorción monomérica de esta ASR con un diametro de agregados de 35nm a pH=8.5 fue estudiada usando distintos monómeros (MMA, BA y S) y alterando las relaciones monómero/ASR desde 0 a 2 durante 6 días. Para el MMA se observaron agregados estables (incluso con MMA/ASR=2) durante el tiempo de ensayo. Sin embargo para BA y S, los agregados fueron estables únicamente para relaciones monómero/ASR menores (1,25 para BA y 0,5 para S).

Estos agregados hinchados de monómero fueron polimerizados satisfactoriamente para obtener látex de alto contenido en sólidos (52% en peso) en un proceso de polimerización en emulsión en dos etapas utilizando MMA, BA y una mezcla al 50% de MMA/BA. En un primer paso, los agregados se hinchan con monómero usando una relación monómero/ASR=0,5 (en todos los casos hay absorción completa) dando un D_{agg} mayor para MMA que para BA y MMA/BA bajo condiciones de reacción (50ºC y agitación). Las reacciones se inician con TBHP/AsAc (adición única) observandose polimerizaciones más rápidas para BA y MMA/BA debido a su mayor número de partículas y a su elevada constante de propagación. Al final

de esta primera etapa se alcanzan conversiones del 97% para BA y MMA/BA y del 88% para MMA. En un segundo paso, las partículas se hinchan con monómero aumentando la relacion monómero/ASR a 1 y se vuelven a polimerizar con THBP/AsAc. Las velocidades de polimerización y el número de partículas siguen las mismas tendencias que en el primer paso. De esta manera se obtuvieron látex estables y monodispersos con diámetro de partícula entre 70-90nm para BA y MMA/BA. Aunque no se observa un coágulo macrocópico para el MMA, la distribución de tamños de partícula presenta un pico a tamaños grandes.

Se han obtenido finalmente látex de MMA/BA (40/60) con menores tamaños de partícula usando ASR más hidrofóbicas mediante la sustitución de parte del MMA por lauril metacrilato (LMA). El menor tamaño de agregados (20nm) se obtuvo para las ASRs con 5, 10 y 20% de LMA. Estas ASRs se ultilizaron en polimerizaciones en emulsión en semicontinuo de MMA/BA con APS como iniciador. Se obtuvieron látex estables con un 40% de contenido en sólidos y tamaños de partícula entre 60-80nm dependiendo del contenido en LMA del ASR.

Como conclusión final puede decirse que las diferentes familias de ASRs sintetizadas pueden utilizarse de manera satisfactoria como emulsificantes en distintas reacciones de polimerización tanto en emulsión como en miniemulsión obteniendo látex estables. La cinética de estas reacciones está afectada tanto por el tipo de ASR como por el monómero y el inicidor utilizado.